Lnc-ITM2C-1 and *GPR55* are Proviral Host Factors for Hepatitis C Virus

Dissertation

for the degree

Doctor rerum naturalium (Dr. rer. nat.)

submitted by Pan Hu, M. Sc.

Institute of Biochemistry

Faculty of Medicine

Justus Liebig University Gießen

Gießen, October 2019

This work was accomplished from May 2015 to October 2019 under the supervision of Prof. Dr. Michael Niepmann in the Institute of Biochemistry, Faculty of Medicine, Justus Liebig University Gießen.

This research was funded by a Land Hessen LOEWE grant (Medical RNomics).

Supervisors:

Prof. Dr. Albrecht Bindereif
Institute of Biochemistry
Faculty of Biology and Chemistry
Justus Liebig University Gießen

Prof. Dr. Michael Niepmann
Institute of Biochemistry
Faculty of Medicine
Justus Liebig University Gießen

Summary

Multiple host factors are known to play important roles in Hepatitis C Virus (HCV) replication, in immune responses induced by HCV infection, or in processes that facilitate virus escape from immune clearance, while yet only few studies examined the contribution of long non-coding RNAs (lncRNAs/lncRs). Using microarrays, we identified lncRNAs with altered expression levels in HCV replicating Huh-7.5 hepatoma cells. Of these, lncR 8/*Lnc-ITM2C-1* was confirmed by quantitative real-time polymerase chain reaction (qRT-PCR) to be upregulated early after HCV infection. Nucleus/cytoplasm fractionation showed a preferential nuclear localization of lncR 8. Expression of lncR 8 in Huh-7.5 could be largely repressed by GapmeRs (GmRs). After suppressing the expression of lncR 8, HCV RNA and protein were downregulated, confirming a positive correlation between lncR 8 expression and HCV replication. LncR 8 knockdown in Huh-7.5 cells reduced mRNA expression level of the neighboring gene G protein-coupled receptor 55 (*GPR55*) at early times, and leads to increased levels of several interferon stimulated genes (ISG) including interferon stimulated gene 15 (*ISG15*), MX dynamin like GTPase 1 (*Mx1*) and interferon induced transmembrane protein 1 (*IFITM1*). Importantly, the effect of lncR 8 on ISGs and *GPR55* precedes its effect on HCV replication. Furthermore, knockdown of *GPR55* mRNA induces ISG expression, providing a possible link between lncR 8 and ISGs. We conclude that HCV induces lncR 8 expression, while lncR 8 indirectly favors HCV replication by stimulating expression of its neighboring gene *GPR55*, which in turn downregulates expression of ISGs. The latter fact is also consistent with a pro-inflammatory role of *GPR55*. These events may contribute to the failure of cells to eliminate ongoing HCV infection.

Content

1. Introduction 4
1.1 Hepatitis C Virus Infection 4
1.2 Hepatitis C Virus Genotypes 5
1.3 Hepatitis C Virus Life Cycle 7
1.3.1 Viral Translation and Replication 8
1.3.1.1 Viral Translation 8
1.3.1.2 Viral Replication 9
1.3.1.3 Host Factors Regulate Translation and Replication 10
1.3.2 Viral Assembly and Secretion 10
1.4 The Antiviral Response Against HCV 11
1.4.1 Innate Immune Response 11
1.4.1.1 Cellular Sensors 13
1.4.1.2 IFN Signaling 13
1.4.1.3 ISGs 15
1.4.2 Adaptive Immune Response 16
1.4.3 HCV Evasion from Immune System 16
1.4.3.1 Viral Proteins Contribute to Immune Escape 17
1.4.3.2 Cellular Sensors Contribute to Immune Escape 17
1.4.3.3 ISGs Contribute to Immune Escape 17
1.4.3.4 Exosomes Contribute to Immune Escape 18
1.5 Long non-coding RNA (lncRNA) 18
1.5.1 HCV or the Antiviral Response Induced LncRNAs 20
1.5.2 Function of LncRNAs 21
1.5.2.1 Antiviral LncRNA 21
1.5.2.2 Proviral LncRNA 22
1.6 Animal Model and Cell Culture System for HCV Research 23
1.7 Aim of Work 24
2. Results 25
2.1 Identification of LncRNAs Deregulated by HCV Replication 25
2.2 HCV Replication Increases the Expression of Four LncRNAs 28
2.3 Low Protein Coding Potential and Subcellular Localization 28
2.4 LncR 8 Favors HCV Viral Replication and Infection 30
2.5 LncR 8 may be a non-polyadenylated RNA 34

2.6 LncR 8 is a Short-Term *Cis*-Acting Regulator of Its Neighbor GPR55 35
2.7 LncR 8 is a Negative regulator of the Antiviral Response 38
2.8 GPR55 Negatively Regulates ISGs 43
2.9 LncR 8 is Induced by poly(I:C) 43
2.10 LncR 8 is Downregulated by JAK/STAT Pathway 46
3. Discussion 48
3.1 Identification of LncRNAs Deregulated by HCV Replication 48
3.2 HCV Replication Increases the Expression of Four LncRNAs 49
3.3 LncR 8 may Regulate GPR55 by *Cis*-regulation 50
3.4 Immune Responses Induced after HCV Infection 50
3.5 LncR 8 is a Negative Regulator of the Antiviral Response 51
3.6 GPR55 Negatively Regulates ISGs 52
3.7 LncR 8 can be Induced by Poly(I:C) 54
3.8 LncR 8 is Downregulated by JAK/STAT Pathway 54
4. Materials and Methods 56
4.1 Materials 56
4.1.1 Bacterial Strains, Cell Lines and plasmid 56
4.1.2 Materials for Bacterial Growth and Cell Culture 56
4.1.3 Chemicals and Reagents 56
4.1.4 Enzymes 57
4.1.5 Antibodies 58
4.1.6 Kits 58
4.1.7 Oligonucleotides and primers 59
4.1.7.1 miR122 duplex 59
4.1.7.2 Anti-miR122 LNA 59
4.1.7.3 LNA^{TM} LongRNA GmR Oligos 59
4.1.7.4 Primers 60
4.1.8 Buffers and Solutions 63
4.1.8.1 Bacterial Growth and Cell Culture Solutions 63
4.1.8.2 General Use Buffer 64
4.1.8.3 Western Blot and Immunofluorescence Buffers 65
4.1.9 Consumables 66
4.1.10 Laboratory Equipment 66
4.2 Methods 67

4.2.1 Cell Culture 67
4.2.1.1 Thawing of Cells 67
4.2.1.2 Passaging Eukaryotic Cells 67
4.2.1.3 Counting Eukaryotic Cells 68
4.2.1.4 Freezing Eukaryotic Cells 68
4.2.2 Transformation of Bacteria and Maxi Plasmid Preparation 69
4.2.2.1 Cultivation of Bacteria 69
4.2.2.2 Transformation of Bacteria by Heat Shock 70
4.2.2.3 Plasmid Preparation 70
4.2.3 Plasmid digestion and *In vitro* Transcription 70
4.2.4 Infectious HCV in Cell Culture 71
4.2.5 Cell Treatment 72
4.2.6 RNA Samples, DNA Removal and cDNA Preparation 73
4.2.7 Sequencing 75
4.2.7.1 Library Preparation and NGS 75
4.2.7.2 Microarray 75
4.2.8 Quantitative RT-PCR (qRT-PCR) 76
4.2.9 Protein Biochemical Techniques 78
4.2.9.1 Immunofluorescence 78
4.2.9.2 Western blot 78
4.2.10 RACE 79
4.2.11 Protein-coding Potential 80
4.2.12 Statistical Analysis 81
5. References 82
6. Abbreviations 95
7. Appendix 99
7.1 Test for Possible Cross Reactions between GmRs 99
7.2 Potential full length sequence of lncR 8 109
7.3 Negative Control β-actin 110
7.4 Plasmid Map of pFK-JFH1-J6 C-846_dg (Jc1)_12961 111
8. Publications 113
7.1 Peer-reviewed Journal 113
7.2 Contributions to Congresses 113
9. Acknowledgements 114

1. Introduction

1.1 Hepatitis C Virus Infection

While it's not clear about the origin of Hepatitis C virus (HCV) and the timing of its introduction into the human population, it was first noticed in mid-1970s that the world's supply of blood was contaminated with an unknown agent resulting in post-transfusion non-A, non-B hepatitis (Lindenbach and Rice, 2005). In 1989, HCV was identified in the serum of a chimpanzee infected with non-A, non-B hepatitis patient sera (Choo et al., 1989).

HCV is a bloodborne pathogen so it is primarily transmitted through large or repeated direct percutaneous exposure to contaminated blood, including intravenous drug use, blood transfusion, organ transplantations, sexual contacts, vertical transmission, and other blood to blood contact, like use of unsterilized injection needles, use of unsterilized instruments for nose and ear piercing or tattoos *et al.* (Franciscus, 2016; Gokhale et al., 2014; Nouroz et al., 2015).

HCV virions turn over rapidly with a half-life about 3 hour, and an estimated 10^{12} viruses are produced and cleared per day in an infected person (Ashfaq et al., 2011; Avidan U. Neumann et al., 1998; Lindenbach and Rice, 2005). This is about 100-fold greater than the rate reported for HIV. High viral loads are observed in the first few weeks after a person is infected with HCV (Lindenbach and Rice, 2005). Inflammatory processes leading to liver injury are usually occurring after 2-3 months (Lindenbach and Rice, 2005). In 75-85% of those infected, the virus is not cleared by 6 months and persists, the infection becomes chronic (Nouroz et al., 2015). Typically, chronically infected patients contain 10^{3}-10^{7} HCV genomes per ml of serum (Lindenbach and Rice, 2005). Anytime from 2 weeks to 6 months after HCV infection, symptoms include jaundice, fatigue, gray-colored stool, joint pain, belly pain, weakness, anorexia, itchy skin and dark urine can appear. Mild cognitive problems and fatigue are the major symptoms of chronic hepatitis C, but it can also be asymptomatic (Nouroz et al., 2015).

Persistent HCV infection may develop into liver fibrosis, and in 15-25% of patients cirrhosis develops after 10 to 40 years. Patients with chronic Hepatitis C and cirrhosis are at high risk for liver failure and hepatocellular carcinoma (Heim and Thimme, 2014; Messina et al., 2015). HCV is the most common

cause of these chronic liver diseases, and remains a global health issue affecting approximately 2% of the global population (Nouroz et al., 2015; Valadkhan and Fortes, 2018). Many antivirals have been developed to cure HCV, like the initial interferon (IFN)-α-based therapy and direct acting antivirals (DAA) available recently, such as sofosbuvir, a RNA-dependent RNA polymerase (NS5B) inhibitor. However, IFN therapy is not very effective and difficult to tolerate in patients, and the highly effective DAA therapy comes with a very high cost (Gokhale et al., 2014). A vaccine for HCV prevention is still urgently needed (Gokhale et al., 2014; Klenerman, 2016).

1.2 Hepatitis C Virus Genotypes

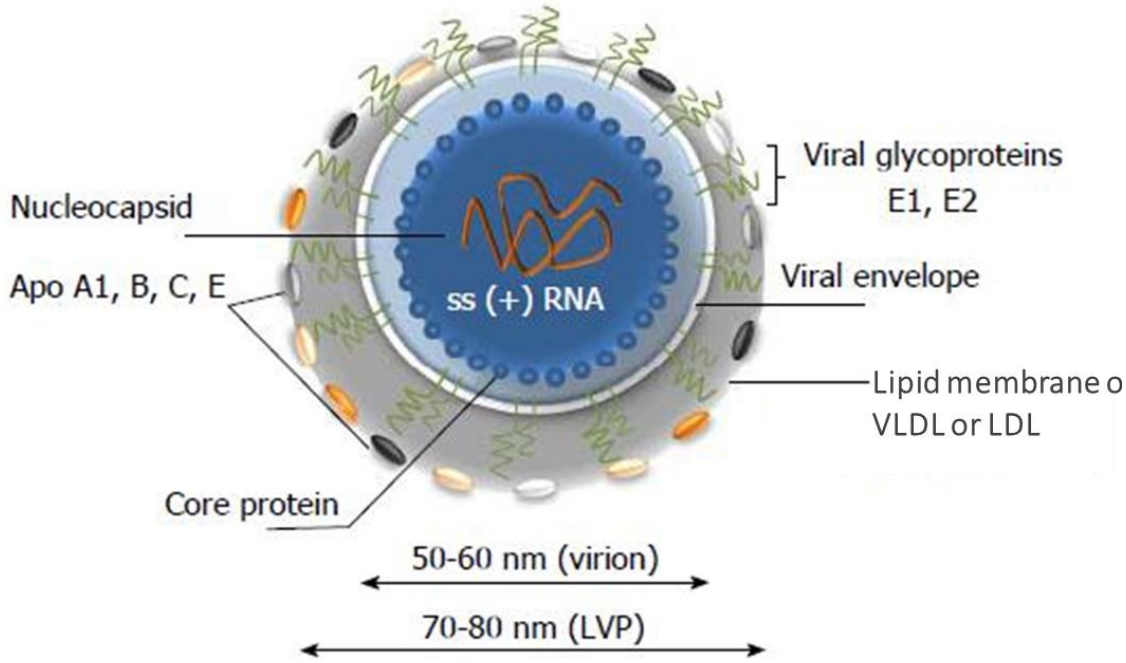

Figure 1.1 A model of hepatitis C virus lipoviral particle. The viral particle is made up of the host cell-derived lipid membrane (given in grey) with the partially embedded viral glycoproteins E1 and E2 (green), and the capsid containing the single stranded RNA genome (orange). Lipid membrane is formed by low density lipoproteins (LDL) and very low-density lipoproteins (VLDL), thus the morphology of the virion is not icosahedral. Picture taken from (Morozov and Lagaye, 2018).

HCV is an enveloped virus with a diameter of 50 nm, belonging to the *Flaviviridae* family (Nouroz et al., 2015) (Figure 1.1). The HCV genome RNA

is 9.6 kb and consists of a long open reading frame (ORF) encoding three structural proteins (core protein and the envelope glycoproteins E1 and E2) and seven non-structural proteins (p7, NS2, NS3, NS4A, NS4B, NS5A, and NS5B), flanked by a 5′untranslated region (UTR) and a 3′UTR (Barriocanal and Fortes, 2017) (Figure 1.2).

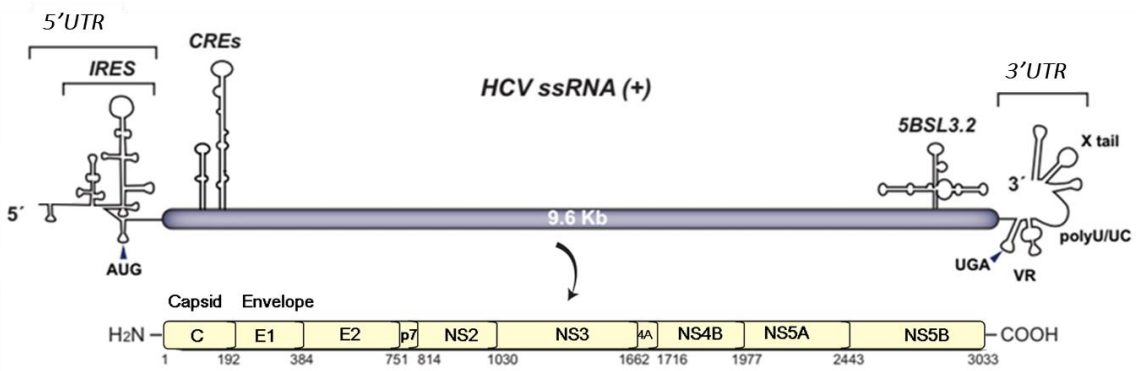

Figure 1.2 HCV genome organization and encoded viral proteins. The HCV genome, which consists of a 9.6-kb open reading frame with 5′- and 3′-UTRs, is translated to a polyprotein of approximately 3000 amino acids. Secondary structures of *cis*-acting RNA elements (CREs) in the untranslated regions (UTRs) and the coding region are schematically depicted. Cellular and viral proteases mediate the proteolytic cleavage of the polyprotein into three structural proteins, core, E1 and E2, and the non-structural proteins p7, NS2, NS3, NS4A, NS4B, NS5A and NS5B. Picture was modified from (Paul et al., 2014).

Due to its high replication rate and lack of a 3′-5′ exonuclease proofreading activity of RNA-dependent RNA polymerase NS5B, HCV sequence shows very high variability, similarly to all RNA positive-strand viruses (Alazard-Dany et al., 2019). The hypervariable region of E1 and E2 glycoprotein show the highest sequence variability between genotypes, while the 5′UTR show the lowest. Based on the highly variable regions in the envelope protein and nonstructural 5A protein, HCV strains are currently classified into seven major genotypes that differ from each other at the nucleotide level by 30-50%. Each genotype contains a variable number of genetically distinct “subtypes” (more than 80 subtypes), designated a, b, c and so on, that differ at 10-30% of nucleotide sites (Ashfaq et al., 2011; Tsukiyama-Kohara and Kohara, 2017). HCV in patients can produce a group of similar descendant HCV genomes differing in the sequence by mutations, known as quasi-species (Valadkhan and Fortes, 2018). The rate of nucleotide mis-incorporation is approximately 10^{-3} base substitutions

per genome site per year (Ashfaq et al., 2011).

Different HCV genotypes show different geographical distributions. HCV genotype 1b is the most prevalent worldwide, while genotype 2a is most prevalent in Europe and Japan (Messina et al., 2015; Nouroz et al., 2015). Infection with genotypes 1a and 1b results in more severe liver diseases than infection with genotype 2. Patients infected with different genotypes show different responsiveness to IFN-α-based therapy (Wong and Chen, 2016), thus genotyping is important for planning of HCV treatment period (Nouroz et al., 2015).

1.3 Hepatitis C Virus Life Cycle

The core, E1 and E2 are the main constituents of infectious virus particles (Jirasko et al., 2010). HCV virions can exist as single hybrid particles, while the majority of HCV virions circulating in the blood are embedded into very low or low-density lipoprotein-like particles (VLDLs and LDLs) formed by triglycerides, apolipoproteins (Apo) E and ApoB and cholesterol or phospholipids (Paul et al., 2014). The association of HCV with lipoprotein is a remarkable feature of HCV (Dubuisson and Cosset, 2014), which leads to low buoyant density (Bartenschlager et al., 2011). This coat may help virions to escape from neutralizing antibodies and aids hepatocyte infection (Valadkhan and Fortes, 2018).

The HCV life cycle is very complicated and needs a coordinated cooperation between viral and cellular components for each step (Figure 1.3). Understanding these host-virus interactions will benefit the strategies development of therapeutic intervention (Pezacki et al., 2010).

The acidic pH in the endosome triggers fusion of the viral envelope with the endosomal membrane, allowing the release of the viral particle into the cytoplasm (White and Whittaker, 2016). The components of the virion particle include the positive strand HCV genomic RNA, HCV structural proteins, some HCV non-structural proteins, including NS5A, and, in some cases, host proteins, including LDLs (Dubuisson and Cosset, 2014; Pezacki et al., 2010). The HCV RNA then moves to ribosomes, and serves as a messenger RNA (mRNA) for translation of the viral proteins (Dubuisson and Cosset, 2014; Lindenbach and Rice, 2013; Pezacki et al., 2010). The encoded polyprotein is processed by viral

and host proteases into mature proteins (Appel et al., 2006b; Niepmann, 2013; Paul et al., 2014). Negative strand RNA intermediates are generated which then act as templates for the synthesis of new positive strand genomic RNA at the endoplasmic reticulum (ER)-derived membranous webs (Paul et al., 2014; Pezacki et al., 2010). Viral assembly and release are the last steps of a complete HCV viral life cycle (Dubuisson and Cosset, 2014; Lindenbach and Rice, 2013; Paul et al., 2014; Pezacki et al., 2010; Vieyres and Pietschmann, 2019).

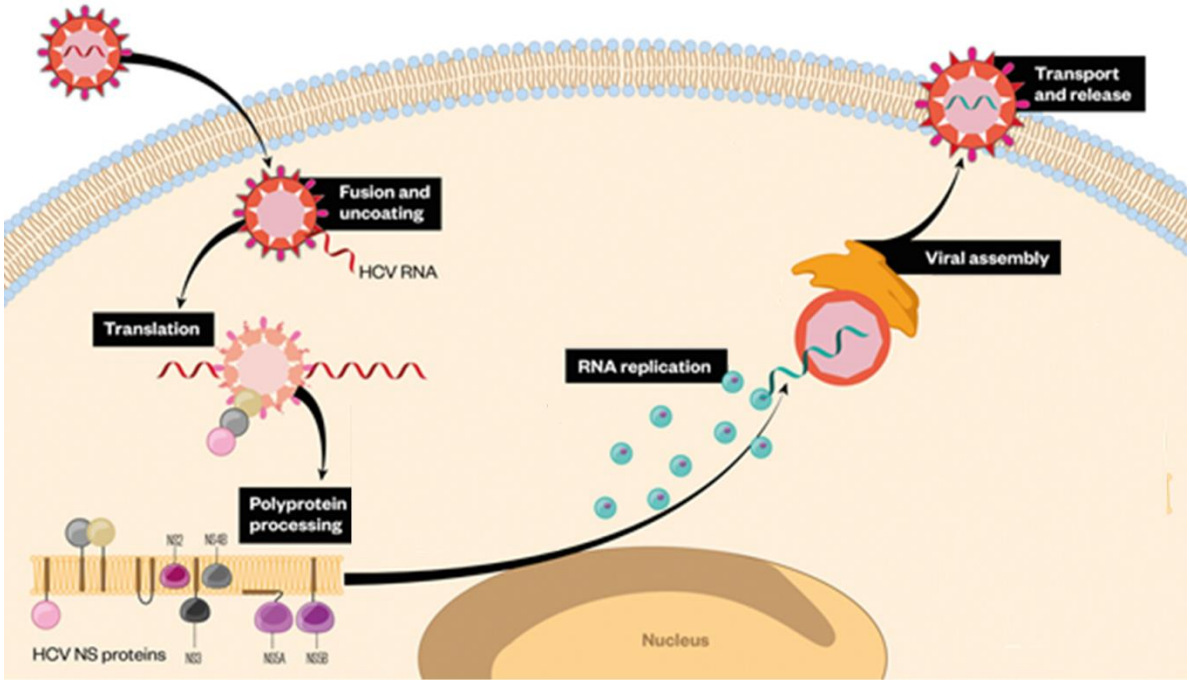

Figure 1.3 HCV life cycle. Virus entry, fusion and uncoating, the internal ribosome entry site (IRES)-mediated translation and polyprotein processing, HCV RNA replication in a specific membrane alteration, the membranous web, virus packaging and assembly, virion maturation and release. Figure was adapted from (Sarpel et al., 2017).

1.3.1 Viral Translation and Replication

1.3.1.1 Viral Translation

As a positive-strand RNA virus, HCV can serve directly as the template for translation of the viral polyprotein (Appel et al., 2006a). Translation is controlled by the IRES (Kohara et al., 1992) in the 5′UTR. Downstream elements like the CRE in the coding region and the 3′UTR are involved in translation regulation (Niepmann et al., 2018).

Eukaryotic translation is usually initiated by the 5′cap structure that guides the small ribosomal 40S subunit to the 5′end of the mRNA by the help of initiation factors (eIFs) (Jackson et al., 2010). In contrast, the 5′UTR of HCV contains an IRES, which constitutes the stem-loops II to IV including a few nucleotides of the core coding region, and binds 40S ribosomal subunits directly, bypassing the need for nuclear RNA processing machinery and allowing cap-independent translation (Niepmann, 2013). Together with the NS4A cofactor, the serine type protease in the NS3 domain forms a stable complex and catalyzes polyprotein cleavage at the NS3-4A, NS4A-B, NS4B-5A, and NS5A-5B sites (Jirasko et al., 2010).

1.3.1.2 Viral Replication

The viral RNA also serves as a template for production of minus strand RNA intermediates, which then act as templates for the synthesis of new positive strand HCV genomic RNA that is produced in 5- to 10-fold excess (Lohmann, 2013). The new positive strand HCV genomic RNA can be used for translation, replication, or packaging (Paul et al., 2014).

NS4B induces modified membranes in the host cell after the synthesis of HCV proteins. The ER-derived membranous webs then become the sites for HCV replication, which is performed by the RNA-dependent RNA polymerase NS5B (Pezacki et al., 2010). Formation of a membrane-associated replication complex, composed of viral proteins, replicating RNA and altered cellular membranes, is a hallmark of all positive- strand RNA viruses investigated so far (Dreux et al., 2009).

First negative strand can be detected in cells 4-6 h after transfection or infection, which represent the time needed for polyprotein translation, the formation of membranous replication compartment and RNA synthesis. Full replication cycle needs 24-48 h (Lohmann, 2013).

The *cis*-elements controlling replication of the viral RNA genome are located mainly in the 5′- and 3′ -UTRs at the genome ends but also in the protein coding region, and in part these signals overlap with the signals controlling RNA translation. The 3′UTR is composed of a variable region, a polyU/UC tract of variable length and a highly conserved 98-bases element designated X-tail or 3′X, encompassing the 3′end of the viral genome. The conserved region of

3′UTR is specifically recognized by viral RNA-dependent RNA polymerase NS5B and other host and viral factors, and is essential for viral RNA replication.

1.3.1.3 Host Factors Regulate Translation and Replication

A number of cellular RNA-binding proteins are involved in the regulation of HCV translation and replication. Like La protein, poly(rC)-binding protein 2 (PCBP2), and RNA binding motif protein 24 (RBM24), which enhance HCV translation (Cao et al., 2018). Heterogeneous nuclear ribonucleoprotein A1 (hnRNPA1) and high mobility group box 1 (HMGB1) exert biological effects on viral replication (Rios-Marco et al., 2016). The cellular ewing sarcoma breakpoint region 1 (EWSR1) protein and the components of the mRNA decay machinery, including LSm1-7, are involved in regulation of the switch from translation to replication of the genome (Bayer et al., 2016; Fehr et al., 2012).

Interestingly, another noncoding host factor was detected, microRNA-122 (*miR-122*) specifically and highly accumulated in liver cells (Chang J. et al., 2004). *miR-122* can bind to two *miR-122* seed sites located between stem-loops I and II of the highly conserved 5′UTR of HCV and at least three additional target sites in the coding region and the 3′UTR (Figure 1.4). It is positively involved in the regulation of HCV RNA stability (Shimakami et al., 2012), translation (Henke et al., 2008) and replication (Jopling et al., 2005).

1.3.2 Viral Assembly and Secretion

Virtually all viral proteins seem to participate in this process (Paul et al., 2014; Vieyres and Pietschmann, 2019). The site of viral particle assembly is on LDs adjacent to the ER and is initiated by the HCV core protein (Pezacki et al., 2010). NS5A molecules from the replication complex facilitate the nucleocapsid assembly by helping the interaction between core protein and viral RNA (Masaki et al., 2008). HCV secretion from Huh-7.5 cells is different from classical secretion via the Golgi apparatus and the trans-Golgi network. It may involve the endosomal pathway and link to the exosome secretory pathway (Bayer et al., 2016). The components of the VLDL secretion pathway are thought to be involved (Bayer et al., 2016; Takacs et al., 2017), given that HCV virions acquire their low buoyant density during secretion.

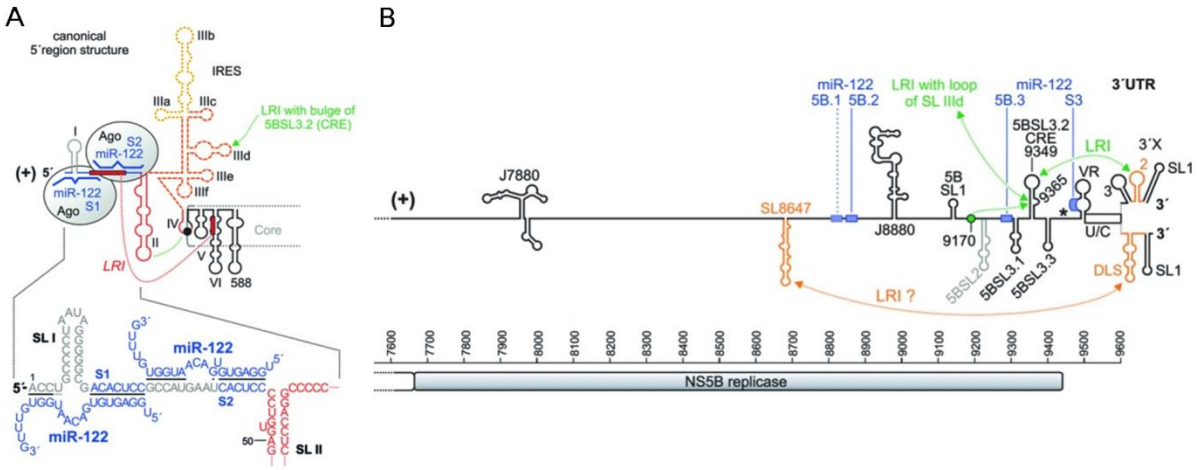

Figure 1.4 *MiR-122* binding sites in HCV genome. (**A**) The canonical HCV 5′UTR structure with the *miR-122* binding sites S1 and S2. The seed region of *miR-122* (nucleotides 2-7 or 2-8) binds to the target sequence (A)CACUCC, and the *miR-122* supplementary region binds to a variable number of target nucleotides. (**B**) The NS5B sequence is shown with nucleotide numbers. The NS5B stop codon is shown by an asterisk, and the 3′X region is shown in its two experimentally validated alternative structures. The *miR-122* binding sites are shown as blue boxes, with the first non-conserved site 5B.1 with a dotted box and the other conserved two sites in the NS5B region (5B.2 and 5B.3) and the *miR-122* target site in the 3′UTR (S3) with solid boxes. Figure was modified from (Niepmann et al., 2018).

1.4 The Antiviral Response Against HCV

During HCV life cycle, the cell develops several mechanisms to recognize the virus and fight against it. Already within days after infection, high viral titres have been measured in the serum and the liver of chimpanzees (Gokhale et al., 2014). The tightly coordinated innate immune signaling pathways in the liver provide the first and significant line of host defense against HCV (Gokhale et al., 2014; Heim and Thimme, 2014), while the adaptive immune response emerges over several weeks (Sun et al., 2015).

1.4.1 Innate Immune Response

Upon HCV infection, specific pathogen-associated molecular patterns (PAMPs) of HCV can be sensed by different pattern recognition receptors (PRRs), like retinoic acid-inducible gene I (RIG-I), melanoma differentiation factor 5 (MDA5), and toll-like receptor 3 (TLR3), leading to the production of pro-inflammatory cytokines, chemokines, and IFN, which include Type I IFN

(IFN-α, IFN-β, and others), Type II IFN (IFN-γ), and Type III IFN (IFN-λ) (Barriocanal et al., 2014; Kambara et al., 2014; Sun et al., 2015; Valadkhan and Fortes, 2018).

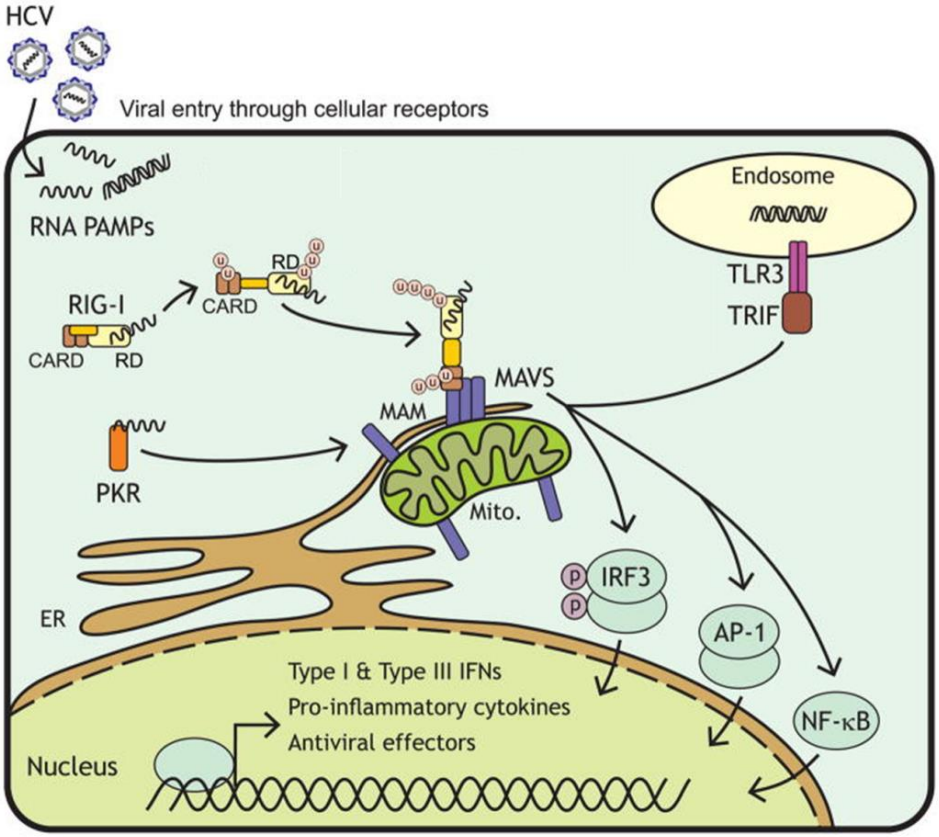

Figure 1.5 Antiviral innate immune responses of HCV in hepatocytes. Following entry of HCV into hepatocytes, viral PAMPs can be sensed by PRRs such as RIG-I, TLR3, and protein kinase R (PKR). Innate immune signaling induction through RIG-I, TLR3, and PKR activates the production of type I and type III IFNs, other pro-inflammatory cytokines, and antiviral effector proteins through the action of transcription factors such as interferon regulatory factor 3 (IRF3), activator protein 1(AP-1), and nuclear factor kappa-light-chain-enhancer of activated B cells (NF-κB). Picture was modified from (Gokhale et al., 2014).

After triggering the Janus kinase/signal transducers and activators of transcription (JAK-STAT) signaling pathway, the final outcome of the IFN signaling is the induction of hundreds of ISGs, which serve as direct effectors of the IFN antiviral defense (Heim and Thimme, 2014; Kambara et al., 2014; Sun et al., 2015; Valadkhan and Fortes, 2018) (Figure 1.5). Antiviral ISGs may target many steps in the HCV life cycle to limit viral replication or promote the IFN antiviral ability (Barriocanal et al., 2014; Valadkhan and Fortes, 2018;

Wong and Chen, 2016). IFN signaling and the subsequent expression of ISGs are central in this antiviral defense (Sumpter et al., 2005). Only combined ISGs can induce a strong antiviral response, while the effect of a single ISG is weak (Thimme et al., 2012; Valadkhan and Fortes, 2018).

1.4.1.1 Cellular Sensors

Upon HCV infection, different PRRs, which are located on the cell surface or in intracellular compartments, can recognize PAMPs of HCV (Gokhale et al., 2014). The phosphorylated 5′end and the poly U/UC sequence near its 3′end of HCV RNA, the IRES near the 5′end of the HCV genome can act as PAMPs (Dustin, 2017). Canonical PRRs include the RIG-I–like helicases (RLHs), the TLRs and the NOD-like receptors (NLRs). RLHs include RIG-I, MDA5, and laboratory of genetics and physiology 2 (LGP2), which all contain DExD/H helicase domain. RIG-I and MDA5 both contain two CARD domains at the N-terminal (Cao et al., 2015). In Huh-7.5 cells, RIG-I is mutated, which is not the reason leading to increased permissiveness of Huh-7.5 and Huh-7.5.1 cells for HCV replication (Feigelstock et al., 2010). HCV infection is capable of inducing interferon production that is mainly dependent upon MDA5 rather than RIG-I (Cao et al., 2015).

1.4.1.2 IFN Signaling

Pathogen recognition by PRRs initiates signaling that activates NF-κB and interferon regulatory factor 3 (IRF3), thereby inducing the production of pro-inflammatory cytokines, chemokines, such as interleukin-6 (IL-6), IL-8, macrophage inflammatory protein 1 (MIP1), and also production of IFN-I and type-III IFN (IFN-λ) (Nishitsuji et al., 2013; Sun et al., 2015).

The IFN response is a central component of the innate immune system and all three classes of mammalian IFNs (types I, II and III) have been shown to possess antiviral activity (Figure 1.6). Most cells are able to launch the type I IFN response (IFN-α, IFN-β, and others). Type III IFNs (IFN-λ) have a more restricted role, most likely in the viral defense at epithelial surfaces in the respiratory and gastro-intestinal tract (Heim and Thimme, 2014).

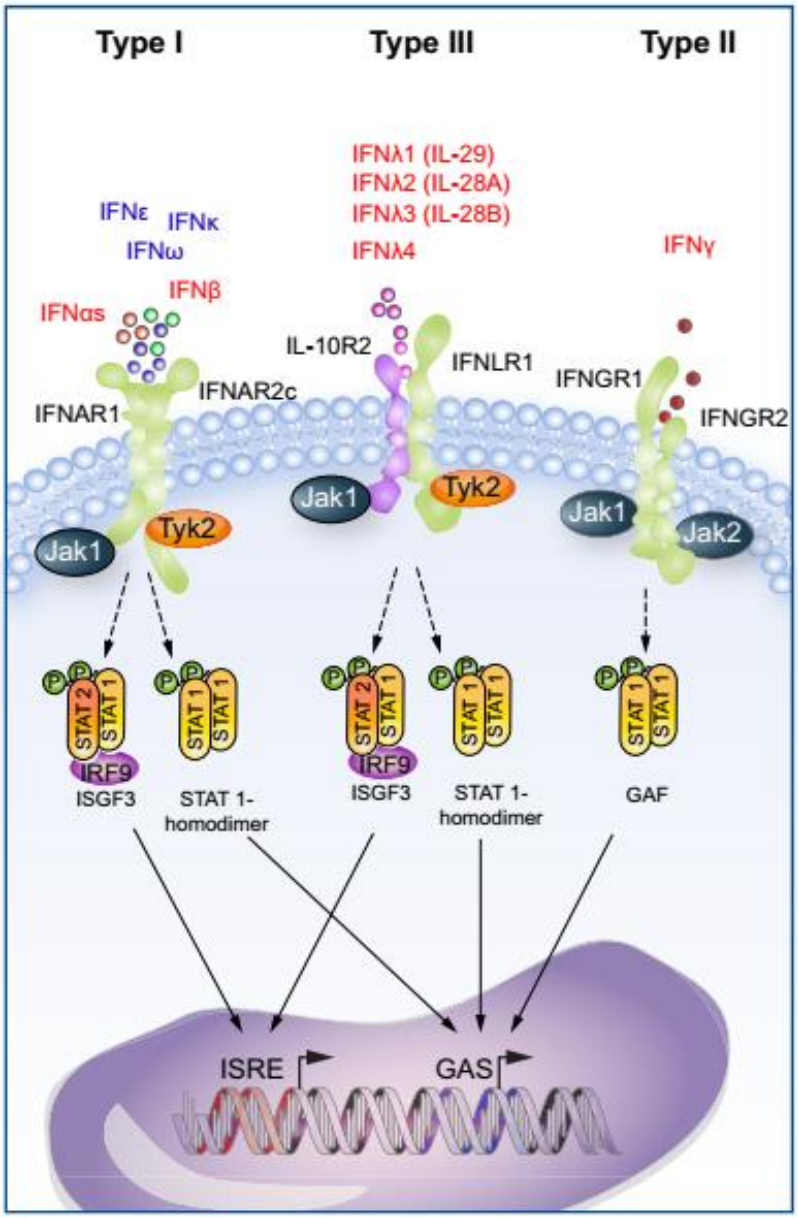

Figure 1.6 IFN signaling through the JAK-STAT pathway. Three types of IFN bind to specific receptor, Type I and III IFNs induce almost identical sets of genes mainly through the activation of IFN-stimulated gene factor 3 (ISGF3) and STAT1 homodimers. Type II IFN activates STAT1, but not ISGF3, and induces a partially overlapping but distinct set of genes. Figure was obtained from (Heim and Thimme, 2014).

Binding of Type I IFN and Type III IFN to their receptors triggers the JAK-STAT signaling pathway, which gives rise to the nuclear translocation of the STAT1/STAT2/IFN regulatory factor 9 (IRF9) complex that binds IFN-stimulated response elements (ISRE) in the promoters of ISGs and leads to transcriptional upregulation ISGs that function as potent antivirals (Kambara et

al., 2014). In contrast, Type II IFN (IFN-γ), produced by natural killer cells and mitogenically activated T cells, binds to the widely expressed IFN-γ receptor, leading to nuclear translocation of STAT1 homodimers, which bind to gamma-activated sequences (GAS) in the promoter of immunoregulatory genes (Barriocanal et al., 2014; Valadkhan and Fortes, 2018).

1.4.1.3 ISGs

The final outcome of the IFN signaling is the transcriptional activation of hundreds of ISGs. ISGs act as direct effectors of the antiviral response (Sun et al., 2015; Valadkhan and Fortes, 2018). However, the synthesis of some ISGs is triggered independent of IFN production (Wong and Chen, 2016).

The specific set of genes differs between IFNs and target cell type (Heim and Thimme, 2014). In general, IFN-α and IFN-λ, which are both modulated by the IRF3 and NF-κB pathways for induction, induce similar sets of ISGs, but the IFN-γ-induced gene set is more distinct (Dustin, 2017; Wong and Chen, 2016). The number of genes regulated by IFNs also differs between cells, it can be hundreds or thousands.

ISG products can target many steps in the HCV replication cycle to limit viral replication, whereas others may promote the IFN antiviral activity against invading viruses, or act as negative feedback regulation of IFN response, which is essential to ensure a later return to cell homeostasis (Barriocanal et al., 2014; Barriocanal and Fortes, 2017; Valadkhan and Fortes, 2018; Wong and Chen, 2016). ISGs belong to the first group are antiviral factors which reinforce the IFN pathway (STAT1 and 2 and IRF1, 3, 7 and 9) or increase cell sensitivity to PAMPs (PKR and 2'-5'-oligoadenylate synthetase (OAS) or ribonuclease L (RNase L)).

Other ISGs affect several steps of the HCV life cycle to block viral entry (Mx, IFITM, and the tripartite motif (TRIM) family, Cholesterol 25-hydroxylase (CH25H)), virus replication, translation and stability (Interferon-induced protein with tetratricopeptide repeats (IFIT), OAS, PKR, interferon-induced guanylate-binding protein 1 (GBP1), and ISG15), or viral assembly and release (viperin and tetherin/bone marrow stromal cell antigen 2 (BST2)) (Barriocanal et al., 2014; Valadkhan and Fortes, 2018).

1.4.2 Adaptive Immune Response

Innate immune response can limit HCV replication and spread, but rarely can eliminate the infection (Dustin et al., 2016). IFNs, ISGs, inflammatory cytokines, and other signals contribute to the initiation and regulation of adaptive immune responses (Dustin, 2017), which develops over several weeks**,** later than innate immune responses. A robust response by both the innate and adaptive the immune system is required for effective elimination of HCV, but the adaptive immune responses are the determinants of the clearance (Gokhale et al., 2014; Sun et al., 2015). Three components of the adaptive immune system, antibodies, $CD4^+$ T cells, and $CD8^+$ T cells, have been shown to be associated with viral clearance (Neumann-Haefelin and Thimme, 2013). Most of the HCV-specific antibodies have no antiviral activity, only a small number of them is able to prevent viral infection and spread by inhibiting virus binding, entry or post-entry steps and are therefore termed neutralizing antibodies. However, viral clearance can occur without the presence of neutralizing antibodies (Neumann-Haefelin and Thimme, 2013). Major antiviral effector cells are $CD8^+$ T cells, HCV-specifc $CD4^+$ T cells help to prevent viral escape from the $CD8^+$ T cell response (Neumann-Haefelin and Thimme, 2013).

1.4.3 HCV Evasion from Immune System

In spite of activated immune response, 75-85% of infected patients develop chronic infection without clearance of HCV (Nouroz et al., 2015), which may develop into chronic hepatitis, cirrhosis and hepatocellular carcinoma (HCC). HCV remains a global health issue affecting approximately 2% of the global population (Messina et al., 2015; Nouroz et al., 2015; Valadkhan and Fortes, 2018). The co-existence of high viral loads and high ISG expression reflects the failure of the innate immune response in clearing HCV (Heim and Thimme, 2014), suggesting strategies used by HCV to evade the host immune response (Gokhale et al., 2014). It was shown that the ineffectiveness of the HCV induced innate immune response can be achieved by cleavage of MAVS by NS3/4A protease, by an ISG translation block mediated by the noncanonical cellular sensors PKR and DEAD box RNA helicase 3 (DDX3X), or by ISGs like ubiquitin specific peptidase 18 (USP18) that downregulates the IFN pathway response as a negative

feedback to ensure homeostasis of the cellular immune response (Barriocanal et al., 2014; Barriocanal and Fortes, 2017; Gokhale et al., 2014; Ramakrishnaiah et al., 2013; Valadkhan and Fortes, 2018; Wong and Chen, 2016). Autophagy induced by HCV might also be involved in the suppression of type I IFN production (Thimme et al., 2012). Moreover, HCV related exosomes also contribute to the immune escape (Ramakrishnaiah et al., 2013).

1.4.3.1 Viral Proteins Contribute to Immune Escape

HCV encodes several proteins that block the innate immune response, including Core, NS3/4A, NS4B, and NS5A (Gokhale et al., 2014). NS3-NS4A cleaves and inactivate MAVS, TIR-domain-containing adapter-inducing interferon-β (TRIF), and Riplet E3 ubiquitin ligase, required for RIG-I ubiquitination. NS4A/B, NS5A and the core proteins block the STAT pathway (Barriocanal and Fortes, 2017; Valadkhan and Fortes, 2018).

1.4.3.2 Cellular Sensors Contribute to Immune Escape

Interestingly, several factors, like noncanonical cellular sensors PKR and DDX3X favor HCV replication, have a proven antiviral role against different viruses (Barriocanal and Fortes, 2017). PKR blocks cap-dependent cellular translation by eukaryotic translation initiation factor 2A (eIF2a) phosphorylation, while it does not affect the translation of viral proteins since the IRES of HCV does not require eIF2a for translation (Barriocanal and Fortes, 2017; Dustin, 2017; Valadkhan and Fortes, 2018). DDX3X facilitates lipid droplet biogenesis and viral assembly by interacting with the 3′UTR region of HCV and activating IKKα and a cascade of lipogenic signaling (Valadkhan and Fortes, 2018).

1.4.3.3 ISGs Contribute to Immune Escape

Some ISGs have proviral effects by negatively regulating IFN signaling to help IFN-induced cells to return to cellular homeostasis, and thus contribute to immune escape (Barriocanal et al., 2014). USP18 (UBP43) displaces ISG15 from its targets and binds to the IFNAR2 receptor, thus interfering with JAK binding and blocking IFN signaling (Barriocanal and Fortes, 2017). Early after infection, ISG15 induced by PKR acts through ISG15 conjugation (ISGylation),

which modifies newly synthesized proteins such as viral proteins and ISGs, and changes protein structure and stability, affecting functionality. It blocks RIG-I ubiquitination and functionality, leading to decreased expression of several ISGs. This promotes HCV replication (Barriocanal and Fortes, 2017; Carnero et al., 2016).

1.4.3.4 Exosomes Contribute to Immune Escape

HCV related exosomes, which contain argonaute 2 (Ago2), heat shock protein 90 (HSP90) and *miR-122* (Shen et al., 2017), enhance HCV transmission to hepatocytes (Ramakrishnaiah et al., 2013; Shen et al., 2017). HCV related exosomes also contribute to the immune escape (Ramakrishnaiah et al., 2013). HCV-infected cells could deliver their virus complex to neighbouring plasmacytoid dendritic cells (pDCs) by exosomes, avoiding the secretion of type I IFN and type III IFNs (Barriocanal and Fortes, 2017; Shen et al., 2017). Furthermore, close proximity and exosome release from HCV-infected cells promoted the secretion of gal-9 from monocytes, leading to T cell inhibition and contributing to adaptive immune escape (Ramakrishnaiah et al., 2013; Shen et al., 2017). The latest research also showed that transforming growth factor beta (TGF-β)-containing exosomes can exacerbate T follicular regulatory (Tfr) cells, likely leading to suppression of T follicular helper (Tfh) cell responses and the generation of high affinity antibody-producing B cells to subvert antiviral immunity (Dustin A. Cobb et al., 2018). Therefore, targeting specific HCV exosomes may represent a therapeutic strategy that enhances HCV treatment effects (Shen et al., 2017).

1.5 Long non-coding RNA (lncRNA)

The human genome may contain more than 90.000 genes, more than 90% of human genome undergoes transcription but does not necessarily code for proteins (Yang et al., 2015). Constituting about 65% of the human transcriptome, lncRNA is defined as RNA with more than 200 nucleotides in length and lacking protein coding capacity or only containing small ORFs (Barriocanal and Fortes, 2017).

Similarly to mRNAs, most lncRNAs are transcribed from RNA polymerase

II and are capped at the 5′end, spliced and polyadenylated. Most lncRNAs are expressed at low levels and more cell type-specific compared to mRNAs (Barriocanal and Fortes, 2017). They show poor sequence conservation among even closely related organisms and lack shared biochemical and structural features (Bevilacqua et al., 2015).

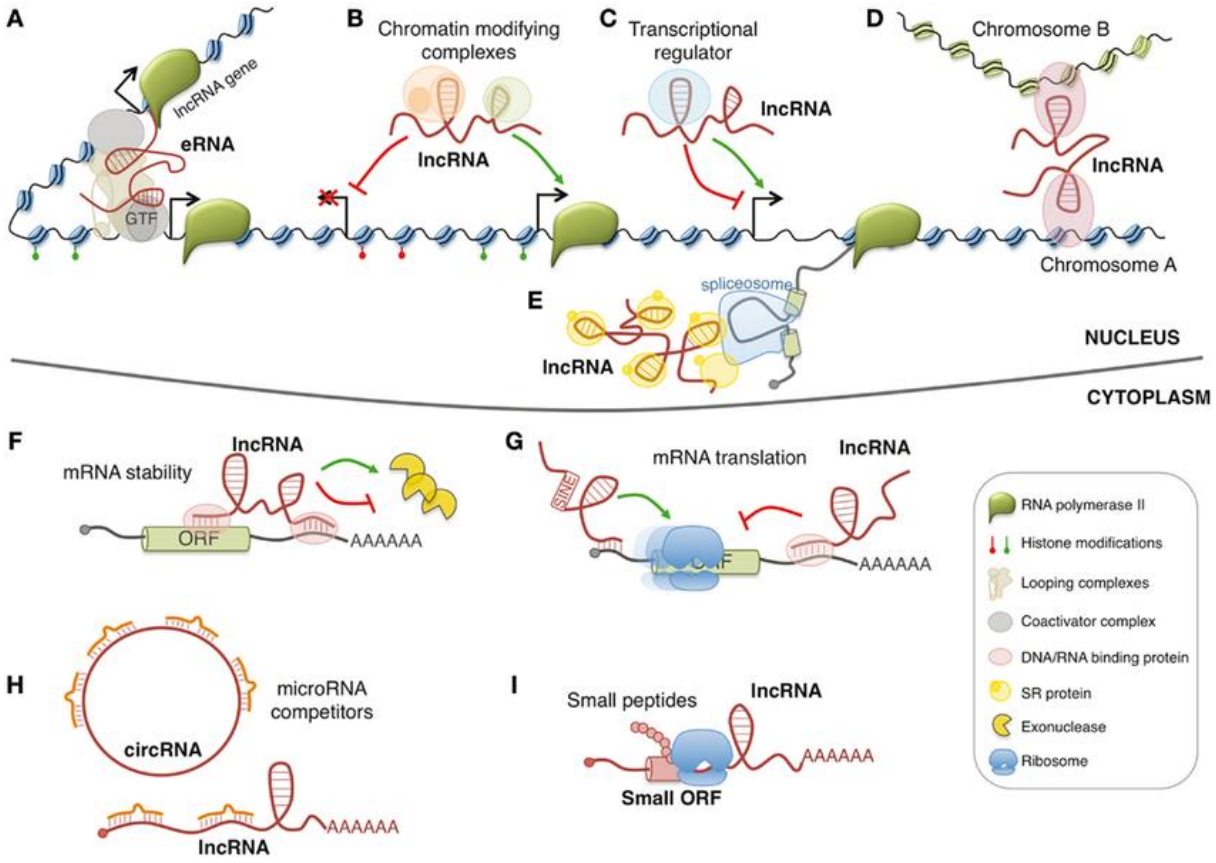

Figure 1.7 lncRNA functions. Nuclear and cytoplasmic lncRNAs may act by different mechanisms. Nuclear lncRNAs can regulate transcription by acting as enhancer RNA (eRNA) (**A**), by recruiting chromatin modifying complexes (**B**), by regulating transcription factors activity (**C**), or by acting on the spatial conformation of chromosomes to regulate gene expression (**D**), or by influencing pre-mRNA splicing (**E**). Cytoplasmic lncRNAs can regulate mRNA expression by regulating mRNA stability (**F**), mRNA translation (**G**), or by competing for microRNA binding (**H**). Few lncRNAs contain small ORFs that can be translated in biological active small peptides (**I**). Figure was taken from (Morlando et al., 2015).

LncRNAs can regulate chromatin remodeling, transcription in *cis* or *trans*, translation, or serve as enzyme cofactors (Wang et al., 2017). Few lncRNAs contain small ORFs that can be translated in biological active small peptides (Morlando et al., 2015). LncRNAs may act by different mechanisms (Figure

1.7). A major functional mechanism of lncRNAs involves regulation of nuclear events, including transcriptional regulation by acting as eRNA, by recruiting chromatin modifying complexes, or by regulating transcription factors activity, and regulation of gene expression by control of the epigenetic state of chromatin, or by influencing pre-mRNA splicing (Morlando et al., 2015; Valadkhan and Fortes, 2018). Cytoplasmic lncRNAs can regulate mRNA expression by regulating mRNA stability, mRNA translation, or by function as a competing endogenous RNA (ceRNA), competing for microRNA binding. It is a hypothesis that all types of RNA transcripts (including protein-coding messenger RNAs and non-coding RNAs such as lncRNA, pseudogenes and circular RNAs) communicate with each other by competing for binding to shared miRNA-binding sites (Morlando et al., 2015; Zhang et al., 2015).

1.5.1 HCV or the Antiviral Response Induced LncRNAs

Increasing evidence suggests that cellular lncRNAs may be deregulated in response to viral replication or to the antiviral pathways induced by infection (Barriocanal et al., 2014; Barriocanal and Fortes, 2017) (Figure 1.8).

HCV induced lncRNAs are upregulated in response to HCV viral replication or other signaling routes activated by HCV infection, but do not change when cells are treated with IFN or PAMPs such as polyinosinic-polycytidylic acid (poly(I:C)) or lipopolysaccharides (LPS), or in cells infected with other viruses (Barriocanal and Fortes, 2017; Valadkhan and Fortes, 2018). HOX Transcript Antisense RNA (*HOTAIR*) is induced by the core protein, which may in turn lead to increased viral replication by silencing the sirtuin family member 1 (SIRT1) promoter and affecting glucose and lipid metabolism (Valadkhan and Fortes, 2018). Urothelial cancer associated 1 (*UCA1*) is also a bona-fide HCV induced lncRNA.

LncRNAs induced by the antiviral response are upregulated both in HCV infected cells and in cells treated with IFN or PAMPs, or when cells are infected with viruses different from HCV (Barriocanal and Fortes, 2017; Valadkhan and Fortes, 2018), including proviral lncRNA (negative regulator of interferon response (*NRIR*), negative regulator of antiviral response lncRNA (*NRAV*), eosinophil granule ontogeny transcript (*EGOT*)), and antiviral lncRNAs (BST2

interferon stimulated positive regulator (*BISPR*), lncRNA upregulator of antiviral response interferon signaling (lncRNA#32/*LUARIS*)).

However, it's sometimes difficult to discriminate whether certain lncRNAs in HCV infected cells are induced by the antiviral responses or by viral infection (Barriocanal and Fortes, 2017).

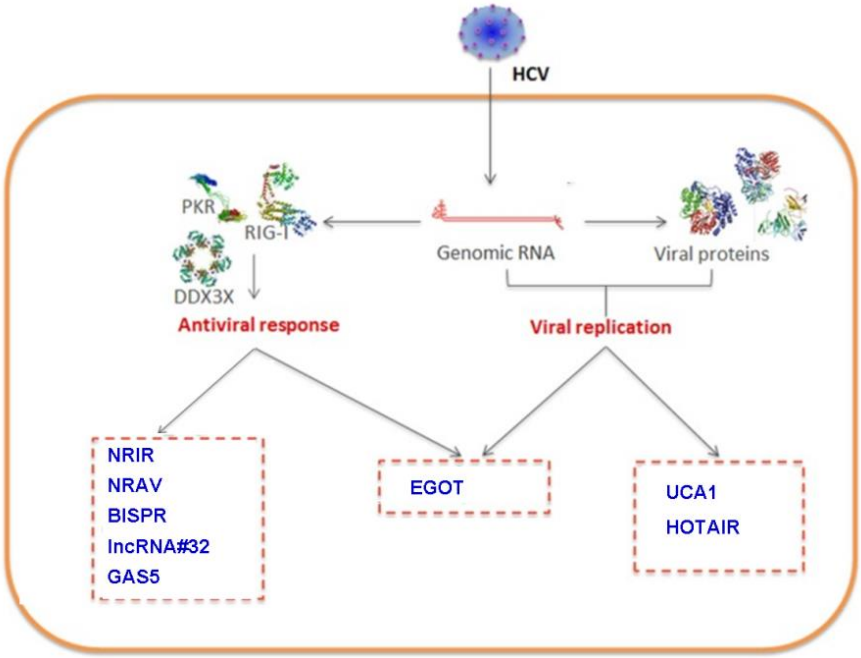

Figure 1.8 LncRNAs are induced by viral replication or antiviral response. Viral replication and HCV infection induced antiviral response deregulate the levels of different cellular lncRNAs. Some are activated by both events. Negative regulator of interferon response: *NRIR*, negative regulator of antiviral response lncRNA: *NRAV*, BST2 interferon stimulated positive regulator: *BISPR*, lncRNA upregulator of antiviral response interferon signaling: lncRNA#32/*LUARIS*, growth arrest-specific 5: *GAS5*, eosinophil granule ontogeny transcript: *EGOT*, urothelial cancer associated 1: *UCA1*, HOX Transcript Antisense RNA: *HOTAIR*. Figure was adapted from (Barriocanal and Fortes, 2017).

1.5.2 Function of LncRNAs

LncRNA may function in the HCV life cycle, the antiviral immune response induced by HCV, or in HCV immune escape, finally exerting a proviral or antiviral role (Barriocanal and Fortes, 2017; Valadkhan and Fortes, 2018).

1.5.2.1 Antiviral LncRNA

LncRNAs, like growth arrest-specific 5 (*GAS5*), *BISPR*,

lncRNA#32/*LUARIS*, and *lncITPRIP-1* can suppress HCV replication by different mechanisms. *GAS5* binds HCV NS3 protein to inhibit its functions or binds *miR-222* to release p27 protein, *lncITPRIP-1* enhances the innate immune response by MDA5 oligomerization and activation (Qian et al., 2016; Xie et al., 2018; Yu et al., 2015). LncRNA#32/*LUARIS* controls the expression of several ISGs (Nishitsujia et al., 2016), while *BISPR* appears to increase the expression of a single target gene, ISG BST2, and thereby leads to decreased virion release (Barriocanal et al., 2014). In fact, *GAS5* was also reported to positively regulate IFN responses in esophageal squamous cell carcinoma (Huang et al., 2018).

1.5.2.2 Proviral LncRNA

In contrast, *NRIR*, also known as *lncRNA-CMPK2*, and *EGOT* are proviral lncRNAs which negatively regulate ISGs and thus antagonize the antiviral response (Barriocanal and Fortes, 2017; Kambara et al., 2014; Valadkhan and Fortes, 2018).

NRIR, induced by IFN, is the first described lncRNA that acts as a negative regulator of the transcription of ISGs (*IFITM1*, *IFIT3*, *CXCL10* and *ISG15*) and benefits viral replication in Huh-7.5 cells (Barriocanal and Fortes, 2017; Valadkhan and Fortes, 2018). Similar to *NRIR*, influenza A virus-induced *NRAV* partially blocks induction of its target ISGs, including *IFITM3* and *MxA*, by modulating H3K4me3 and H3K27me3 marks (Barriocanal and Fortes, 2017). The proviral function of *EGOT* resembles what has been described for the LncRNAs *NRIR* and *NRAV* (Valadkhan and Fortes, 2018). *EGOT* mediates downregulation of ISGs, including *GBP1*, *ISG15*, *Mx1*, *BST2*, *ISG56*, *IFI6* and *IFITM1*, some of which have already been described as negative regulators of HCV or semliki forest virus (SFV) entry, replication or release (Carnero et al., 2016). *NORAD* binds *miR-373*, resulting in release of their common target Wee1 and thereby deregulation of cell growth in HCV infected cells (Sur et al., 2018). *lncIGF2-AS* and *lnc7SK*, induced by STAT3 activation, which help membranous web formation by increasing the level of phosphatidylinositol 4-phosphate kinase, thus benefit viral replication (Valadkhan and Fortes, 2018).

Some lncRNAs control the expression of the ISGs that are located in the close genome (Barriocanal and Fortes, 2017). Similarly, *NRIR* is next to *CMPK2* and *viperin*/radical S-adenosyl methionine domain containing 2 (*RSAD2*), and

BISPR to *BST2* (Barriocanal and Fortes, 2017). Interestingly, *BISPR* and *NRIR* are also bona-fide ISGs themselves (Valadkhan and Fortes, 2018). In fact, investigation in esophageal squamous cell carcinoma also supports that *GAS5* is an ISG which regulates the expression of other ISGs (Huang et al., 2018). *EGOT* is induced in response to the antiviral response, but not a bona fide ISG.

The discovery of the proviral role of *NRIR*, *NRAV* and *EGOT* points to a prominent role for lncRNAs in negative feedback loops controlling the IFN response, thus contribute to virus immune escape (Valadkhan and Fortes, 2018). Future studies are likely to identify many additional lncRNAs that regulate different steps of the innate immune response and reveal lncRNAs which regulate the steps upstream of IFN genes, thus acting as global regulators of the IFN response (Valadkhan and Fortes, 2018).

1.6 Animal Model and Cell Culture System for HCV Research

Major obstacles to studying the HCV life cycle include the lack of suitable small animal models and cell culture systems, and the difficulty to obtain samples from acutely infected patients who successfully eliminated the virus, which is because of the lack of distinct symptoms during the acute phase of HCV infection (Sun et al., 2015).

The Chimpanzee model, the only non-human primate susceptible to experimental HCV infection, has been the best animal model for HCV infection, but has been terminated by National Institutes of Health (NIH). Several genetically modified HCV-permissive mouse models have been developed. Since 2005, the full viral life cycle can be investigated with the help of complete viral replication systems, replacing the selectable replicon systems and retrovirus-based pseudotyped particles, which have been used to understand HCV genomic replication and virus entry (Dubuisson and Cosset, 2014).

In this study we will use Huh-7.5 cell lines, the most permissive "cured" subline identified so far (Blight et al., 2002), which support high levels of subgenomic HCV replication in >75% of transfected cells. It should be noted that Huh-7-derived hepatoma cells lack many features of hepatocytes. Primary human hepatocytes or human liver slices have therefore been developed to validate some experiments in more physiological models (Dubuisson and Cosset, 2014). However, besides highly expressing tumor markers like alpha-fetoprotein,

Huh-7.5 cells also express liver-specific genes at high levels, like those for albumin and various apolipoproteins (Gerresheim et al., 2019).

1.7 Aim of Work

Given the high prevalence of the virus, the severity of the associated HCC, the lack of good diagnostic and prognostic markers, and the absence of broadly effective treatment strategies, research about HCV infection should not stop but remain in focus of intensive research. It is hoped that a detailed understanding of HCV life cycle and pathogenesis will lead to effective means to treat or control infection (Li and Lo, 2015; Valadkhan and Fortes, 2018).

Accumulating data suggest a critical role of lncRNAs during HCV infection. Particularly, the protein-hostile environment caused by the combined action of PKR and the ISGylation and ubiquitination pathways in HCV infected cells make it important for virus and host to achieve functionality through the expression of functional non-coding RNAs (Valadkhan and Fortes, 2018). However, only a small number of lncRNAs, even less for HCV-related lncRNAs, has been functionally studied (Valadkhan and Fortes, 2018).

In this study, we examined cellular lncRNAs with altered expression after fully established replication of HCV to identify additional lncRNAs that may regulate different steps of the HCV life cycle and the innate immune response. Two novel lncRNA candidates identified in this study, with anti- or proviral function for HCV replication, underline an involvement of lncRNAs in the battle of HCV and host cells.

2. Results

2.1 Identification of LncRNAs Deregulated by HCV Replication

To identify deregulated lncRNAs induced by HCV replication, we carried out a gene expression microarray assay. Huh-7.5 cells were electroporated either with *miR-122* only or with *miR-122* plus HCV full-length genomic RNA, and then left for 6 days. Since Huh-7.5 cells contains somewhat lower levels of *miR-122* than primary hepatocytes, *miR-122* transfection was performed one day before and three days after the electroporation of HCV RNA to mimic a high level of *miR-122*, which is essential for HCV replication (Chang J. et al., 2004; Henke et al., 2008; Jopling et al., 2005; Niepmann et al., 2018). The 6-day duration of HCV replication was chosen to analyze the changes in expression levels of low abundance lncRNAs under conditions similar to long term infection. A large fraction of the cells contained replicating virus at the harvest day, as evaluated by immunofluorescence and western blotting against HCV protein (Figure 2.1 A & B) and by qRT-PCR targeting HCV RNA in the NS3 coding region (Figure 2.1 C). Cells transfected with anti-*miR-122* locked nucleic acid (LNA) only or anti-*miR-122* LNA plus HCV full-length genomic RNA were also prepared. Anti-*miR-122*-LNA-DNA mixmer sequesters endogenous *miR-122* and by that disables HCV replication. The effect of this anti-*miR-122*-LNA on HCV replication is shown in Figure 2.1 C and in the Western Blot in Figure 2.1 B, it serves as a negative control.

RNA samples from two independent biological replicates were used to hybridize an array in the Human G3 v3 Microarray Kit (in collaboration with Dr. Jochen Wilhelm, UKGM Giessen). Analysis of the expression changes in transcripts showed 68 deregulated genes with fold changes > 4 and $p < 0.01$ (log fold change > 2, $\log_{10}$P value > 2) in HCV treated cells compared to control cells (Figure 2.1 D). They were involved in different cellular process including immune response, amino acid metabolism, cell cycle, lipid homeostasis and alcoholism according to the KEGG analysis (Figure 2.1 G). Eighteen putative lncRNAs and 48 protein coding mRNAs showed a significant change of expression level in Huh-7.5 cells upon HCV replication (Figure 2.1 E & F; fold change > 4, $p < 0.01$).

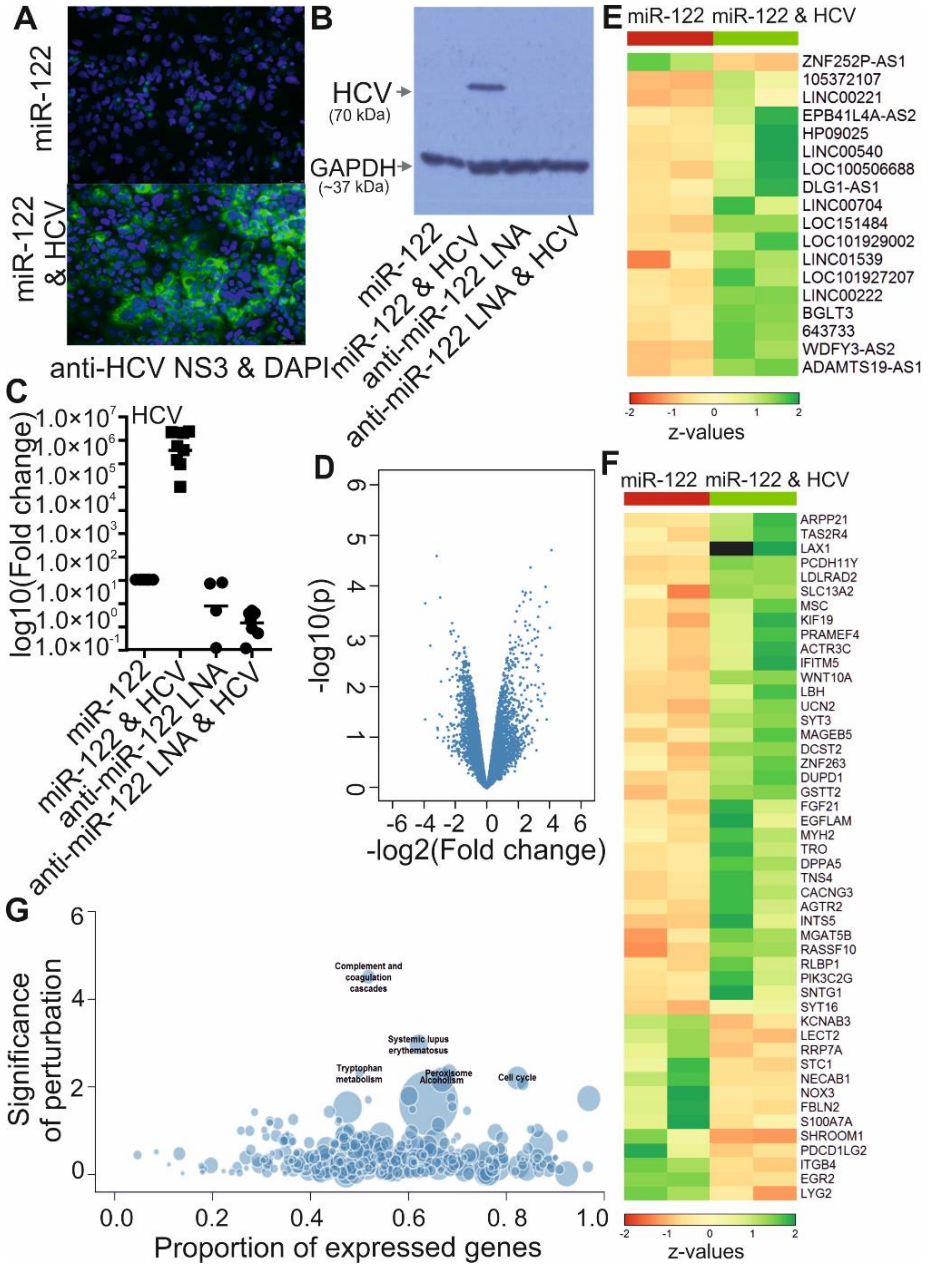

Figure 2.1 Transcriptome analysis of HCV-deregulated genes in Huh-7.5 cells. HCV NS3 protein level was detected by immunofluorescence (**A**) and western blotting (**B**) 6 days after transfection of HCV full length RNA with *miR-122* duplex or *miR-122* only as described (section 4.5). Treatment with anti-*miR-122* LNA mixmer alone or with HCV was also performed. qRT-PCR was performed to check the HCV RNA targeting the NS3 coding region (**C**). Glyceraldehyde 3-phosphate dehydrogenase (*GAPDH*) was used as a reference gene for normalization. * $p<$ 0.05.Total RNA was isolated from Huh-7.5 cells with above treatments in two independent experiments. These RNAs were used for microarray experiments. Comparison of expression levels of sequences from HCV infected cells to uninfected cells was carried out. The volcano plot shows the results for all genes (**D**). Deregulated lncRNAs (**E**) and protein-coding genes (**F**) with fold change > 4 and $p<$ 0.01 (log fold change > 2, $\log_{10}$P value > 2) are shown in the heatmap. Z value was calculated. The color scale is shown at the bottom. Information about lncRNAs is listed in Table 3. The bubble plot shows enriched KEGG pathway annotation of differentially expressed genes (**G**).

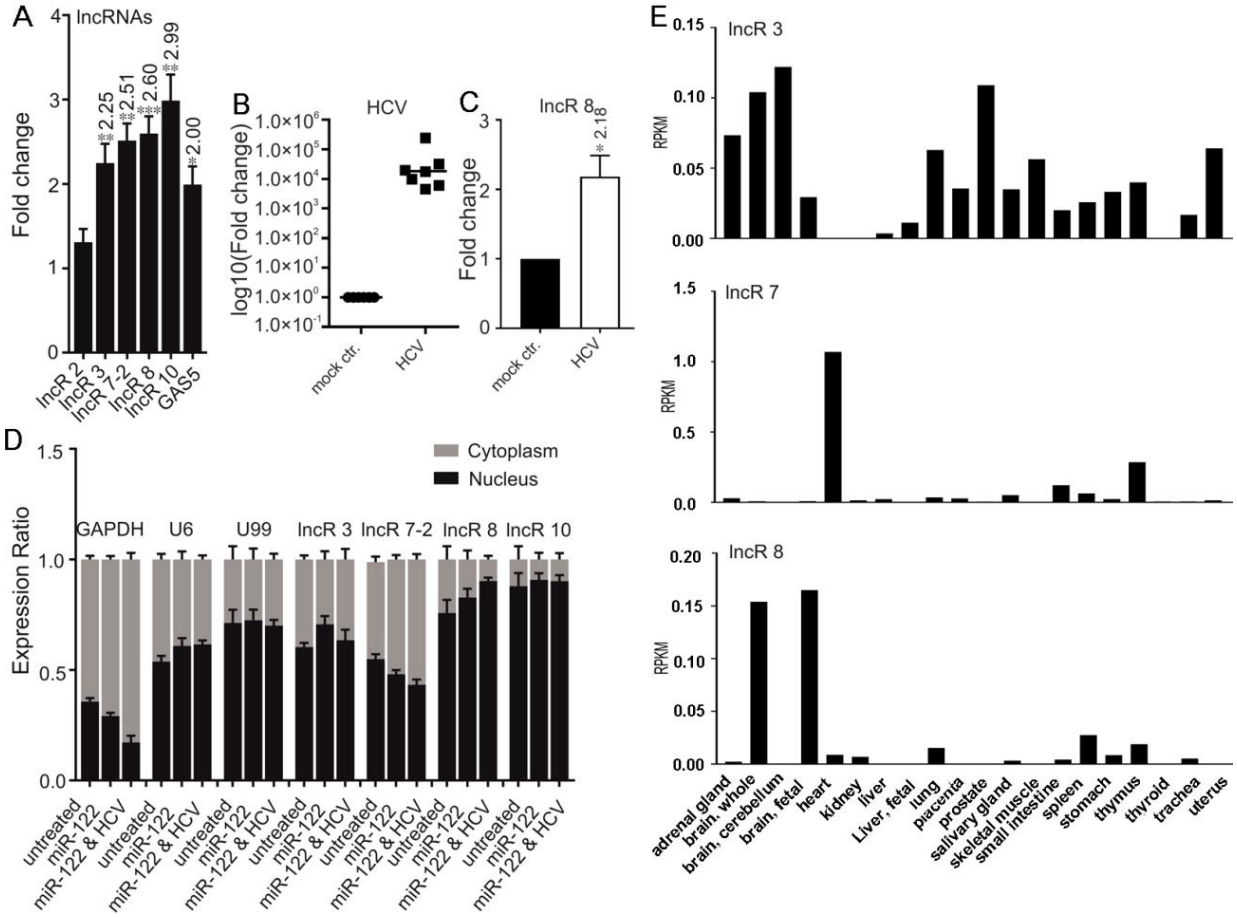

Figure 2.2 Four selected lncRNA candidates are upregulated by HCV. (**A**) The differential expression of five selected lncRNAs was confirmed by qRT-PCR 6 days after HCV transfection. GAS5 was used as a positive control. Data were normalized to *GAPDH*. Fold changes of lncRNA expression comparing HCV-treated cells to control cells are indicated at the top of each bar when statistically significant. Experiments were repeated a minimum of three times, with at least two replicates each time, and are represented as mean ±standard error of the mean (SEM). * $p \leq 0.05$, ** $p \leq 0.01$, and *** $p \leq 0.001$. (**B**) HCV NS3 level and (**C**) lncR 8 indicated similar upregulation after HCV transfection in samples treated as described above but without ectopoic *miR-122* for 6 days**.** (**D**) The subcellular localization of lncR 3, lncR 7-2, lncR 8, and lncR 10 was measured by qRT–PCR after cell fractionation. RNA was collected from untreated cells, *miR-122* treated, and *miR-122* plus HCV RNA treated Huh-7.5 cells. *GAPDH* was used as cytoplasmic control. *U6* and *U99* were used as nuclear controls. Percentage of nuclear and cytoplasmic RNA levels were calculated depending on $2^{-\Delta Ct}$, where ΔCt = Ct of the gene in nucleus - Ct in cytoplasm. qRT-PCR data was normalized to GAPDH. The data are shown as the mean ± SEM of at least three independent experiments. * $P \leq 0.05$, ** $P \leq 0.01$, *** $P \leq 0.001$, and **** $P \leq 0.0001$. (**E**) Tissue distribution of lncR 3/LINC00222, lncR 7-2/*Lnc-SLC12A7-4:5* (SLC12A7: solute carrier family 12 member 7) and lncR 8/*Lnc-ITM2C-1* was retrieved from online transcriptome data of total RNA from 20 human tissues by RNA sequencing (https://www.ncbi.nlm.nih.gov/gene/). Data of lncR 10/ZNF252P Antisense RNA 1(*ZNF252P-AS1*) was missing. Data are normalized by RPKM (Reads Per Kilobase of transcript per Million mapped reads).

2.2 HCV Replication Increases the Expression of Four LncRNAs

In total, 11 lncRNAs (here renamed to lncR 1-10, nine upregulated and one downregulated in response to HCV replication; whereby lncR 7 has two variants, labeled as lncR 7-1 & 2) were selected for further investigation. To our knowledge, none of them had been functionally studied to date. Changes of the transcript levels observed in HCV replicating samples versus control were verified by qRT-PCR. GAS5 (Qian et al., 2016) was used as a positive control. Two variants of lncR 7 have 70 bp difference in sequence, they were amplified separately by variant specific primers (see Table 4.1). Six candidates were discarded due to failed (lncR 5, 6) or poor amplification (lncR 1, 4, 7-1, 9), which is mainly caused by their very low expression levels. A consistent result between the data of the qRT-PCR and microarray analysis was observed for lncR 3, 7-2, and 8 (Figure 2.2 A). Samples after HCV or mock treatment without adding ectopic *miR-122* were also prepared. Similar upregulation of lncR 8 was also observed in samples without ectopic *miR-122* but only containing endogenous *miR-122* (Figure 2.2 B & C). LncR 2 expression was not altered by HCV replication, while lncR 10 was upregulated (Figure 2.2 A), showing a result opposite to the microarrays (Figure 2.1 E). In this context, it is interesting to note that lncR10 was reported to be upregulated in HCC tissues compared to adjacent non-tumor tissues in another study (Zhang et al., 2015). Concerning this possible link between HCV infection and HCC, we therefore also proceeded with lncR 10.

2.3 Low Protein Coding Potential and Subcellular Localization

ORF Finder (National Center for Biotechnology Information (NCBI)) was used to determine all possible ORFs in four candidate lncRNAs. Putative ORFs longer than 100 amino acids (aa), which was set as a noncoding threshold, were screened for the presence of Kozak sequences (A/GCCACC or A/GCC) at the initiation codon. No results indicating coding capacity for these four lncRNA candidates were obtained (Data not shown). LncR 8 was predicted as a coding gene according to CPAT (69.31%) but not interpreted as coding RNA according to PhyloCSF (-112.1426), and it was also not present in the PRIDE archive, and not in the Lee and the Bazzini coding RNA lists (Table 2.1). LncR 3, 7-2, and 10

were all described as non-coding RNA in LNCipedia, indicating a very low probability for coding (Table 2.1).

Table 2.1 Protein-coding potential of lncRNAs

Metric	lncR 3	lncR 7-2	lncR 8	lncR 10
CPAT coding probability	1.33%	10.83%	69.31%	80.45%
PhyloCSF score	-67.4569	13.6639	-112.1426	11.7381
PRIDE reprocessing 2.0	0	0	0	0
Lee translation initiation sites	0	0	0	0
Bazzini small ORFs	0	0	0	0

The table lists the results of analysis using different metrics to address the protein-coding potential of candidates from LNCipedia. 5.2 (http://www.lncipedia.org).

The preference of nuclear or cytoplasmic location can give clues for the function of a lncRNA (Morlando et al., 2015; Valadkhan and Fortes, 2018; Zhang et al., 2015). To gain insight into the potential roles of the lncRNAs, we evaluated the subcellular localization of lncRs 3, 7-2, 8, and 10 in untreated Huh-7.5 cells and Huh-7.5 cells treated with *miR-122* alone or *miR-122* plus HCV. As expected, glyceraldehyde 3-phosphate dehydrogenase (*GAPDH*) reference transcripts accumulate preferentially in the cytoplasm in treated or untreated Huh-7.5 cells (Figure 2.2 D). In contrast, more *U6* RNA was found to be in the nucleus compared to cytoplasm. The relatively high ratio of *U6* reference transcripts in the cytoplasm may be due to a leakage during nucleus/cytoplasm fractionation, which was also found in a previous study (Pessa et al., 2008). Therefore, we used *U99* RNA as an additional control; *U99* RNA was more localized in the nucleus. Importantly, lncR 8 and 10 were dominantly accumulated in the nucleus, while LncR 3 and 7-2 were found in both fractions. The nuclear enrichment of lncR 8 and 10 further confirmed their noncoding nature. No obvious difference in subcellular translocation due to the treatment with *miR-122* or with HCV was observed. Thus, the different subcellular locations of our lncRNA candidates indicate different function and regulation mechanisms. In particular, lncR 8 (which is further analyzed below) is localized in the nucleus.

Most lncRNAs are tissue-specific. According to the transcriptome results of RNA sequencing of total RNA from 20 human tissues, lncR 8 is predominantly present in brain, lncR 7 in heart, while lncR 3 was ubiquitously expressed (Figure

2.2 E). However, all lncRNAs showed very low abundance in liver, which is consistent with the relatively high CT values we detected in Huh-7.5 cells by qRT-PCR (data not shown).

2.4 LncR 8 Favors HCV Viral Replication and Infection

To evaluate the role of the lncRNAs in viral replication, we depleted lncRNAs from cells with GapmeRs (GmRs), thereby independently targeting two different sites in the respective lncRNA to largely exclude off-target effects. LNA™ longRNA GmRs are single-stranded antisense oligonucleotides that contain a central block of deoxynucleotide monomers, flanked by LNA stretches for strong target binding and nuclease resistance. The central DNA block induces RNase H mediated degradation of the target RNA and can be used for knockdown of lncRNA and mRNA in cell cultures and even in animal models (Chan et al., 2006; Lennox and Behlke, 2016). GmRs are effective at degrading both nuclear and cytoplasmic lncRNAs (Lennox and Behlke, 2016). Cells were transfected with the specific GmRs or with negative control GmR (Neg. ctr. GmR, which contains a randomized targeting sequence) one day prior to transfection with HCV RNA and collected at indicated time points. The Neg. ctr. GmR transfection serves to level out unspecific effects that may be caused by the transfected GmRs in general. To display GmR binding specificity in the genome, CLUSTAL and NBLAST analyses were done. The results show that the Neg. ctr. GmR does not bind specifically to any target in the human transcriptome, and all GmRs specific for lncRNAs used in this study are very specific for their genuine targets, except that lncR 10-GmR1 has a single off-target with only 1 nt difference (Appendix 6.1).

The suppression of targeting lncRNAs 48 h after HCV transfection was examined by qRT-PCR (Figure 2.3 A). Reference gene *GAPDH* was used for normalization. Since qRT-PCR detection of expression levels may significantly differ when targeting the 5′ or the 3′ side of the GmR target sequences (Prediger, 2016), two different sets of primers targeting both sides of lncRNA sequence were checked and compared (Data not shown). Primers amplifying 5′ side sequence of lncRs 3 and 7-2, and 3′ side primers for lncRs 8 and 10 were used to determine GmR effects in this study. Both GmRs against lncRNAs functioned efficiently (Figure 2.3 A).

HCV RNA level after lncRNA knockdown was examined by qRT-PCR. Since *GAPDH* was used for 'well-to-well' normalization within each experiment to correct for slight variations in samples, another house-keeping gene β-actin was used as a negative control gene, which is not supposed to be affected by the treatment (Figure 2.3 B). β-actin did not show changes due to treatment. Two GmRs targeting lncR 3 stimulated HCV RNA expression, but the stimulation by lncR3-GmR 1 was not statistically significant, whereas lncR3-GmR 2 significantly induced upregulation of HCV protein level (Figure 2.3 C). No change of HCV RNA levels was observed after the silencing of lncRs 7-2 and 10 (Figure 2.3 B). However, HCV protein level was upregulated in lncR 7 knockdown samples and in lncR 10-GmR 1 treated samples (Figure 2.3 C). Considering the extremely low level of lncR 7-1 in Huh-7.5 cells that was not detected by qRT-PCR in our study, the upregulated HCV protein after lncR 7 knockdown was believed to be mainly the effect of suppression of variant 2 by GmRs that target both variants. These results pointed out a negative regulation of HCV translation, but not replication, by lncR 7-2. Given the inconsistent effects caused by two GmRs targeting lncRs 3 and 10, we cannot exclude that the changes of HCV expression is caused by off-target effect of lncR3-GmR 2 and lncR 10-GmR 1. In contrast, viral RNA and viral protein were both decreased after lncR 8 suppression (Figure 2.3 B & C). Based on these results, we learned that lncR 7-2 is a negative regulator of HCV, while lncR 8 supports HCV replication. When higher concentration of lncR 8-GmR was added in cells, HCV RNA expression showed a stronger decrease, further confirming a correlation between lncR 8 level and HCV replication level (Figure 2.3D). Therefore, lncR 8 is required for efficient HCV replication. Accordingly, we further focused on lncR 8 in the following.

To understand the function of lncR 8 in real HCV infection, HCV infectious particles were prepared and used to infect Huh-7.5 cells at MOI of 0.3 for 12 h, 24 h, 2 d, and 6 d. lncR 8 was upregulated by HCV infection (Figure 2.4 B). In cells first treated with GmR for 24 h and then infected with HCV for 48 h, lncR 8 was decreased by GmRs, and HCV viral genome abundance and virus titer were decreased (Figure 2.4 C, D, & E).

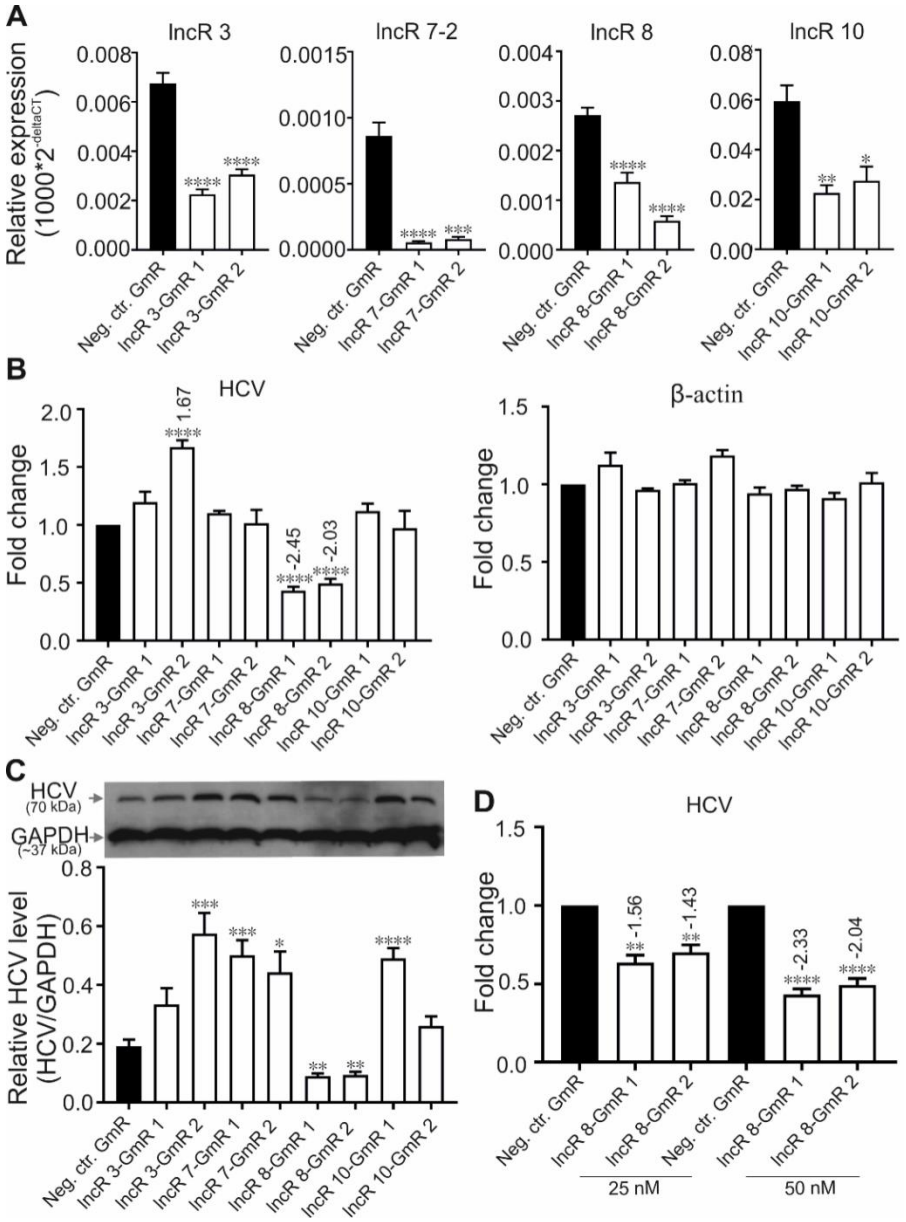

Figure 2.3 Suppression of lncR 8 inhibits HCV replication. (**A**) The efficiency of GmRs suppressing lncRs 3, 7-2, 8, and 10 was determined by qRT-PCR in Huh-7.5 cells. One day prior to HCV treatment, GmRs targeting lncRNA candidates and Neg. ctr. GmR were transfected in Huh-7.5 cells. Cells were collected at 48 h post HCV transfection. HCV RNA and protein level after GmR treatment were detected by qRT-PCR (**B**) and western blotting (**C**). HCV RNA level after different concentration of lncR 8-GmR treatment was detected by qRT-PCR (**D**). qRT-PCR data of targeted genes was normalized to *GAPDH*. Another housekeeping gene β-actin was used as a negative control. Altered HCV level with significance are marked with numbers at the top of the bar. The numbers indicate fold changes of HCV RNA expression after GmRs treatment, where positive numbers mean upregulation, negative numbers mean downregulation. The upper panel in (**C**) is representative western blot of HCV NS3 protein. The lower panel is the quantification of protein bands from western blot was performed by using Image J (NIH). IntDen ratio of each NS3 band relative to each GAPDH band was presented. The data are shown as the mean ± SEM of at least three independent experiments.* $p \leq 0.05$, ** $p \leq 0.01$, *** $p \leq 0.001$, and **** $p \leq 0.0001$.

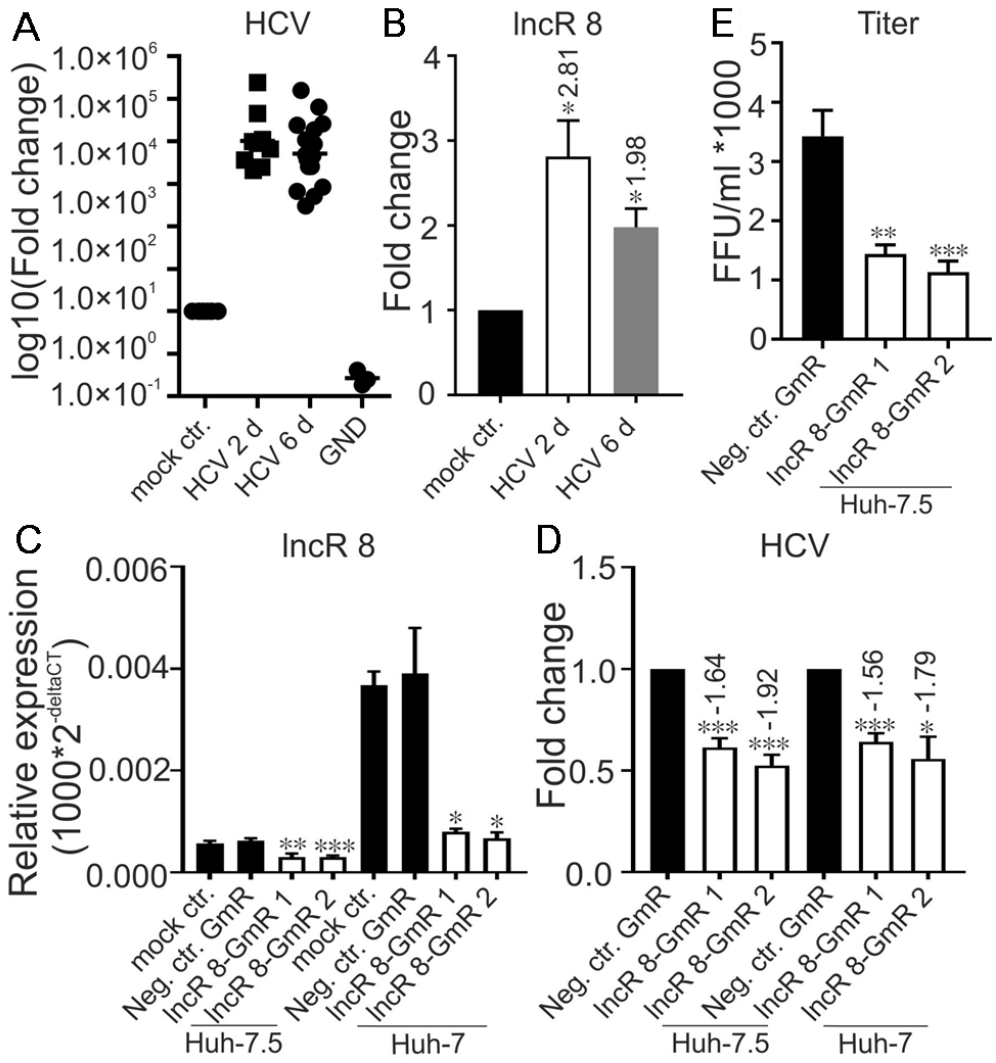

Figure 2.4 LncR 8 is upregulated by HCV infection in Huh-7.5 cells and suppression of lncR 8 inhibits HCV infection in both Huh-7.5 and Huh-7 cells. The expression of HCV (**A**), and lncR 8 (**B**) were confirmed by qRT-PCR at 2 or 6 days post HCV infection. NS3 level was also tested in cells infected with a replication defective mutant version of the HCV genome (NS5B replicase inactivating "GND" mutation). The efficiency of GmRs suppressing lncR 8 was determined by qRT-PCR in Huh-7.5 and Huh-7 cells (**C**). One day prior to HCV infection, GmRs targeting lncRNA candidates and Neg. ctr. GmR were transfected in cells. Cells treated with mock ctr. (without GmRs) were also detected to show that no unspecific influence was induced by Neg. ctr. GmR on lncR 8. Cells were collected at 48 h post HCV infection. HCV RNA and virus titer after GmR treatment were detected by qRT-PCR (**D**) and fluorescent focus assay (FFA)(**E**). qRT-PCR data of targeted genes was normalized to *GAPDH*. Fold changes of mRNA expression comparing to control cells are indicated at the top of each bar when statistically significant. Experiments were repeated a minimum of three times, with at least two replicates each time, and are represented as mean ± SEM. * $p \leq 0.05$, ** $p \leq 0.01$, *** $p \leq 0.001$, and **** $p \leq 0.0001$.

2.5 LncR 8 may be a Non-polyadenylated RNA

LncR 8 was chosen for further study. We first determined that lncR 8 is a transcript without poly(A) tail. Considering cDNA synthesized by using Oligo(dT) also generates cDNA through internal poly(A) sequence (Nam et al., 2002), non-polyadenylated genes can also be amplified from Oligo(dT)-reverse transcribed cDNA. LncR 10 and GAS5, known to have poly(A) tail, were used as positive control genes. Lower or similar 30-ΔCt value was observed for lncR 10 and GAS5 when using random primer instead of oligo-dT for reverse transcription (Figure 2.5 A). Thus, slightly higher 30-ΔCt value observed in samples using random primer for reverse transcription compared to the samples using oligo-dT may be an indicator for non-polyadenylation of lncR 8 (Figure 2.5 A). This phenomenon was maintained in both *miR-122* and *miR-122* plus HCV treated samples.

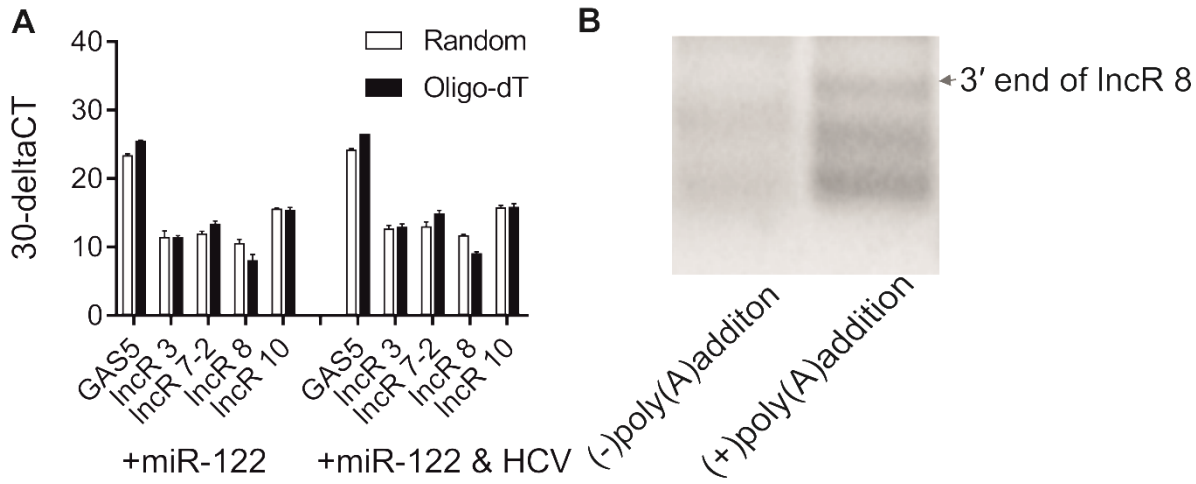

Figure 2.5 LncR 8 may be a non-polyadenylated RNA. (**A**) The 30-ΔCt of GAS5, lncR 3, 7-2, 8 and 10 were examined by qRT-PCR both in Oligo(dT)- and random primer - reverse transcribed cDNA using samples after 6 days of *miR-122* only or *miR-122* plus HCV transfection. (**B**) The agarose gel image of products from the 3′ RACE 2nd round PCR using cDNA template which was reverse transcribed from RNA with or without poly(A) tail addition. RACE: rapid amplification of cDNA ends.

Accordingly, the transcripts of lncR 3 and lncR 7-2 may contain poly(A) tails. The agarose gel image also showed that the 3′ end sequence of lncR 8 is absent from the 3′ rapid amplification of cDNA ends (RACE) 2nd round PCR using a cDNA template which was reverse transcribed from RNA without

poly(A) tail addition (Figure 2.5 B). RACE experiments extended sequences of both 3′ and 5′ end of lncR 8 in addition to sequence from the RefSeq database (NR_038238.1), 5′-GAACCATTTGAGCTTTGAAGGTG-3′ to the 5′ end and 5′-CTCAGTCTGCAGTGTTTTATTATGGCAGCTCAGGTAGACTGACAA-3′ to the 3′end, making it 1961 bp long (Appendix 6.2). Sequence alignment showed that lncR 3 and lncR 8 were conserved among primates (Data not shown). In contrast, low conservation was observed in lncR 7-2 and lncR 10, since ortholog sequence of human lncR 10 was only found in *Pan troglodytes*, while no ortholog sequence was found for human lncR 7-2.

2.6 LncR 8 is a Short-Term *Cis*-Acting Regulator of Its Neighbor *GPR55*

Previous studies showed that lncRNAs can regulate neighboring genes (Kopp and Mendell, 2018). The genes for Integral Membrane Protein 2C (*ITM2C*) and G protein-coupled receptor 55 (*GPR55*) are within 10 kb distance of lncR 8 in the genome (Figure 2.6 A). To gain further insight into the regulatory mechanism of lncR 8 during HCV replication, we evaluated the expression of neighboring genes at 6 days after HCV RNA transfection as well as 2 days after lncR 8 suppression in Huh-7.5 cells. Though *ITM2C* was identified with high expression level in HCV-induced HCC tissues compared to HCV-induced HCC non-tumor liver tissues (Hu and Gao, 2012), we found only a very mild increase of *ITM2C* induced by HCV replication in Huh-7.5 cells (Figure 2.6 B). Furthermore, no change of *ITM2C* mRNA levels was observed after lncR 8 knockdown (Figure 2.6 C). This rules out a *cis*-regulatory activity of lncR 8 on *ITM2C* during HCV replication.

The mRNA expression of the other neighboring gene *GPR55* was not significantly altered after 6 days of HCV replication (Figure 2.6 B). Similar results were observed when cells are treated without ectopically added *miR-122* (Figure 2.6 C). HCV triggered lncR 8 expression but did not change *GPR55* expression after 6 days, on first glance arguing against a correlation between lncR 8 and *GPR55*. However, lncR 8 knockdown suppressed *GPR55* expression at 48 h post GmR and HCV treatment in Huh-7.5 cells (Figure 2.6 D). In addition, samples obtained after lncR 8-GmRs treatment and further HCV transfection for 12 h and 24 h were examined. Downregulation of *GPR55* mRNA levels was also

observed at these early time points when lncR 8 was suppressed efficiently (Figure 2.6 E & F), while HCV RNA level was not changed (Figure 2.6 G).

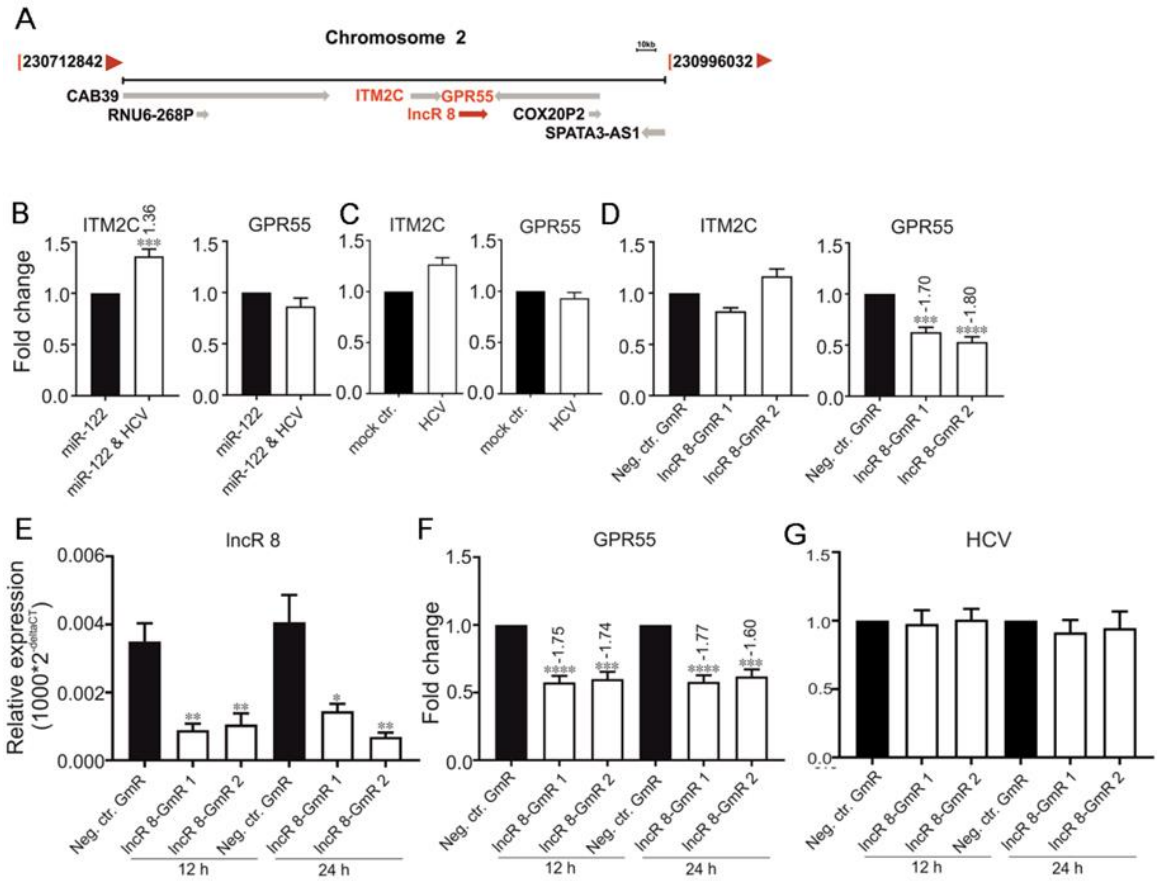

Figure 2.6 LncR 8 positively regulates neighboring gene *GPR55*. (**A**) Genomic location of lncR 8 and the relationship with the genes encoding *ITM2C* (Integral Membrane Protein 2C) and *GPR55* (G protein-coupled receptor 55). (**B**) *ITM2C* and *GPR55* expression in HCV-transfected samples and controls was measured 6 days after transfection and compared. Cells were treated as described in Figure 2.1. (**C**) *ITM2C* and *GPR55* expression in HCV-transfected cells with same treatment but without ectopically added *miR-122* was also measured. (**D**) *ITM2C* and *GPR55* expression level at 2 days after lncR 8-GmRs and HCV transfection was measured**.** The knockdown of lncR 8 (**E**), the effect on neighboring gene *GPR55* (**F**) and HCV RNA (**G**) were examined at earlier time points by qRT-PCR. Huh-7.5 cells were treated with Neg. ctr. GmR and lncR8-GmRs one day prior to HCV transfection. Cells were collected at indicated time points post HCV transfection. To illustrate the differences in basal expression levels, the values of lncR 8 expression level are shown relative to *GAPDH*, expressed as $2^{-\Delta Ct}$. qRT-PCR data was normalized to *GAPDH*. The data are shown as the mean ± SEM of at least three independent experiments. * $p \leq 0.05$, ** $p \leq 0.01$, *** $p \leq 0.001$, and **** $p \leq 0.0001$.

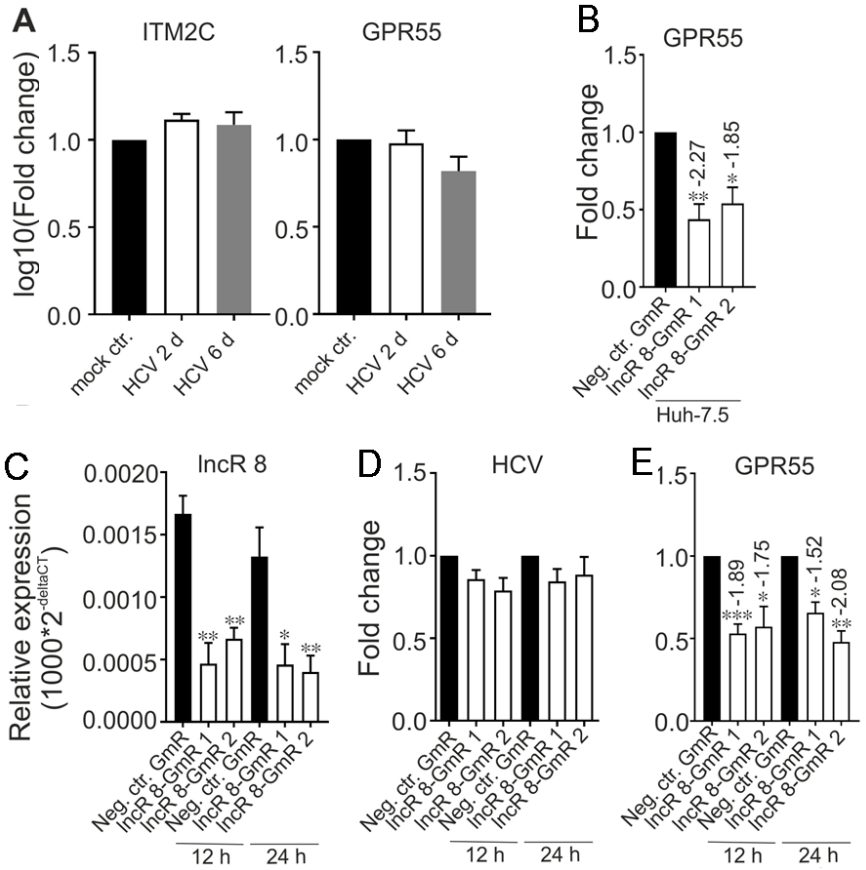

Figure 2.7 Suppression of lncR 8 inhibits *GPR55* expression in HCV infected cells. The expression of neighboring genes (**A**) was confirmed by qRT-PCR at 2 or 6 days post HCV infection. *GPR55* (**B**) expression after GmR-lncR 8 treatment in HCV infected Huh-7.5 cells was detected by qRT-PCR. One day prior to HCV infection, GmRs targeting lncRNA candidates and Neg. ctr. GmR were transfected in Huh-7.5 cells. Cells were collected at 48 h post HCV infection. Cells from earlier time points were also collected (12 h and 24 h). The efficiency of GmRs suppressing lncR 8 (**C**) was determined by qRT-PCR in Huh-7.5 cells. HCV RNA (**D**) and *GPR55* (**E**) after GmR treatment were detected by qRT-PCR. qRT-PCR data of targeted genes was normalized to *GAPDH*. Altered mRNA expressions with significance are marked with numbers at the top of the bar. The numbers indicate fold changes of expression after GmRs treatment, where positive numbers mean upregulation, negative numbers mean downregulation. The data are shown as the mean ± SEM of at least three independent experiments. * $p \leq 0.05$, ** $p \leq 0.01$, and *** $p \leq 0.001$.

These data strongly indicate a positive regulation of *GPR55* by lncR 8 in HCV transfected cells. Considering the different time length in the experimental settings, we hypothesize that lncR 8 controls *GPR55* at early times (12, 24, 48 h), while at late times (6 d) the effect of lncR 8 on *GPR55* expression may be counteracted by other mechanisms. Taken together, the positive effect of lncR 8

on *GPR55* by *cis*-regulation may act only within a short time period after HCV replication.

Similar to the results observed when cells were transfected with HCV *in vitro* transcribed RNA (Figure 2.6 B, D & F), both *ITM2C* and *GPR55* mRNA level were not changed at 2 d and 6 d post HCV infection (Figure 2.7 A), and *GPR55* was downregulated by lncR 8 knockdown at all the time points we tested (Figure 2.7 B & E), similar to what we observed when cells were transfected with HCV RNA (Figure 2.6 D & F). The downregulation of HCV RNA only occurred at 48 h (Figure 2.4 D & 2.7 D), while the upregulation of *GPR55* expression was observed early at 12 h post GmR treatment and HCV infection (Figure 2.7 E), indicating that the downregulation on *GPR55* expression by lncR 8 silence happened earlier than the downregulation on HCV infection.

2.7 LncR 8 is a Negative regulator of the Antiviral Response

Several lncRNAs were proven to affect HCV replication by regulating the interferon response (Barriocanal et al., 2014; Carnero et al., 2016; Huang et al., 2018; Kambara et al., 2014; Nishitsujia et al., 2016; Ouyang et al., 2014). To investigate this possibility for lncR 8, we examined the expression levels of four ISGs, *CXCL10*, *ISG15*, *Mx1*, and *IFITM1*, which are involved in immune responses against HCV (Valadkhan and Fortes, 2018). In accordance with previous studies, these four ISGs showed increased expression levels after 6 days of HCV replication in the presence of endogenous plus ectopically added *miR-122* (Figure 2.8 A) or without ectopically added but only with endogenous *miR-122* in the Huh-7.5 cells (Figure 2.8 B), showing a successfully induced immune response after HCV replication in Huh-7.5 cells. Furthermore, 48 h post HCV transfection followed by lncR 8 silencing for 24 h in Huh-7.5 cells, significant increases of ISG levels compared to control cells were also observed (Figure 2.8 C), except for *CXCL10* when lncR 8-GmR 1 was used. This indicates that lncR 8 is a negative regulator of ISGs.

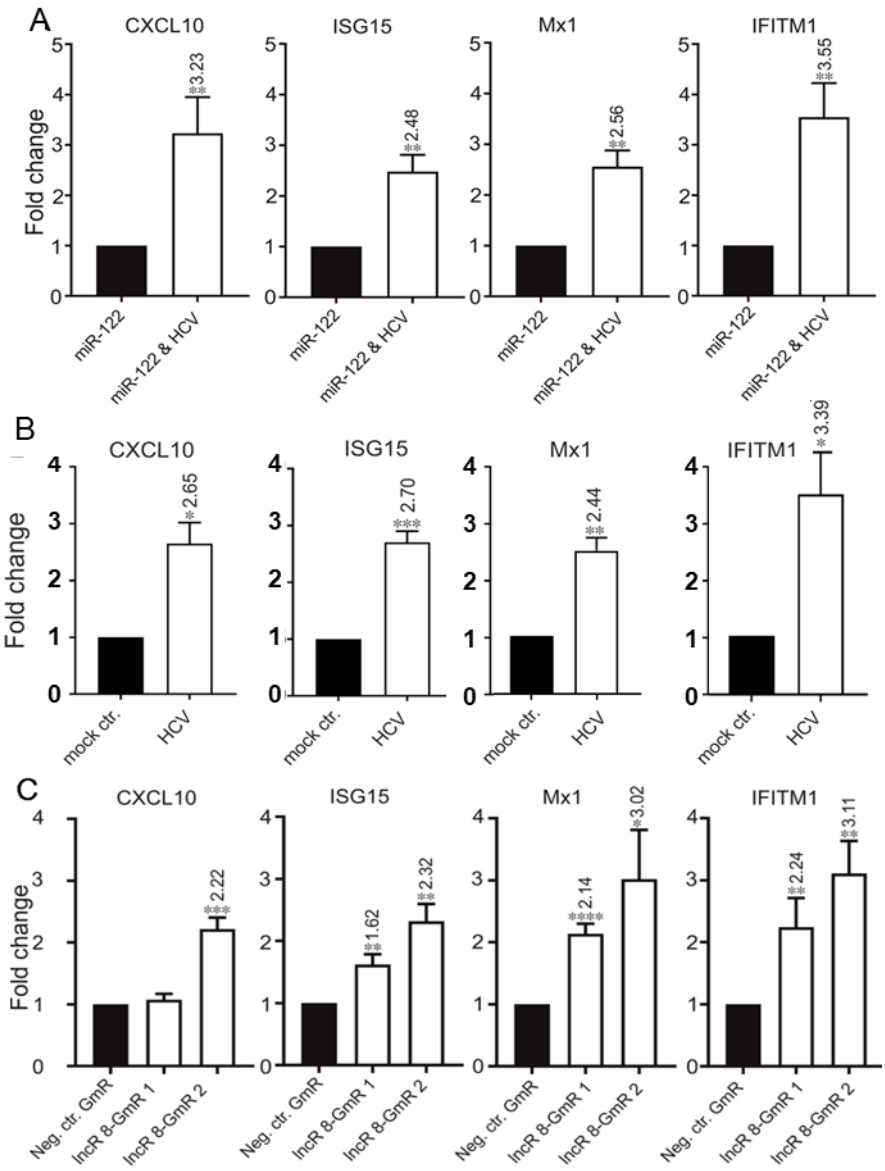

Figure 2.8 LncR 8 negatively regulates ISGs expression. (**A**) Indicated ISGs expression in samples treated as described in Figure 2.1 were measured 6 days after HCV transfection**.** (**B**) Indicated ISGs expression were also measured in samples treated as described in Figure 2.1 but without ectopically added *miR-122* 6 days post HCV transfection**.** (**C**) ISGs expression level at 48 h after GmRs and HCV transfection were measured**.** Cells were treated in the same condition as described in Figure 2.3 A. qRT-PCR data was normalized to *GAPDH*. The data are shown as the mean ± SEM of at least three independent experiments. * $p \leq 0.05$, ** $p \leq 0.01$, *** $p \leq 0.001$, and **** $p \leq 0.0001$.

In addition, following 24 h of lncR 8-GmR incubation, samples were obtained at 12 and 24 h post HCV transfection. Under these conditions, ISGs, except for *CXCL10*, were upregulated by lncR 8 silencing (Figure 2.9), while HCV RNA level was not altered (Figure 2.6 G). Since *GAPDH* was used for data

normalization, an additional house-keeping gene (β-actin) was used as a negative control target, which was not changed due to lncR 8-GmR treatment compared to negative control cells (Appendix 6.3)**.** These results show that the upregulation of ISGs expression by lncR 8 suppression occurs earlier than the decrease of HCV RNA levels. Taken together, our data indicate that the suppression of HCV may be the result of ISGs′ increase induced by lncR 8 knockdown.

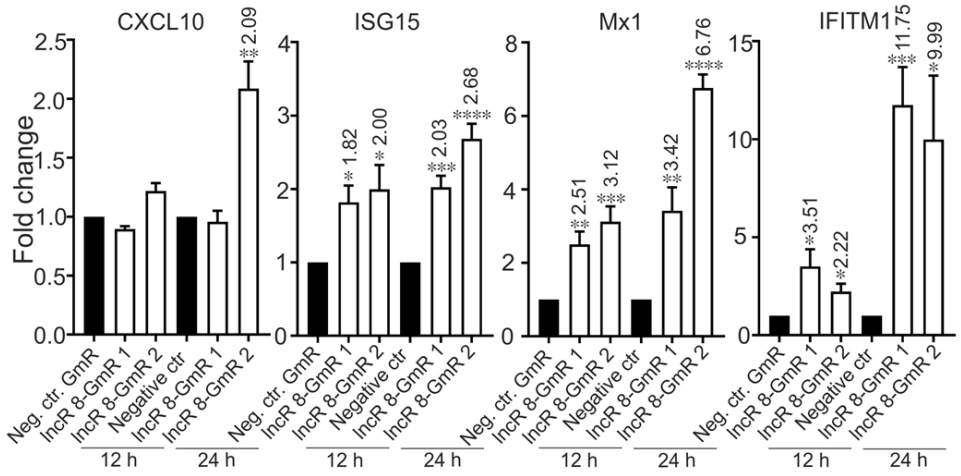

Figure 2.9 Regulation of ISGs by lncR 8 is earlier than regulation of HCV in HCV transfected cells. ISGs expression level at early time points (12 h and 24 h) were examined by qRT-PCR in the samples described in Figure 2.6. *GAPDH* was used to normalize. The data are shown as the mean ± SEM of at least three independent experiments. * $p \leq 0.05$, ** $p \leq 0.01$, *** $p \leq 0.001$, and **** $p \leq 0.0001$.

Furthermore, *IFN-β* was not changed due to HCV infection, while another type I IFN, *IFN-α*, and type III IFN, interleukin-28 isoform A (*IL28A*), were upregulated at 2 d and 6 d post infection (Figure 2.10 B). *ISG15* and *IFITM1* were upregulated at 6 d post HCV infection (Figure 2.10 C), similar to that we observed after HCV RNA transfection (Figure 2.8 A & B). At earlier time, *IFITM1* expression level was also increased due to HCV infection, while *CXCL10* was only induced at 12 h post HCV infection, and *Mx1* was downregulated after HCV infection for 12 h, 24 h, and 2 d but increased only after 6 d.

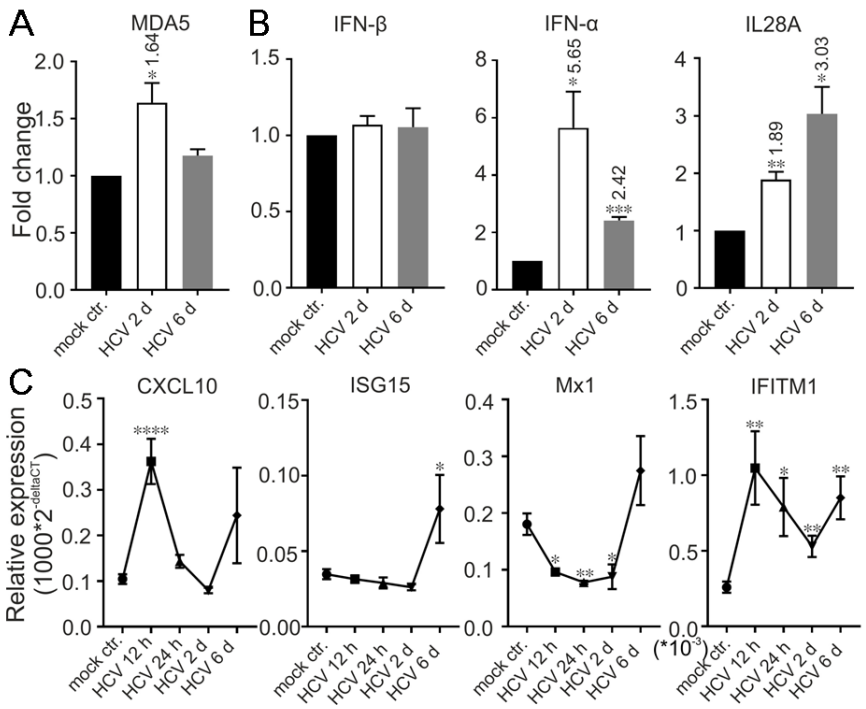

Figure 2.10 *ISG15* and *IFITM1* are upregulated by HCV infection. The expression of *MDA5* (A) and indicated IFNs (B) were confirmed by qRT-PCR at 2 or 6 days post HCV infection. Expression of ISGs (C) was also detected at earlier time points post HCV infection. Data were normalized to *GAPDH*. Fold changes of mRNA expression comparing HCV infected cells to control cells are indicated at the top of each bar when statistically significant. Experiments were repeated a minimum of three times, with at least two replicates each time, and are represented as mean ± SEM. * $p \leq 0.05$, ** $p \leq 0.01$, *** $p \leq 0.001$, and **** $p \leq 0.0001$.

In cells first treated with GmR for 24 h and then infected with HCV for 48 h, representative ISGs were upregulated in HCV infected cells with lncR8-GmR treatment compared to negative control (Figure 2.11 C). Similar upregulation of ISGs by lncR 8 knockdown were also observed in Huh-7 cells (Figure 2.11 C). Similar to the results observed when treated with HCV *in vitro* transcribed RNA (Figure 2.9), the upregulation of ISGs expression was observed early at 12 h post GmR treatment and HCV infection (Figure 2.11 E), while the downregulation of HCV RNA only occurred at 48 h (Figure 2.4 D & 2.7 D), indicating that the downregulation on ISGs expression by lncR 8 happened earlier than the downregulation on HCV infection (similar as after HCV RNA transfection).

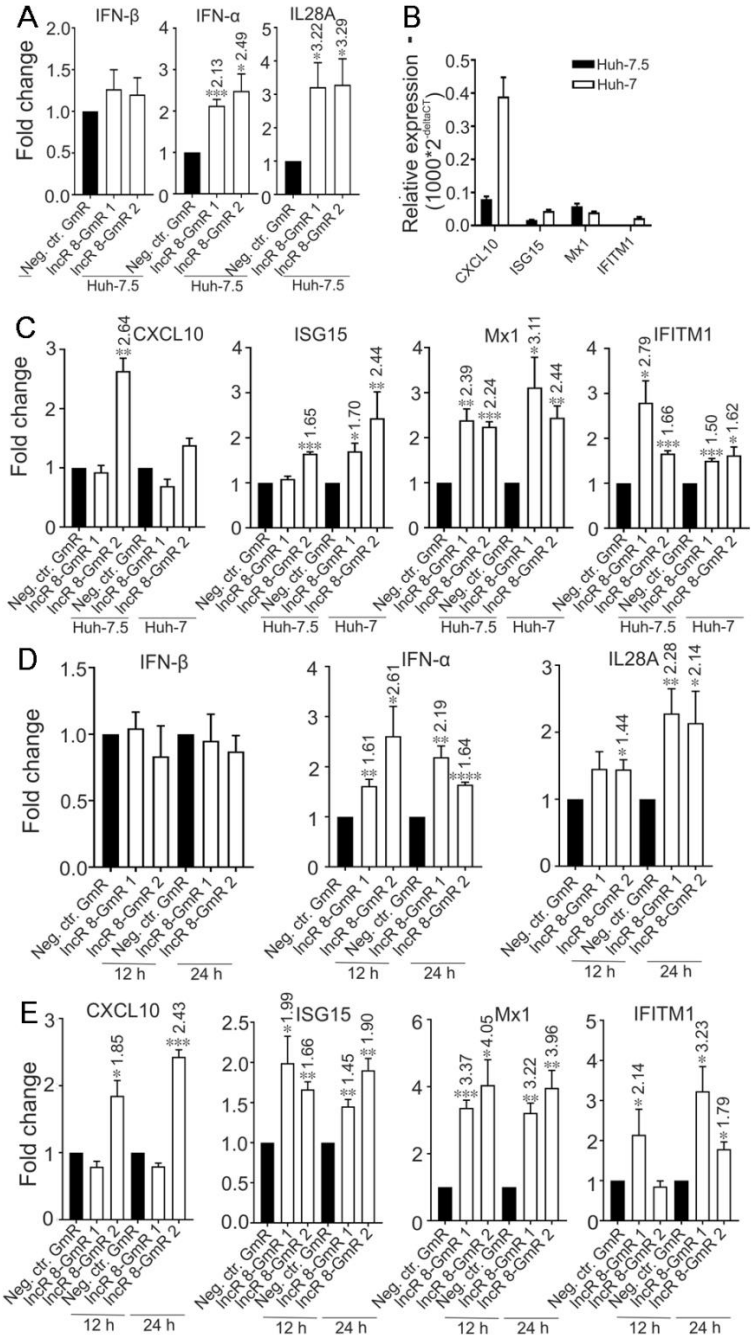

Figure 2.11 Suppression of lncR 8 promotes ISGs expression in HCV infected Huh-7.5 cells. IFNs (**A**) and ISGs (**C**) expression after GmR treatment were detected by qRT-PCR. Basal relative expression level of ISGs expression in Huh-7.5 and Huh-7 cells was shown in (**B**). One day prior to HCV treatment, GmRs targeting lncRNA candidates and Neg. ctr. GmR were transfected in cells. Cells were collected at 48 h post HCV infection. At 12 h and 24 h post HCV infection, indicated IFNs (**D**) and ISGs (**E**) after GmR treatment were also detected by qRT-PCR. qRT-PCR data of targeted genes was normalized to *GAPDH*. Altered mRNA expressions with significance are marked with numbers at the top of the bar. The numbers indicate fold changes of expression after GmRs treatment, where positive numbers mean upregulation, negative numbers mean downregulation. The data are shown as the mean ± SEM of at least three independent experiments. * $p \leq 0.05$, ** $p \leq 0.01$, and *** $p \leq 0.001$.

Though *IFN-β* was not influenced by lncR 8 change at the time points we tested, both *IFN-α* and *IL28A* were upregulated by lncR 8 inhibition in Huh-7.5 cells (Figure 2.11 A & D). Taken together, lncR 8 is positively regulated by HCV and has a role in stimulating HCV replication by suppression of interferon responses.

2.8 *GPR55* Negatively Regulates ISGs

Since both *GPR55* and ISGs are negatively regulated by lncR 8, it is interesting to know whether there is a correlation between *GPR55* and ISG expression. Therefore, *GPR55* expression was inhibited by two different GmRs in Huh-7.5 cells for 48 h. Suppression of *GPR55* promotes the expression of *ISG15*, *Mx1*, and *IFITM1* (Figure 2.12). This finding provides a possible link between lncR 8 and ISGs expression, suggesting that ISG suppression after lncR 8 induction may be mediated by GPR55.

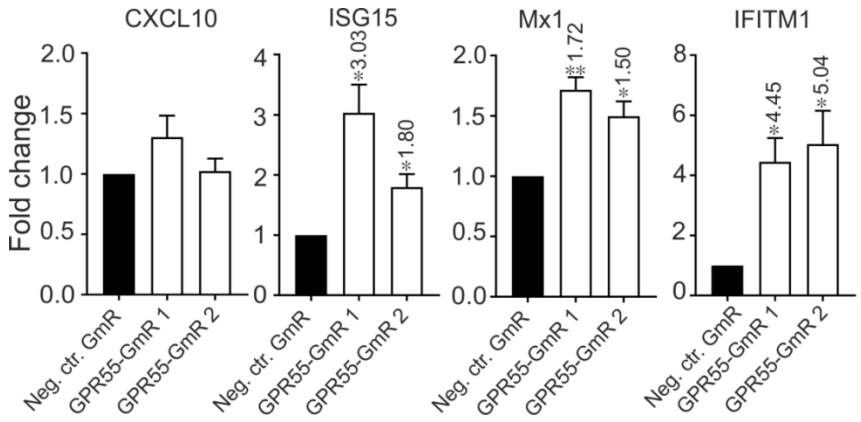

Figure 2.12 Suppression of *GPR55* promotes several ISGs expression. Two GmRs targeting *GPR55* and Neg. ctr. GmR were transfected in Huh-7.5 cells. Cells were collected at 48 h later and ISGs expression was measured by qRT-PCR. qRT-PCR data was normalized to *GAPDH*. The data are shown as the mean ± SEM of at least three independent experiments. * $p \leq 0.05$ and ** $p \leq 0.01$. Altered mRNA level with significance are marked with numbers at the top of the bar. The numbers indicate fold changes of mRNA expression after GmRs treatment.

2.9 LncR 8 is Induced by poly(I:C)

Poly(I:C) is a synthetic analog of double-stranded RNA (dsRNA), a molecular pattern associated with viral infection that induces the innate immune

response. Thus, poly(I:C) can be used to distinguish between virus-specific and unspecific effects of a treatment which are just due to elevated amounts of foreign nucleic acids in the cell.

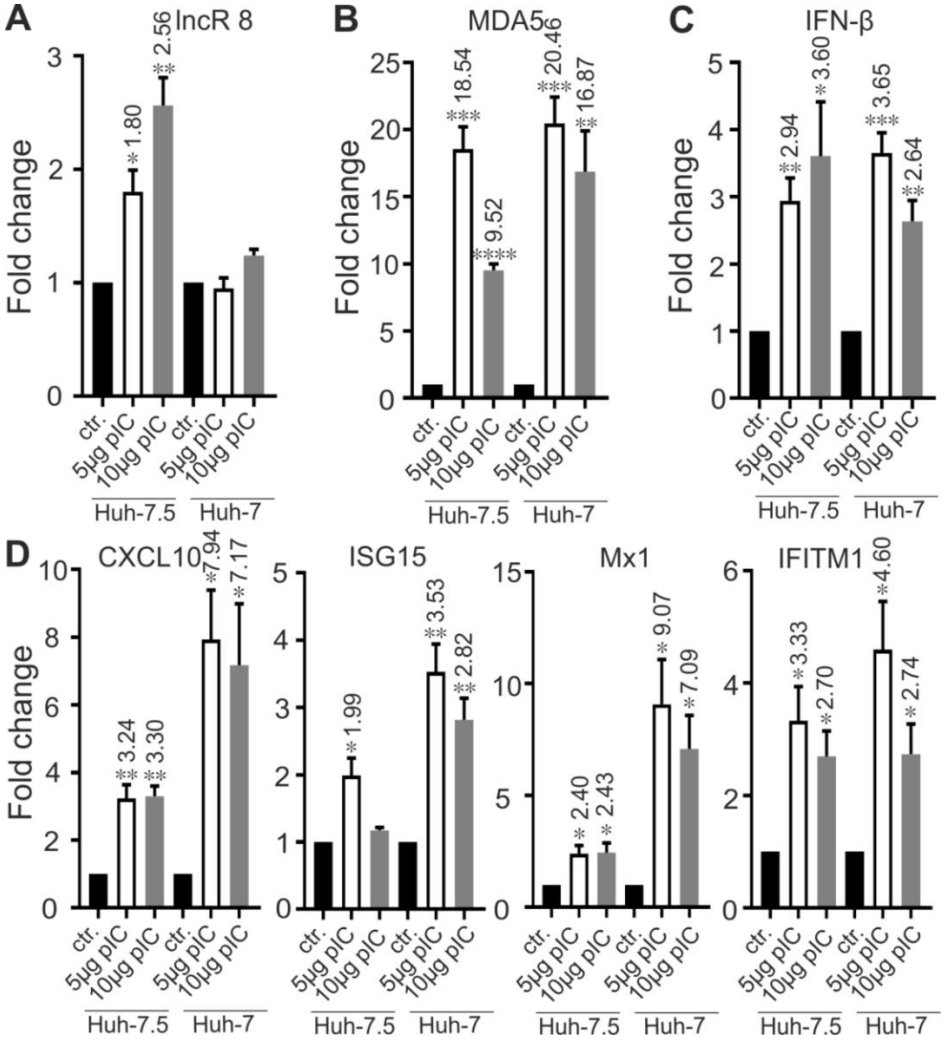

Figure 2.13 LncR 8 is efficiently induced by poly(I:C) treatment in Huh-7.5 cells but not in Huh-7 cells. Cells were treated with 5ug or 10 ug poly(I:C) and collected after 8 h incubation. qRT-PCR data of targeting genes, including lncR 8, *MDA5*, *IFN-β* and ISGs, was normalized to *GAPDH*. The data are shown as the mean ± SEM of at least three independent experiments. * $p \leq 0.05$, ** $p \leq 0.01$, *** $p \leq 0.001$, and **** $p \leq 0.0001$. Altered mRNA level with significance are marked with numbers at the top of the bar. The numbers indicate fold changes of mRNA expression after treatment, where positive numbers mean upregulation, negative numbers mean downregulation.

When poly(I:C) was used to treat Huh-7.5 and Huh-7 cells, increasing expression level of ISGs were observed in both cells. LncR 8 was upregulated in

Huh-7.5 cells (Figure 2.13 A), which suggests that lncR 8 can also be induced by PAMPs independently of HCV. However, lncR 8 was not changed after poly(I:C) treatment in Huh-7 cells (Figure 2.13 A), indicating different responses in these two cells. Poly(I:C) is known to trigger *MDA5*-mediated interferon signaling (Cao et al., 2015). Given that Huh-7.5 cells have deficient RIG-I and TLR3, PKR can also be considered to be the sensor for poly(I:C) in Huh-7.5 cells. *MDA5* and *IFN-β* showed upregulation both in Huh-7.5 and Huh-7 cells treated with poly(I:C) (Figure 2.13 B & C), while PKR was only upregulated in Huh-7.5 cells after poly(I:C) treatment (Data not shown). Relatively lower levels of ISGs were induced by poly(I:C) treatment in Huh-7.5 cells compared to that in Huh-7 cells (Figure 2.13 D), which is consistent with the similar level of ISGs expression increase in HCV infected Huh-7.5 cells and also consistent with the nature of Huh-7.5 cells with higher permissiveness for HCV replication compared with Huh-7 cells, and also consistent with the trigger of lncR 8 only in Huh-7.5 cells.

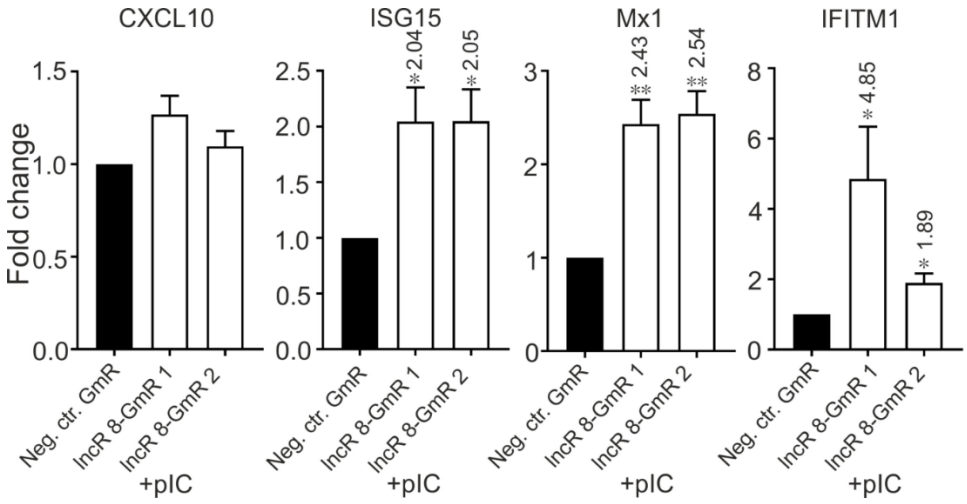

Figure 2.14 Knockdown of lncR 8 upregulates representative ISGs after poly(I:C) treatment. One day prior to poly(I:C) treatment, GmRs targeting lncR 8 and Neg. ctr. were transfected in Huh-7.5 cells. Cells were treated with 5 μg poly(I:C) and collected after 8 h incubation. qRT-PCR data of ISGs was normalized to *GAPDH*. Altered mRNA level with significance are marked with numbers at the top of the bar. The numbers indicate fold changes of mRNA expression after treatment, where positive numbers mean upregulation, negative numbers mean downregulation. The data are shown as the mean ± SEM of at least three independent experiments. * $p \leq 0.05$ and ** $p \leq 0.01$.

Importantly, when Huh-7.5 cells were treated with poly(I:C) in combination with lncR 8 GmRs for lncR 8 knockdown for 8 h, the ISGs showed further increased expression level even compared with control cells with only poly(I:C) treatment (Figure 2.14). This shows that lncR 8 negatively regulates representative ISGs expression even when poly(I:C) was used instead of HCV, demonstrating the specific suppression of ISGs by lncR 8 independent of their unspecific induction by poly(I:C).

2.10 LncR 8 is Downregulated by JAK/STAT Pathway

To learn whether lncR8 is an ISG which can be induced by IFN-α like other known lncRNAs, Huh-7.5 cells were treated with IFN-α and collected after 8 h. qRT-PCR results show that lncR 8 was negatively regulated by IFN-α (Figure 2.15 A).

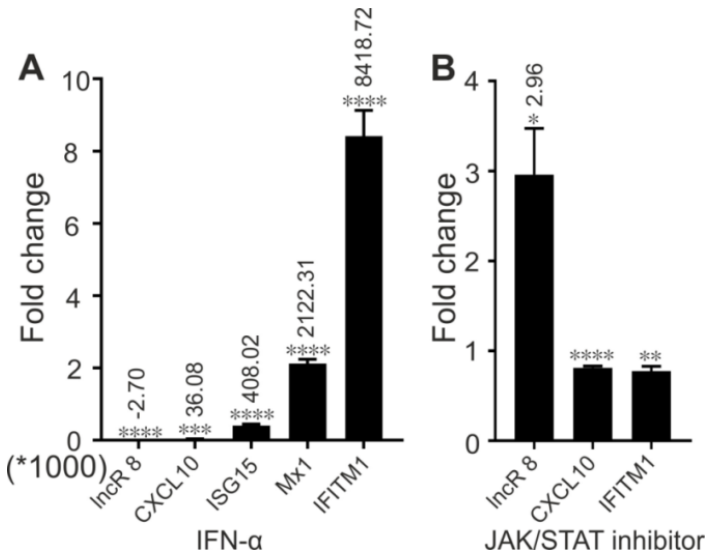

Figure 2.15 IFN treatment depresses lncR 8 through JAK/STAT pathway. Cells were treated with either mock or IFN-α, and collected after 8 h incubation (**A**). For JAK/STAT inhibition, JAK/STAT inhibitor or mock was added 1 h before IFN treatment (**B**). qRT-PCR data of targeting genes was normalized to *GAPDH*. The data are shown as the mean ± SEM of at least three independent experiments. * $p \leq 0.05$, ** $p \leq 0.01$, *** $p \leq 0.001$, and **** $p \leq 0.0001$. Altered mRNA level with significance are marked with numbers at the top of the bar. The numbers indicate fold changes of mRNA expression after treatment, where positive numbers mean upregulation, negative numbers mean downregulation.

To determine whether the negative regulation of lncR 8 by IFN-α is

dependent on JAK-STAT pathway, we treated the Huh-7.5 cells with or without the JAK inhibitor, ruxolitinib, followed by IFN-α treatment. Increased lncR 8 expression was observed when ruxolitinib was added (Figure 2.15 B), indicating that lncR 8 is not an ISG, but lncR 8 is negatively regulated by the immune response through the JAK-STAT signaling pathway.

In summary, the above results indicate that:
1. HCV induces lncR 8 and lncR 8 favors HCV replication.
2. LncR 8 induces *GPR55* expression at early time points after HCV infection.
3. HCV triggers antiviral innate immune responses. LncR 8 and *GPR55* repress ISG expression earlier than HCV expression change.
4. LncR 8 is not specifically induced by HCV, it can also be triggered by poly(I:C).
5. LncR 8 is negatively regulated by IFN-α through the JAK-STAT signaling pathway.

3. Discussion

3.1 Identification of LncRNAs Deregulated by HCV Replication

Next generation sequencing (NGS) results of cDNA library we prepared in this study were largely divergent between two independent samples (Data not shown).By using microarray assays, 68 transcripts showed altered expression level upon HCV treatment in Huh-7.5 cells (log fold change > 2, $\log_{10}$P value > 2) (Figure 2.1 D). Compared to the lncRNAs identified in the study of Carnero and coworkers (Carnero et al., 2016), the number we obtained is much lower. Surprisingly, among the 68 altered candidates, no overlapping genes were found between these two studies (Carnero et al., 2016) (Figure 2.1 F & G).

It is reasonable to consider that the different experimental conditions in these two studies are the major reason for this difference. Consistent with other previous studies, the coding genes we identified as HCV-upregulated (Figure 2.1 G), like wingless-type MMTV integration site family member 10A (*WNT10A*), dual specificity phosphatase and pro isomerase domain containing 1 (*DUPD1*), and fibroblast growth factor 21 (*FGF21*), were previously described to be upregulated by HCV (Ahmad et al., 2012; Kukla et al., 2012; Liu et al., 2011). Phosphatidylinositol-4-phosphate 3-kinase catalytic subunit type 2 gamma (*PIK3C2G*) is required for HCV replication (Berger et al., 2009). Downregulated leukocyte cell-derived chemotaxin 2 (*LECT2*) is a direct target of Wnt/β-catenin signaling in HCC and could be a potential biomarker of HCC in patients (Okabe et al., 2014; Ovejero et al., 2004). Thus, our findings of most coding genes we identified conform with previous studies. In contrast, not in line with previous data and also not consistent with our qRT-PCR results (Valadkhan and Fortes, 2018), ISGs *CXCL10*, *ISG15*, *Mx1*, and *IFITM1* were not found to be deregulated in the microarrays. *MDA5*, which is the main sensor in *RIG-I* defective Huh-7.5 cells (Cao et al., 2015), was not detected to be differentially regulated in the microarrays (data not shown). Known lncRNAs like GAS5 and EGOT did not show changes due to HCV replication, which is in contrast to previous studies (Carnero et al., 2016; Qian et al., 2016). In another study, only 7 of the 60 lncRNAs show statistically significant correlation between the results of the RT-qPCR and microarray analysis (Nishitsujia et al., 2016).

In addition to the different experimental settings, the discrepancy between our microarray results with previous studies and our qRT-PCR results can be caused by several other factors. In the first place, low abundancies of lncRNAs could cause high variance of sequencing results (Barriocanal et al., 2014). Perhaps even more importantly, low reproducibility of microarray results can occur when experiments are performed by different laboratories, or in the same laboratory but not in a close time period (Jaksik et al., 2015). Adequate number of biological replicates is needed to exclude major sources of variances and exert reliable biological effects (Chen et al., 2007; Jaksik et al., 2015; Stretch et al., 2013). These factors may also be the major reasons leading to failed NGS. Except for what mentioned above, different sequencing methods could also lead to largely different results, like the candidates that were successfully obtained by NGS in our recently published paper (Gerresheim et al., 2019), which I contributed to the initial sample preparation.

3.2 HCV Replication Increases the Expression of Four LncRNAs

Nevertheless, four lncRNA candidates identified by microarray assays, lncRs 3, 7-2, 8, and 10, were verified by qRT-PCR to be HCV-upregulated lncRNAs (Figure 2.2 A). We performed knockdown of lncRNAs to address their effect on HCV replication. Suppressing lncRs 3, 7-2, and 10 did not change the expression of the HCV RNA genome, except that lncR 3-GmR 2 induced a moderately increased level of HCV RNA (Figure 2.3 B). Upregulation of HCV protein expression was observed after knockdown of lncR 7 by two GmRs (Figure 2.3 C). These results pointed out an antiviral role of lncR 7-2 by negatively regulating HCV translation, but not replication. In addition, the presence of lncR 7-2 in both nucleus and cytoplasm fractionation (Figure 2.2 D) indicates that lncR 7-2 may regulate mRNA stability or translation, protein transport or post-translational modifications, in addition to regulation of nuclear events (Morlando et al., 2015; Zhang et al., 2015). Previously, lncR 7-2 was reported to be a direct target of Notch and was positively regulated in T-cell acute lymphoblastic leukemia (Durinck et al., 2014). Since hepatitis C virus NS3 protein can activate the Notch-signaling pathway (Iwai et al., 2011), upregulated lncR 7-2 may be the result of the activated Notch pathway that was induced by

HCV. Further investigation is still needed to decipher the regulation mechanism of lncR 7 by HCV.

A previous report showed that lncR 3 was downregulated in Insulin-like growth factor-1 (*IGF-1*) overexpressing human umbilical cord-derived mesenchymal stem cells when compared to controls (Liu et al., 2016), suggesting a possible negative correlation between *IGF-1* and lncR 3. In turn, *IGF-1* levels were significantly lower in HCV infected patients and HCV-related HCC compared to controls (Ghada and Nancy, 2009; Kasprzak and Adamek, 2012). This suggests that the increased lncR 3 may have been induced by decreased *IGF-1* in HCV infected cells. Interestingly, lncR 10 is also upregulated in HCC tissues compared to adjacent non tumor tissues (Zhang et al., 2015), pointing to an involvement of lncR 10 in HCC development.

In contrast, lncR 8 suppression with two independent GmRs consistently decreased HCV genomic RNA and protein production (Figure 2.3 B & C), indicating that lncR 8 is required for HCV replication in Huh-7.5 cells. In this study, we further investigated lncR 8.

3.3 LncR 8 may Regulate *GPR55* by *Cis*-regulation

LncRNAs can often regulate their neighboring genes *in cis*, so we examined the expression of nearby genes, *ITM2C* and *GPR55*. *GPR55* was downregulated after lncR 8 suppression at 12, 24, and 48 h in HCV-transfected cells (Figure 2.6 D & F), though this regulation was apparently not maintained at later times since no change of *GPR55* expression was observed when lncR 8 was upregulated 6 days post HCV replication (Figure 2.2 A & 2.6 B). Thus, lncR 8 may regulate *GPR55* by *cis*-regulation only within a short period after the begin of HCV replication. Similar results were observed when cells were infected with HCV virus instead of RNA transfection (Figure 2.7 B & E).

3.4 Immune Responses Induced after HCV Infection

Type I IFN, *IFN-α*, was upregulated at 2 d and 6 d post HCV infection, while *IFN-β* was not changed (Figure 2.10 B). Considering that *IFN-β* induction represents the immediate response of cells to viral infection and precedes the transcription of most *IFN-α* species (Li et al., 2005), it is possible that *IFN-β*

induction happened at earlier time points. However, a slight increase of *IFN-β* mRNA level was only observed at 9 h post HCV infection in Huh-7.5 cells, which was also reported by another group (Omura et al., 2019), pointing to a possible IFN-β defect in Huh-7.5 cells. Nevertheless, it was demonstrated recently that IFN-λ is the major IFN produced by HCV infected cells (Sung et al., 2015). This is supported by our data that type III IFN, *IL28A* (*IFN-λ2*), was elevated at 2 d and 6 d post infection (Figure 2.10 B).

3.5 LncR 8 is a Negative Regulator of the Antiviral Response

To elucidate the mechanism of proviral activity of lncR 8, ISG expression were examined after lncR 8 suppression. Surprisingly, two selected ISGs in this study, *ISG15* and *IFITM1*, were upregulated after lncR 8 knockdown in both HCV RNA transfected and virus infected Huh-7.5 cells (Figure 2.8 C & 2.11 C). This suggests that lncR 8 negatively regulates *Mx1* and *IFITM1* during HCV replication and infection. Moreover, the negative effect of lncR 8 on ISGs was also observed at early times when HCV RNA genome abundance was not yet changed (Figure 2.6 G, 2.7 D, 2.9 & 2.11 E), suggesting that the HCV suppression was probably caused by ISGs increase induced by lncR 8 knockdown. Both HCV RNA transfection and virus infection in Huh-7.5 cells triggered increase of lncR 8 expression compared to untreated cells (Figures 2.2 A & 2.4 B).

Considering the different chromosome locations of ISGs and lncR 8, the negative regulation on ISGs by lncR 8 must occur through a *trans*-acting mechanism, which resembles the effect of *EGOT* and *NRIR* on HCV (Carnero et al., 2016; Kambara et al., 2014). Enrichment of lncR 8 in the nucleus (Figure 2.2 D) suggests that the regulation on ISGs could be through regulation of a nuclear event like transcriptional regulation, epigenetic DNA/chromatin modification, or control of pre-mRNA splicing (Kopp and Mendell, 2018; Morlando et al., 2015; Valadkhan and Fortes, 2018). Other lncRNAs, such as lncRNA#32/*LUARIS*, ISR12 and *NRAV*, are also regulators of ISGs through a *trans*-acting mechanism (Carnero et al., 2016; Nishitsujia et al., 2016; Ouyang et al., 2014).

Interestingly, though HCV RNA transfection can induce increased ISGs expression despite of the negative regulation of lncR 8 on ISGs (Figure 2.8 A, B), HCV infection did not trigger increase of *CXCL10* and *Mx1* in Huh-7.5 cells

(Figure 2.10 C). Since transfection sends the HCV RNA directly into the cells, successfully bypassing the membrane recognition and fast immune response induced by membrane receptors, this may lead to longer survival time of HCV replication. Furthermore, it is RIG-I but not MDA5 that recognize *in vitro* transcribed RNAs in the cytosol (Wienert et al., 2018), while HCV infection is capable of inducing IFN production that is mainly dependent upon MDA5 rather than RIG-I (Cao et al., 2015). It is worth noting that Huh-7.5 cells have impaired RIG-I pathways. Thus, HCV RNA added through transfection may have failed to be recognized in the Huh-7.5 cells cytosol. Taken together, HCV RNA transfection and HCV viral infection in Huh-7.5 cells are two different processes and trigger different upstream pathways to induce immune factors. This may explain the different results observed in HCV RNA transfected and HCV infected cells that the pathways triggering expression of *CXCL10* and *Mx1* in RNA transfected Huh-7.5 cells failed to exert the same effect in infected cells.

Similar upregulation of ISGs and downregulation of HCV NS3 expression by lncR 8 knockdown were also observed in Huh-7 cells (Figure 2.11 C & 2.4 D), indicating that lncR 8 is also required for HCV infection in Huh-7 cells and this regulation may be independent of RIG-I.

Most ISGs function by increasing the antiviral response or by inhibiting viral replication. IFITM1 blocks viral entry by interacting with the CD81 receptor (Narayana et al., 2015). Mx1 traps viral components and prevents them from re-location (Garcia-Alvarez et al., 2017). ISG15 inhibits HCV replication by IFN-mediated ISGylation of NS5A (Domingues et al., 2015; Kim and Yoo, 2010). However, ISG15 induced by PKR can also modify ISGs, and change the structure and stability, affect functionality of host cellular protein through ISGylation, which favors HCV replication. As a result, ISG15 is now emerging as playing a proviral role in case of HCV infection (Arnaud et al., 2011).

3.6 *GPR55* Negatively Regulates ISGs

At basal levels, lncR 8 level is relatively low. Upon HCV infection, lncR 8 level was increased to silence ISGs and promote *GPR55*, thus repress the innate immunity and allow inflammation. It would be very interesting to understand how lncR 8 can regulate transcription of both neighboring and distal genes. To elucidate the possibility that lncR 8 regulates ISGs through its neighboring gene

GPR55, *GPR55* was inhibited by two different GmRs in Huh-7.5 cells for 48 h. Interestingly, suppression of *GPR55* promotes the expression of *ISG15*, *Mix1*, and *IFITM1* (Figure 2.12). This finding provides a possible link between lncR 8 and ISGs expression, indicating that lncR 8 favors HCV replication by regulating its neighboring gene *GPR55*, which in turn negatively regulates expression of ISGs (Figure 3), while not excluding that lncR 8 suppresses ISGs also by other mechanisms. Recently, GPR55 has gained much attention due to its activation by endogenous cannabinoids (EC) and a proinflammatory role in innate immunity (Chiurchiu et al., 2015; Yang et al., 2016; Zhou et al., 2016). ECs have been associated with fibrosis progression in HCV infected patients (Pesce et al., 2018).

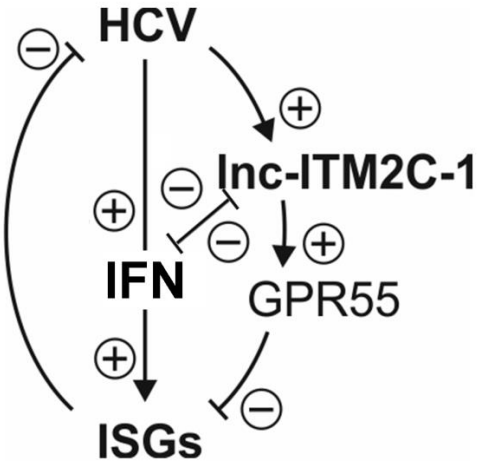

Figure 3.1 A model depicts the role of lncR 8 and *GPR55* during HCV replication. Indicated is that HCV induces lncR 8 expression, while lncR 8 favors HCV replication by regulating its neighboring gene *GPR55*, which in turn negatively regulates expression of ISGs. LncR 8 negatively regulates IFN and also is negatively regulated by IFN through JAK/STAT signaling pathway.

On the other hand, elevated levels of ECs were reported in plasma of patients with chronic hepatitis C and indicated potential immunosuppressive and profibrogenic roles (Patsenker et al., 2015). GPR55 is a third cannabinoid receptor which is novel because it is different from the other two classical receptors, CB_1 and CB_2 (Yang et al., 2016). High levels of GPR55 were found in monocyte and natural killer (NK) cells. GPR55 enhances IL-12 and tumor necrosis factor-α (TNF-α) production in monocytes and stimulates signature

cytokines as well as cytolytic activity in NK cells (Chiurchiu et al., 2015). While the detailed function of *GPR55* during HCV replication remains to be determined, the involvement of *GPR55* in the negative regulation of ISGs by lncR 8 indicates a potential pro-inflammatory role of *GPR55* and lncR 8 during early HCV replication.

3.7 LncR 8 can be Induced by Poly(I:C)

LncR 8 is induced not only HCV-specific, but it can also be induced by poly(I:C) in Huh-7.5 cells (Figure 2.13 A). When lncR 8 was suppressed in Huh-7.5 cells, upregulation of ISGs expression was observed (Figure 2.14). This negative regulation of representative ISGs expression by lncR 8 upon poly(I:C) treatment was similar when cells were infected with HCV instead of poly(I:C).

Generally, lncRNAs deregulated by the antiviral response can also be altered in response to several viruses, different PAMPs and/or IFNs, including like *NRIR*, *lncISG1*5, and *BISPR* (Barriocanal and Fortes, 2017). Given that poly(I:C) induces the innate immune response, and lncR 8 expression was altered by both poly(I:C) and HCV infection, we speculate that lncR 8 is deregulated by the antiviral response and might also response to other viruses.

3.8 LncR 8 is Downregulated by JAK/STAT Pathway

Unlike other lncRNAs that can be induced by *IFN-α*, lncR8 is negatively regulated by IFN-α (Figure 2.15 A) through the JAK-STAT pathway (Figure 2.15 B), thus, lncR 8 is not an ISG. We know that irrespective of persistent immune and inflammatory response induced by HCV *in vivo*, HCV survives in the infected cell. This indicates that HCV develops strategies to bypass the immune response (Heim and Thimme, 2014; Thimme et al., 2012), i.e. uncouple lncR 8 from the control of IFNs. We speculate that lncR 8 is normally maintained at low expression level and upregulated upon HCV infection by unknown mechanisms irrespective of the elevated IFN levels.

In the battle of HCV and host cells, increased levels of ISGs should be induced by the immune response against HCV. Most ISGs function by increasing the antiviral response or by inhibiting viral replication. Paradoxically,

high expression of ISGs even indicates failed therapy in the HCV patients (Arnaud et al., 2011; Thimme et al., 2012). In fact, the level of most ISGs induced by the endogenous IFN system is lower than the level induced by recombinant IFN therapy (Boldanova et al., 2017), pointing to existence of factors blocking efficient ISG expression in patients. The innate immune response is insufficient to control viral replication. Host cells do not lack immune responses in general, but they rather lack effective immune responses (Sun et al., 2015).

Nevertheless, lncR 8 induced by HCV helps HCV replication by positively regulating its neighboring gene *GPR55*, which in turn negatively regulates ISGs, like *ISG15*, *Mx1*, and *IFITM1*, at early time points (Figure 2.11 E). By this mechanism, lncR 8 may contribute to the failure of interferon action and elimination of ongoing HCV infection. Due to our findings, lncR 8/ *lnc-ITM2C-1* was renamed as GPR55 *cis* regulatory suppressor of immune response RNA (*GCSIR*) by the HUGO gene nomenclature committee (https://www.ncbi.nlm.nih.gov/gene?Db=gene&Cmd=DetailsSearch&Term=151484). Though further studies will be required to elucidate the underlying mechanisms, our study benefits a better understanding of lncRNAs in the HCV-host battle and provides us with hints to better control HCV infections.

4. Materials and Methods

4.1 Materials

4.1.1 Bacterial Strains, Cell Lines and plasmid

One Shot® TOP10 Chemically Competent E. coli (Life Technologies) is highly transformable and ideal for stable replication of high-copy plasmids. Along with the usage of commercial stocks, self-made chemically competent E.coli TOP10 was also applied for transformations.

Human hepatocarcinoma derived Huh-7.5 cells and naïve Huh-7 cells were kindly provided by Charles Rice (Rockefeller University, New York, USA) and Ralf Bartenschlager (Heidelberg, Germany) respectively. Huh-7.5 is a derivative of Huh-7 cells generated after removal of the HCV replicon by IFN treatment. Huh-7.5 appeared to be highly permissive for the HCV RNA.

Plasmid pFK-JFH1-J6 C-846_dg (briefly: Jc1) as previously described (Pietschmann et al., 2006), kindly provided by Ralf Bartenschlager (Heidelberg, Germany) (Appendix 6.4).

4.1.2 Materials for Bacterial Growth and Cell Culture

Material	Company
LB-Broth (Lennox)	Carl Roth
Agar-Agar, Kobe I	Carl Roth
Ampicillin sodium salt	Carl Roth
Dulbecco's Modified Eagle's Medium (DMEM)	Life Technologies
100 × Penicillin-streptomycin solution (Pen/Strep)	Life Technologies
Fetal Bovine Serum (FBS)	Life Technologies
10 × 0.5 % Trypsin-ethyendiamintetraacetic acid (EDTA)	Life Technologies
Dimethyl Sulfoxide (DMSO)	Carl Roth
Roti-Stock 10 × Phosphate buffered saline (PBS)	Carl Roth

4.1.3 Chemicals and Reagents

Chemicals and reagents	Company
Acetic Acid	Sigma-Aldrich
Acetone	Sigma-Aldrich
Ammonium Persulfate	Carl Roth
Bovine serum albumin (BSA)	Sigma-Aldrich

β-Mercaptoethanol	Sigma-Aldrich
Chloroform	Sigma-Aldrich
dNTPs (separate solutions of dATP, dGTP, dCTP and dTTP) (100 mM each)	Carl Roth
Ethanol (ACS reagent, > 99.5 %)	Sigma-Aldrich
EDTA	Carl Roth
Fluoroshield Mounting Medium With DAPI	Abcam
GeneRuler DNA Ladder Mix	Life Technologies
GeneRuler 50 bp and 100 bp (0.5 µg/µL)	Life Technologies
Glycerol	Carl Roth
Glycine	Sigma-Aldrich
GlycoBlue (15 mg)	Life Technologies
HyperLadder 1 kb	Bioline
Lipofectamine 2000	Life Technologies
Methanol	Carl Roth
$MgCl_2$ (25 mM)	NEB
NTPs (separate solutions of ATP, GTP, CTP and UTP) (100 mM each)	Carl Roth
PageRuler Prestained Protein Ladder (10 to 250 kDa)	Life Technologies
Poly-L-Lysin 0.1 mg/mL (30000-70000)	Sigma-Aldrich
Paraformaldehyde	Sigma-Aldrich
Potassium chloride (KCl)	Carl Roth
Skimmed milk powder	EDEKA Krenschker
Sodium chloride (NaCl)	Carl Roth
Sodium Dodecyl Dulfate (SDS)	Carl Roth
Tris base	Carl Roth
Triton X-100	Bio-rad
TRIzol	Life Technologies
Tween20	Sigma-Aldrich
5 x DNA Loading Buffer	Bioline
2 x RNA Loading Dye	NEB

4.1.4 Enzymes

Enzyme	**Company**
*Mlu*I-HF, CutSmart (Recognition sequence :A↓CGCGT)	NEB
Antarctic Phosphatase, 10 × Antarctic Phosphatase reaction buffer	NEB
DNase I (RNase-free), 10 × DNase I reaction buffer	NEB
T4 DNA Ligase, 10 × T4 DNA Ligase buffer	NEB
One Taq DNA Polymerase, 5 × OneTaq standard reaction buffer	NEB
T7 RNA polymerase, 10 × RNAPol reaction buffer	NEB

SuperScript® IV Reverse Transcriptase	Life Technologies
TrueStart Hot start Taq DNA Polymerase, 10×TrueStart Hot start Taq Reaction Buffer	Life Technologies
RNase H	NEB
Terminal deoxynucleotidyl-transferase	NEB

4.1.5 Antibodies

Antibody	Description	Company
Anti-Hepatitis C Virus NS3 antibody [8 G-2]	A mouse monoclonal antibody to HCV NS3 that efficiently reacts towards the JFH-1 strain (genotype 2a).	Abcam
Anti-GAPDH antibody	A mouse monoclonal antibody to a cytoplasmic housekeeping protein GAPDH	Abcam
Anti-mouse IgG HOR antibody conjugated with peroxidase		Sigma-Aldrich
Goat anti-mouse IgG1, Alexa Fluor® 488 conjugate		Life Technologies

4.1.6 Kits

Kit	Purpose	Company
GeneJET Gel Extraction Kit	Purification of DNA fragments from agarose gels	Life Technologies
GeneJET PCR Purification Kit	Purification and concentration of DNA fragments from PCR reactions	Life Technologies
GeneJET Plasmid Maxiprep Kit	Endotoxin-free plasmid preparation; maxi scale	Life Technologies
GeneJET Plasmid Miniprep Kit	Plasmid preparation; mini scale	Life Technologies
GeneJET RNA Cleanup Micro Kit	RNA cleanup and concentration after DNase I treatment	Life Technologies
qScript Flex cDNA Kit	Reverse transcription of a specific gene from total RNA samples	Quanta Biosciences
PerfeCTa SYBR Green FastMix	Real-time quantitative PCR	Quanta Biosciences
Qubit quantification assay Kits (dsDNA BR, RNA BR)	Quantification of DNA and RNA concentration	Life Technologies
SuperSignal West Femto Chemiluminescent Substrate	Western blot substrate	Pierce
TA Cloning® Kit	Clone PCR products into vector	Life Technologies

RNeasy Mini Kit	RNA clean up	Qiagen

4.1.7 Oligonucleotides and primers

4.1.7.1 *miR122* duplex

miR-122 RNA oligos were supplied by biomers.net (Germany). The sequences were:

miR-122 mat, 5′-(phos) UGGAGUGUGACAAUGGUGUUUG-3′;

*miR-122**, 5′-(phos) AACGCCAUUAUCACACUAAAUA-3′;

miR-124 mat, 5′-(PHOS)UUAAGGCACGCGGUGAAUGCCA-3′;

*miR-124**, 5′-(PHOS)GUGUUCACAGCGGACCUUGAUU-3′;

Duplexes were formed by annealing same amounts of the guide (mat) and its complementary passenger strand (*) in a thermocycler by a steady temperature decrease from 90 ℃ to 4 ℃ (1 ℃ per minute (min)).

4.1.7.2 Anti-*miR122* LNA

The LNA mixmer oligo for sequestering *miR-122* was ordered from Exiqon (Denmark). The sequence was:

5′-+C*C*A*+T*T*G*+T*C*A*+C*A*C*+T*C*+C-3′, where (+) indicates a following LNA residue and G*, A*, T*, C* indicate phosphorothioate DNA bases.

4.1.7.3 LNA™ LongRNA GmR Oligos

LNA™ longRNA GmR oligos targeting different lncRNA candidates were designed using online Antisense GmR Designer (https://www.qiagen.com/de/shop/genes-and-pathways/custom-products/custom-assay-products/antisensegapmerdesigner/) and purchased from Qiagen (Germany). The sequences of the GmRs were:

GmR Negative Control A (Neg. ctr. GmR): 5′-AACACGTCTATACGC-3′;

GmR 1 for lncR 3 (lncR 3-GmR 1): 5′-GCGTGATTAAATGGAT-3′;

GmR 2 for lncR 3 (lncR 3-GmR 2): 5′-GACGATAAGAGGTAAC-3′;

GmR 1 for lncR 7 (lncR 7-GmR 1): 5′-TGATTAACAGAACGGA-3′;

GmR 2 for lncR 7 (lncR 7-GmR 2): 5′-ATAAGTGTCTAGTTAG-3′;
GmR 1 for lncR 8 (lncR 8-GmR 1): 5′-GTTACCAGTGAAGCGG-3′;
GmR 2 for lncR 8 (lncR 8-GmR 2): 5′-TCGGATTGGTCACATG-3′;
GmR 1 for lncR 10 (lncR 10-GmR 1): 5′-GTTAATCTGATCTTGC-3′;
GmR 2 for lncR 10 (lncR 10-GmR 2): 5′-TCTGAGCTTGATCACT-3′;
GmR 1 for *GPR55* (GPR55-GmR 1): 5′-GGCGAATCAGATTAAT-3′;
GmR 2 for *GPR55* (GPR55-GmR 2): 5′-AGGACCATCTTGAATG-3′;

There is a phosphorothioate backbone between the nucleotides. The position of LNA modification is not shown.

Add 100μL Nuclease-free water to 5nmol GmR so to make 50μM store solution. Aliquot 20ul/tube and store at -20°C. Target lncR7 two variants both

CLUSTAL for possible cross reactions and NBLAST analyses to display GmR binding specificity in the genome were provided in Appendix 6.1. The complete hybridization of each GmR to its genuine target, as well as each the best 5 matches to unrelated genomic sequences were depicted. These results show that the Randomized control GmR does not bind specifically to any target in the human transcriptome, and virtually all GmRs specific for lncRNAs used in this study are very specific for their genuine targets (only lncR 10 GmR-1 has a single off-target with only 1 nt difference).

4.1.7.4 Primers

Primers were purchased from biomers.net. Primers used for reverse-transcription (RT) reaction and qRT-PCR of lncRNA candidates are listed in Table 4.1 (Amplifications using primers for lncRs 1, 4, 5, 6, and 9 are failed). Primers for other genes are listed in Table 4.2. Most primers were designed by the PrimerPremier5 program (United Kingdom). Primers to amplify *GAS5*, small nucleolar RNA U99, H/ACA box 57 (snoRNA U99, *U99*), *ISG15*, *Mx1*, and interferon induced transmembrane protein 1 (*IFITM1*) fragments were obtained from previous reports (Carnero et al., 2016; Kambara et al., 2014; Qian et al., 2016; Wang et al., 2016). Primers for Integral membrane protein 2C (*ITM2C*), G protein-coupled receptor 55 (*GPR55*), C-X-C motif chemokine ligand 10 (*CXCL10*), melanoma differentiation-associated protein 5(*MDA5*, also named *IFIH1*), interferon beta 1, fibroblast (*IFN-β*) were from PrimerBank (https://pga.mgh.harvard.edu/primerbank/). Two different sets of primers

targeting two sites of the sequences were designed for lncRs 3, 7, 8, and 10. qRT-PCR detecting expression after *miR-122* with or without HCV treatment, and detecting cytoplasm/nucleus location were performed using 5′ side primers. To test the effect after GmR knockdown, 5′ side primers for lncRs 3 and 7, 3′ side primers for lncRs 8 and 10 were used.

Table 4.1 Primers for lncRNAs

Target gene	Primer sequences (5′-3′)	Amplicon size (bp)
LncR1	F: ACAACGAAGTACCACCTGACAAC R: AACTGGCACTCCGTGGCTT	92
LncR 2	F: CTCCCAGAACCTATCGGCAT R: CACAAAGCCTGCGTTCATTC	130
LncR 3	F: AGGATGTGACTGCCAGGTAATG R: CAGACCCAGCCTAGCACACAG	100
LncR $3^{3'}$	F: GTGACCCAACTAGAGCCAATAGG R: CTCAAATCAGCTCATGACCATAAG	135
LncR4	F:GGACTCCCGAGCTCATTACG R:TTTGCTGAATGTCCTGAAGAAG	108
LncR5	F:TTCAGGTTTCCGAGACAATGG R:TCGTGGTGGTTGAAAGCCC	86
LncR6	F:AGGTGTTACCCAAACTCTGACG R:AAGCAAAAGATGCAGCGGA	151
LncR 7-1	F: AGGCTACAGGAGGCACTGAGGG R: GGAGCCATCTGGGAGAATGAAATAC	144
LncR 7-2	F: GAGGCTACAGGAGGCACTCTTTG R: GGAGCCATCTGGGAGAATGAAATAC	79
LncR $7^{3'}$	F: TCGGGTTCTTGATTTGATTCTC R: TGGACCAAGTATCCTCTAAAAATG	142
LncR 8	F: GGTTTTTTGACCTTGGCAATG R: GTGACCCTTGGTGGCTGTTTAT	102
LncR $8^{3'}$	F: GATTCTGTCTCATCCAATCAAGACT R: GTTGTGCTGAGGATTCTGGGT	123
LncR9	F: CCTGGTTGGCTGATGGAAAGA R: GCCCTAAAACTCATTCCCAAAAG	122
LncR 10	F: CGGAAATGCCTAATCTGAACTT R: TAGAGCGGACCCACGAAAC	80
LncR $10^{3'}$	F: CCCCTGATGCTTCATAATGG R: AGTTCTAACCTAATTTCCCATCAC	111

This table lists the sequence of primers for each lncRNA target and the size of amplicons. Two different sets of primers were purchased for lncRs 3, 7, 8, 10. One targets the 5′ end of the sequence, the other the 3′ end. Primers targeting the 3′end of the lncRNA sequences were labeled with 3′. F: Forward, R: Reverse.

Table 4.2 Primers for HCV, reference genes, and ISGs

Target gene	Primer sequences(5′-3′)	Amplicon size (bp)
GAPDH	F: GAGTCAACGGATTTGGTCGT R: GATCTCGCTCCTGGAAGATG (= RT)	224
U6	F: CTCGCTTCGGCAGCACA R: AACGCTTCACGAATTTGCGT	94
U99	F: CCTCCTTTTCTTGGCGGGGA R: CGTTTGAGGATAGAACCAGC	138
β-actin	F: CATGTACGTTGCTATCCAGGC R: CTCCTTAATGTCACGCACGAT	250
Jc1-NS3	RT: GTATGCCACGGCATTCAAG F: GATATAGGTCGACGGCTCCA R: TTCCTCGGAACAACCATCTC	190
GAS5	F: CCTGTGAGGTATGGTGCTGG R: GGTCCAGGCAAGTTGGACTC	383
ITM2C	F: GTGGTGTGCTGTATGAGGACT R: CGTAGTTCTCGTCGAGGTAGAT	93
GPR55	F: GAAAACCCTACAGTTTGCAGTCC R: GAGGTGGCAGCATAATCGGG	123
CXCL10	F: GTGGCATTCAAGGAGTACCTC R: TGATGGCCTTCGATTCTGGATT	198
ISG15	F: ACTCATCTTTGCCAGTACAGGAG R: CAGCATCTTCACCGTCAGGTC	88
Mx1	F: TGCATCGACCTCATTGACTC R: ACCTTGCCTCTCCACTTATC	218
IFITM1	F: ACTCCGTGAAGTCTAGGGACA R: AGAGCCGAATACCAGTAACAG	149
MDA5	F:TCGAATGGGTATTCCACAGACG R:GTGGCGACTGTCCTCTGAA	152
IFN-β	F:GCTTGGATTCCTACAAAGAAGCA R:ATAGATGGTCAATGCGGCGTC	166
IFN-α	F: GGAGGTTGTCAGAGCAGA R: AATGACAGAATTCATGAAAGCGT	150
IL28A	F: CAGCCTCAGAGTGTTTCTTCT R: TCCAGTCACGGTCAGCA	117

This table lists the sequence of primers and the size of amplicons for targets including HCV NS3 coding region, reference genes and ISGs. F: Forward, R: Reverse, RT: Reverse transcription.

Table 4.3 Specific primers for RACE

Target gene	Primer Sequence(5′-3′)	Start position
lncR3	3GSPouter: ACAGTATAGTTCTGGGAGTTGC	1500
	3GSPinner: TGGAACAGATGGAGATAAATTGG	1578
	5GSP RT: TAACACAGGCACCAAGGATT	285
	5GSPouter: CTGGCAGTCACATCCTCTTCA	250
	5GSPinner: TCTTCACTTCACAATTACAGATAGC	235
lncR7-2	3GSPouter: ATGGGATGTATTTCCGTTGGTT	3059
	3GSPinner: GTGTATAGCGGTGCTACTGAT	3239
	5GSP RT: GAGGAGGTTGGAAGATAAGTGTC	456
	5GSPouter: AGCCATCTGGGAGAATGAAATAC	129
	5GSPinner: AAAGAGTGCCTCCTGTAGCCT	74
lncR8	3GSPouter: TACCACAGTCAGCACCCAACAT	1432
	3GSPinner: CGAGATCTTACCCGCTTCACT	1705
	5GSP RT: CATCATCTACCTGAACGGGAAT	494
	5GSPouter: GCAGCAAGGATACGGAGATG	233
	5GSPinner: CGTGACTGCCGACCCTTCT	199
lncR10	3GSPouter: CCCTGATGCTTCATAATGGTT	2874
	3GSPinner: ACTCTGCCTTCATAGAACTTGTC	3088
	5GSP RT: CTCCACCGCAATAGGTCTG	587
	5GSPouter: GAGAACAACCCCCGGTTGAG	345
	5GSPinner: TAGAGCGGACCCACGAAAC	158

oligo(dT)16AP: 5′-CTGATCTAGAGGTACCGGATCCTTTTTTTTTTTTTTTT-3′, AP(Adaptor Primer): 5′-CTGATCTAGAGGTACCGGATCC-3′, 3RACE-R: 5′-TCTAGAGGTACCGGATCC-3′, GSP: Gene specific primer.

4.1.8 Buffers and Solutions

4.1.8.1 Bacterial Growth and Cell Culture Solutions

Solution	Composition
LB growth medium	For 1 L: 20 g LB-Broth Fill with de-ionized H_2O and sterilize by autoclaving.
2 % Agar-LB plates	For 200 mL: 4 g LB-Broth 4 g agar Fill with de-ionized H_2O Antibiotic is added after autoclaving (100 µg/mL)
1 x PBS	For 1L: 100mL 10×PBS 900mL de-ionized H2O

	autoclaving
Complete 10 % DMEM	For 500 mL: 5 mL Pen/Strep 50 mL FBS
Cryomedium	For 50 mL: 10 mL FBS (20 %) 5 mL DMSO (10 %)
Cytomix	120 mM KCl, 0.15 mM CaCl2, 10 mM K2HPO4/KH2PO4 (pH 7.6), 25 M HEPES, 2 mM EGTA, 5 mM MgCl2, pH 7.6; add before use: 2 mM ATP 5 mM reduced glutathione (GSH)
0.5 % Trypsin-EDTA	For 50mL: 5mL 0.5 % Trypsin-EDTA 45mL 1 × PBS.

4.1.8.2 General Use Buffer

Solution	**Composition**
1 M Tris-HCl (pH 8.0)	For 100 mL: 12.12 g Tris Fill with ddH_2O to 80 mL ~ 4.2 mL HCl, pH 8.0 Fill with ddH_2O
0.5 M EDTA（pH 8.0）	For 500 mL: 73.0625g EDTA 350 mL ddH_2O ~10g NaOH, pH 8.0 Fill with ddH_2O
50×TAE Buffer	For 500 mL: 121 g Tris 28.55 mL Acetic acid 50 mL 0.5 M EDTA (pH 8.0) Fill with ddH_2O
10% SDS	For 500mL: 50 g SDS Fill with ddH_2O Adjust pH to 7.2

4.1.8.3 Western Blot and Immunofluorescence Buffers

Solution	Composition
10 × Lysis buffer	For 100 mL: 10 mL 1M Tris HCl, pH 8,0 (10 mM) 8,2 g NaCl (140 mM) 0,25 g NaN_3 (0,025 %) 10 ml Triton X-100 (1 %)
2 × PPPC	For 50 mL: 5 mL 1 M Tris HCl pH 6,8 (100 mM) 12 mL Glycerin (24 %) 4 g SDS (8 %) 0,01 g Coomassie-blue G-250 (0,02 %) 1 mL ß-Mercaptothanol (2%) Fill with ddH_2O
PBS-T	1 × PBS 0,5 % Tween® 20
Transfer buffer	For 1 L: 5,8 g Tris-Base (48 mM) 2,9 g Glycin (39 mM) 3,7 mL 10 % SDS (0,037 %) 200 mL Methanol (20 %) Fill with ddH_2O
Tricine-Gel buffer	For 500 mL: 181,5 g Tris-Base (3M) 15 ml 10 % SDS (0,3 %) with concentrated 37 % Hydrochloric acid adjust to pH 8.45, fill with ddH_2O
10 × SDS Running Buffer	For 1L: 10 g SDS 30 g Tris 144 g Glycine Fill with de-inonized H_2O
1000 × Ampicillin	5 g ampicillin 25 mL ddH_2O 25 mL absolute ethanol
Blocking solution	5-10 % (w/v) dry milk Fill with PBS-T
4% paraformaldehyde	For 1L: 40 g paraformaldehyde Fill with 1 ×PBS
Glycin-PBST	1% BSA 22.5 mg/mL glycine Fill with PBS-T

4.1.9 Consumables

Consumable	Company
9 cm tissue culture dish	Sarstedt
Adhesive film, optically clear	Sarstedt
Autoclavable Waste Bags	Sarstedt
Chromatography Paper 3MM Chr (Whatman Paper)	VWR
Filter Tips (10 µL, 20 µL, 200 µL, 1250 µL)	Sarstedt
Gene Pulser / Micro Pulser electroporation cuvettes	Biorad
Polyvinylidenfluoride (PVDF) Membrane Immobilon-P, 0.45 µm	Milipore
96 Fast PCR-Plate full skirt	Sarstedt
96 Fast PCR-Plate half skirt	Sarstedt
Reaction Tubes (15 mL, 50 mL)	Sarstedt
Reaction Tubes (1.5mL, 2.0 mL)	Sarstedt
Sterile Serological Pipettes (5 mL, 10 mL, 25 mL)	Greiner
Tissue Culture Flasks (25 cm^2, 75 cm^2, 175 cm^2)	Sarstedt
Tissue culture plates (48-wells, 24-wells, 6-wells)	Sarstedt

4.1.10 Laboratory Equipment

Device	Company
CB series CO_2 Incubator	Binder
Centrifuge 5417R	Eppendorf
Cronex Lightning Plus X-ray cassette	DuPont
Destamat, bi-destiller	Heraeus
Digital-pH-Meter 644	Knick Elektronische Messgeräte
Duomax 1030 shaker	Heidolph
ED240 hot-air cabinet	Binder
FastBlot B44 semidry blotting chamber	Biometra
Fluorescent microscope	Olympus
GelDoc XR gel documentation system	Bio-Rad
HA 2448 BS LaminAir lamina flow	Heraeus
Heat-stir US152 magnetic stirrer	Stuart
Isopropanol tank	Qualilab
Julabo 7A water bath	Julabo
Julabo U3 water bath	Julabo
LB 124 Geiger counter	Berthold Technologies
Leica DM IL invers microscope	Leica Microsystems
MagnaRack magnetic separation rack	Life Technologies
Micropipettors (2 µL-1000 µL)	Gilson

Multifuge 3L-R	Heraeus
Pipetboy comfort pipettor	Integra Biosciences
Qubit 2.0 Fluorimeter	Life Technologies
Severin 700 microwave	Severin
Tecan infinite M200 multimode reader	Tecan Deutschland
TProfessional PCR cycler	Biometra
V150 autoclave	Systec
Vortex Genie 2	Scientific Industries

4.2 Methods

4.2.1 Cell Culture

Human hepatocarcinoma derived Huh-7.5 cells and naïve Huh-7 cells, kindly provided by Charles Rice (Rockefeller University, New York, USA) and Ralf Bartenschlager (Heidelberg, Germany) respectively, were maintained in DMEM (Life Technology) supplemented with 10% FBS and 1% Pen/Strep (10,000 U/mL), and grown at 37 ℃ in a 5% CO2 incubator.

4.2.1.1 Thawing of Cells

To thaw cells stored in a liquid nitrogen tank, it is necessary to use of protective eyewear as well as gloves since residual nitrogen may reside in the vial. The cryovials were placed in a 37 ℃ water bath to accelerate the thawing process. The cells were then transferred to a 25 cm^2 tissue culture flask containing 5 ml of pre-warmed DMEM supplemented with 10 % FBS and 1 % Pen/Strep (DMEM 10 %) and incubated at 37 ℃ overnight. Cells will adhere to the bottom of the flask. The medium was changed to fresh DMEM 10 %. This is necessary to remove cells that died during the freezing and thawing procedure, as well as to remove residual DMSO that was part of the freezing medium.

4.2.1.2 Passaging Eukaryotic Cells

To ensure a constant growth of an adherent cell line it is necessary to split the cells on a regular basis to keep them from getting too confluent. Cell cultures that are grown too thickly have the tendency to detach from the growing surface and to die. Usually cells were passaged when they reached 80 % - 95 %

confluency to ensure that they are in the log phase of growth. The old culture medium was discarded and the cells were washed with PBS. Afterwards, the cells were treated at 37 °C with an appropriate amount of 0.5 % Trypsin-EDTA until they detached (for 75 cm^2 flask 3 ml Trypsin were used, for 175 cm^2 flask 5 ml Trypsin were used). Trypsin was inactivated by adding at least the same amount of fresh DMEM 10 %. The cells were resuspended in the DMEM 10 % by pipetting up and down. Subsequently, an appropriate amount of cell suspension was given into a new flask along with fresh DMEM 10 % and cultured for several days. A normal amount of Huh-7.5 or Huh-7 cells that was given into the new flask was 1/20 of the cell suspension for 5 days of cultivation.

4.2.1.3 Counting Eukaryotic Cells

To determine the total amount of cells in a cell suspension the cells were counted using a Neubauer improved hemocytometer. The counting chamber has a depth of 0.1 mm and is divided into several squares of different sizes. For determining the cell number the squares of 1 mm^2 (Figure 4.1, highlighted in blue) were counted. Cells that touched the upper or right edge of the square were not included in the calculations. Cells touching the left or lower edge of the square were included into the count. The total cell number of all five 1 mm^2 squares (including the central one) was averaged and this mean value was multiplied by 10000, resulting in the number of cells per mL.

4.2.1.4 Freezing Eukaryotic Cells

Eukaryotic cells change their behavior with the number of passages and the time they are cultured. Sometimes transfection efficiencies and growth rate can drop dramatically. At this time point it is necessary to thaw new cells that were stored in the vapour phase of a liquid nitrogen tank. The cryomedium was made by mixing 20 % FBS with 10 % DMSO as a cryoprotectant. The cells were grown in DMEM 10 % until they reached log phase growth at approximately 80 - 90 % confluency. The old culture medium was discarded, the cells were washed twice with PBS and treated with 0.5 % Trypsin-EDTA until they detached. The trypsination was stopped by adding one volume cryomedium. Subsequently, the cells were centrifuged for 10 min at a speed of 150 rcf and

4 ℃. The cells were resuspended in cryomedium at a concentration of about 1 × 10^6 cells per ml and dispersed in to cryovials, 1 ml per vial. The cryovials were placed in an alcohol bath (Nalgene cell freezing container containing 100 % Isopropanol) that was pre-cooled to 4 ℃. The cells were then placed in a -80 ℃ freezer. After one to two days the cryovials were transferred into the gas phase of a liquid nitrogen tank.

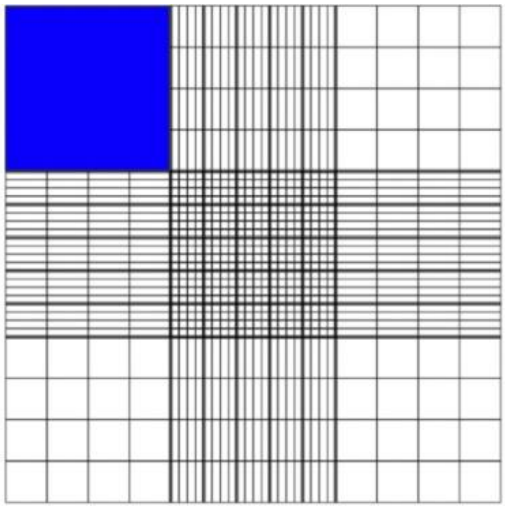

Figure 4.1 Neubauer hemocytometer. The hemocytometer has a depth of 0.1 mm and is divided in several squares ranging from 0.0025 mm^2 to 1 mm^2. The square used to determine the amount of cells in a suspension is highlighted in blue and has an area of 1 mm^2. Cell touching the right and upper rim of the square were not counted. The picture was taken from http://www.microbehunter.com and modified.

4.2.2 Transformation of Bacteria and Maxi Plasmid Preparation

All steps involving bacteria were carried out in close proximity to a Bunsen burner to ensure sterility of the bacterial culture. Metal and glass ware such as glass pipettes or beakers were either disinfected by dry heat sterilization or were singed. The surface of the working space was disinfected by wiping it down with 70 % ethanol.

4.2.2.1 Cultivation of Bacteria

Bacteria were grown on agar plates forming colonies or liquid LB medium. For agar plates, 3.75 g of bactoagar were added per 250 ml of LB medium dissolved in deionized water before autoclaving. For seeding a petri dish, the

agar was heated and cooled down to approximately 60 ℃, only then was (1:1000) ampicillin added. About 20 ml of the agar were poured into a petridish. After turning solid the bacteria were dropped on the agar and spread with a bacterialspreader until the liquid seeped into the plate.

For liquid cultures, a pre-culture containing 3-5 ml of LB medium (1:1000 ampicillin) was prepared firstly. This pre-culture was inoculated with one bacterial colony picked from an agar plate and grown for several hours until the medium turned turbid, then 1/10 of this culture was used to inoculate a bigger flask of LB medium, ranging in size from 10 ml - 500 ml.

4.2.2.2 Transformation of Bacteria by Heat Shock

Take competent cells out of -40 ℃ and thaw on ice (approximately 20-30min). Then gently mix cells with the pipet tip and aliquot 50 µl of cells for each transformation into 1.5 mL tubes that have been pre-chilled on ice. 1µg DNA was added to the cells and was mixed gently by pipetting up and down. The competent cell/DNA mixture was then placed on ice for 15 min. Plate some or all of the transformation onto a 10 cm LB plates/agar plates containing the appropriate antibiotic

4.2.2.3 Plasmid Preparation

Bacteria were transformed with the plasmid of choice and grown (usually overnight) at 37 ℃ under constant shaking at 180 - 250 rpm for about 8 - 12 h until they reached log phase growth. Afterwards the cells were pelleted by centrifugation (5000 rcf, 4 ℃, 10-15 min) and lysed by using GeneJET Plasmid Maxiprep Kit or Miniprep Kit (Thermo Scientific).

4.2.3 Plasmid digestion and *In vitro* Transcription

Restriction Enzyme *Mlu* I	1 µL (10 units) per ug DNA
DNA	500 µL
3.1 10×NEBuffer	75 µL (1×)
Fill with H_2O to	750 µL

Plasmid pFK-JFH1-J6 C-846_dg (briefly: Jc1) was used to generate full-length HCV Jc1 genomes (J6/JFH1 chimeric genotype 2a) by *in vitro* transcription. The Jc1 plasmid was first digested with *Mlu* I-HF (NEB) for 2 hours (h) at 37 ℃ using the following protocol:

Next, linearized DNA was purified by phenol/chloroform extraction and ethanol precipitation. Then, the concentration of dissolved DNA was measured by Qubit 2.0 Fluorimeter (ThermoFisher). The DNA size and linearization were checked on 1 % TAE agarose gels. When an electric current is applied to the gel the negatively charged nucleic acids will move though the gel and small fragments will pass thought the gel more quickly than larger ones. The samples were mixed with DNA loading buffer containing xylencyanole and bromphenol blue. The resulting bands in the gel was visualized by staining the gel with ethidium bromide and exposing it to UV light.

In vitro transcription was performed using T7 RNA Polymerase (ThermoFisher) in the presence of 3.75 mM of each NTP, additional 5 mM $MgCl_2$ and 10 mM DTT, and 30 ng/µL of linearized plasmid DNA. After 2 h of incubation at 37 ℃, another 1 U/µL of T7 RNA Polymerase was added for 2 h more. Template DNA was then digested by 2 U RNase-free DNase I (NEB) per 1 µg of DNA for 1 h at 37 ℃. HCV full-length Jc1 RNA transcripts were dissolved in equal amounts of RNase-free water. After removing the enzymes using GeneJET RNA Clean-up Kit (ThermoFisher), transcripts were checked for integrity by agarose gel electrophoresis and quantified by Qubit Fluorimeter.

It is necessary to take precautions when working with RNA since RNases are ubiquitous and easily to dissolve RNA samples. All glass and metal ware was baked overnight at 280 ℃. Reusable plastic ware was soaked for 1 hour in 0.1 M NaOH and 1 mM EDTA solution and subsequently rinsed with ddH_2O and wrapped with aluminum foil and autoclaved. Self-made buffers (except gel running buffers like TBE or TAE) were prepared in RNase-free materials and glass ware, and subsequently autoclaved. Furthermore, only nuclease-free certified filter tips and sterile serological pipettes were used to handle the buffers and RNA solutions

4.2.4 Infectious HCV in Cell Culture

The Jc1 *in vitro*-transcribed RNA was transfected into Huh-7.5 cells by electroporation. The culture supernatants collected at 6 day (d) after transfection were distributed into split Huh-7.5 cells. After additional multiplication passages on naïve cells, the cell-free supernatants containing HCV were concentrated approximately 50-fold using Amicon Ultra-15 Centrifugal Filters (Millipore, Billerica, MA, USA). Aliquots were stored at -80 ℃ until use. Virus titers were determined by fluorescent focus assay (FFA). Huh-7.5 cells were seeded at 0.25×10^5 cells per well in 24-well plates and cultured overnight. Test samples were diluted serially 10-fold and each dilution was inoculated into the cells. After incubation for 4 h at 37 ℃, the cells were supplemented with fresh complete DMEM and cultured for 48 h. The cells were then immunofluorescence-stained for HCV NS5A. HCV-positive foci were manually counted under a fluorescence microscope. The virus titer was expressed as focus-forming units per milliliter of supernatant (FFU/mL), as determined by the average number of NS5A-positive foci detected in a whole well.

4.2.5 Cell Treatment

To identify HCV altered transcriptome, transfection of 500 ng *miR-122* duplex into Huh-7.5 cells in T175 flask was performed using Lipofectamine 2000 (Invitrogen) 24 h prior to HCV RNA electroporation. Cells were transfected at about 70% confluency. Oligos and Lipofectamine were first prepared as master mixtures in separate tubes in serum/antibiotic-free DMEM (50 µL/reaction). After 5 min at room temperature, each sample was mixed together with Lipofectamine and incubated for 15 min. Then, 100 µL Lipofectamine-oligo mixed solution was carefully applied to the cells dropwise. At 3 h post transfection, the cells were washed in PBS, and fresh medium was added. The *in vitro* transcribed Jc1 HCV RNA together with *miR-122* duplex, or *miR-122* duplex only, were transfected into 400 µL of cells at 1.0×10^7 cells/ml by electroporation one day later. *miR-122* duplexes with or without 8 µg HCV RNA were separately prepared for each treatment. Anti-*miR-122* LNA mixmer, which sequesters endogenous *miR-122* and by that disables HCV replication, was also used to treat cells alone or with HCV transfection. The setting for Gene Pulser Xcell (Biorad, USA) was: square wave, 270 V, 20 ms, 1 Pulse, 4 mm cuvette. The cells were washed with PBS to remove dead cells at 6 h post incubation (hpi).

Cells were further incubated with complete DMEM for 72 h, and another round of *miR-122* duplex transfection was carried out to compensate for *miR-122* loss and degradation after three days incubation in cells. HCV infection was allowed to proceed and cells were harvest 48 h later (i.e., 6 d after HCV RNA transfection).

For knockdown experiments, cells were seeded at 1.5×10^5 cells/mL in 12-well plates 24 h before GmR treatment. 50 pmol of GmRs targeting lncRNA candidates in a final volume of 1 mL were transfected with Lipofectamine 2000 24 h prior to HCV transfection or infection. The medium was not supplemented with antibiotics. Medium from the cells was then substituted by fresh DMEM supplemented with antibiotics and FBS, and full-length HCV genome was transfected at 0.375 μg/well using Lipofectamine 2000. Cells were harvested after 12, 24, and 48 h incubation.

To study HCV infection, cells were infected with HCV at the multiplicity of infection (moi) of 0.3 for 4 h. After 4 h of infection, medium supernatants were removed and fresh medium was added to the cells. Cell supernatants and pellets were harvested at the indicated times post-infection. A replication defective mutant version of the HCV genome (NS5B replicase inactivating "GND" mutation) was also prepared to infect cells. PAMP poly(I:C) high molecular weight (HMW) (Invivogen) was also used to treat Huh-7.5 cells and Huh-7 cells at 2.5 μg or 5 μg per well for 8 h. In experiments with JAK-STAT inhibitor, Huh-7.5 cells were treated with the JAK inhibitor ruxolitinib (Invivogen) (0.8 μM) for 1 h, with a subsequent treatment with IFN-α2 (100 units/mL) or mock control for 8 h followed by harvest of RNA.

Experiments were repeated a minimum of three times, with at least two replicates each time.

4.2.6 RNA Samples, DNA Removal and cDNA Preparation

Total RNA was isolated from cells using TRIzol (Invitrogen). After DNase Itreatment, the total RNA was purified using GeneJET RNA Clean-up Kit. Nuclear and cytoplasmic cell fractionation was obtained using the Paris kit following the manufacturer’s instructions (Life Technologies). RNA integrity was checked by agarose gel electrophoresis, and RNA concentrations were measured by Qubit 2.0.

Reverse transcription (RT) was performed using the qScript Flex cDNA Kit

(Quanta Biosciences). Random primers or Gene-specific primers were used in the RT reaction. To determine whether lncRNA candidates are polyadenylated, cDNA with oligo-dT primer was also prepared. No template control (NTC) and no reverse transcription control (NRC) samples are also prepared to check contamination of solutions, primer dimer and DNA presence.

Total RNA for microarray was lysed by using a protocol combining TRIzol Reagent and RNeasy Kit (Qiagen). Next, total RNA was resuspended in RNase-free water. The quality of the RNA was analyzed by Bioanalyzer (Agilent Technologies, Santa Clara, CA, USA). Only RNAs with RNA Integrity Number (RIN) >9.5 were used for subsequent experiments (Figure 4.2).

For 3′ RACE first strand cDNA, when target genes have no poly(A) tail in the RNA sequence, poly(A) tail was added by using E.coli PolyA polymerase (NEB) prior to the RT reaction. RNA was purified using GeneJET RNA Clean-up Kit. The RT reaction was assembled using SuperScript® IV Reverse Transcriptase (Life Technology) following the protocol. OligodT(16)AP (5′-CTGATCTAGAGGTACCGGATCCTTTTTTTTTTTTTTT-3′) was used as RT primer for 3′ RACE cDNA, while gene-specific primers (Table 4.3) were used to synthesize 5′ RACE cDNA.

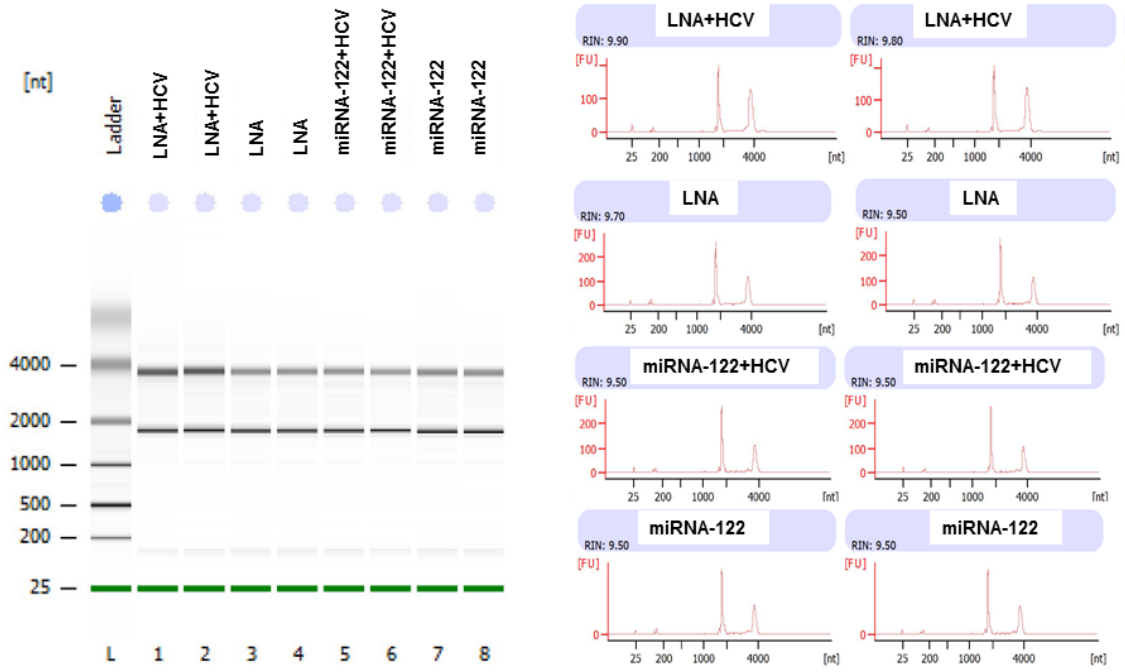

Figure 4.2 Electropherograms of total RNA. Total RNA samples after treatment were analyzed using Bioanalyzer 2100. RNA peaks and RNA Integrity Number (RIN) value were shown in the electropherograms.

4.2.7 Sequencing

4.2.7.1 Library Preparation and Next Generation Sequencing (NGS)

Total RNA was treated by Ribo-Zero rRNA Removal kit (Epicenter) to remove ribosomal RNAs. RNA-seq libraries were made with TruSeq stranded total RNA (illumina) according to the manufacturer's instructions. Assess library quality on a Bioanalyzer (Agilent High Sensitivity Chip) and only libraries showing a narrow distribution with a peak size approximately 300 bp on the electropherogram were used for future sequencing (Figure 4.3).

Sequencing was performed on an Illumina HiSeq 2500 instrument at a depth of ~70 million paired-end, 100 bp long, strand-specific reads per sample (BGI, China). In total, two independent RNA-seq experiments were sequenced to ensure the reproducibility of the data

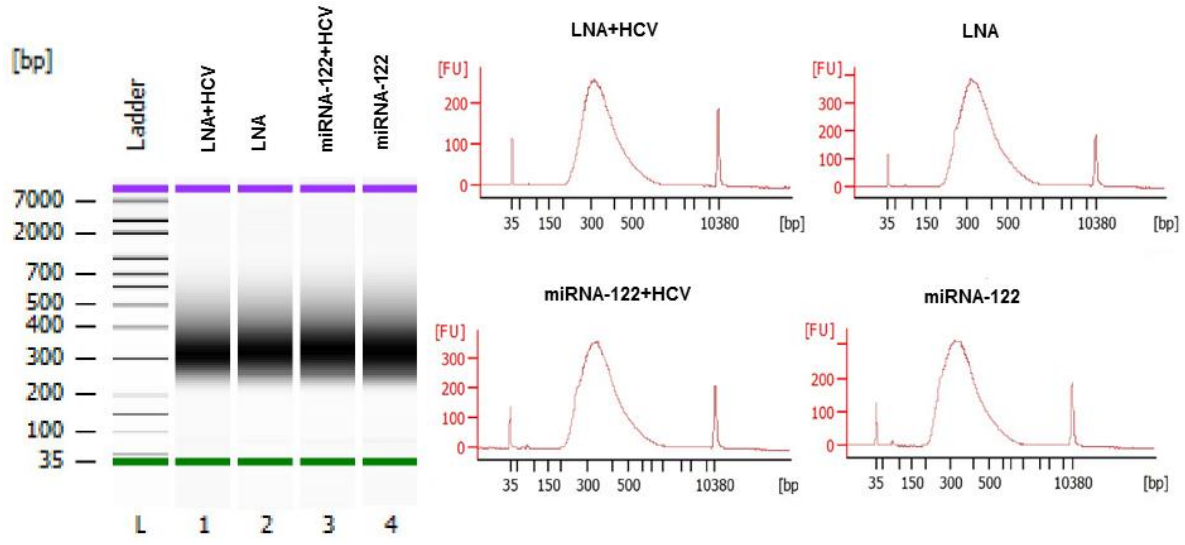

Figure 4.3 Electropherograms of cDNA samples. cDNA samples prepared using high quality total RNA were analyzed using Bioanalyzer 2100. Electropherogram shows a narrow distribution with a peak size approximately 300 bp for each sample.

4.2.7.2 Microarray

Purified total RNAs after *miR-122* with or without HCV treatment were amplified and Cy3-labeled using the LIRAK kit (Agilent Technologies) following the kit instructions. These experiments were performed in collaboration with Dr. Jochen Wilhelm. Per reaction, 200 ng of total RNA was used. The

Cy3-labeled RNA was hybridized overnight to 8×60K 60 mer oligonucleotide spotted microarray slides (Agilent Technologies, design ID 072363). Hybridization and subsequent washing and drying of the slides were performed following the Agilent hybridization protocol. The dried slides were scanned at 2 μm/pixel resolution using the InnoScan 900 (Innopsys, Carbonne, France). Image analysis was performed with Mapix 6.5.0 software, and calculated values for all spots were saved as GenePix results files. Stored data were evaluated using the R software (Team, 2007) and the limma package (Ritchie et al., 2015) from BioConductor (Gentleman et al., 2004). Mean spot signals were background corrected with an offset of 1 using the NormExp procedure on the negative control spots. The logarithms of the background-corrected values were quantile-normalized (Ritchie et al., 2015; Silver et al., 2009). The normalized values were then averaged for replicate spots per array. From different probes addressing the same NCBI gene ID, the probe showing the maximum average signal intensity over the samples was used in subsequent analyses. Genes were ranked for differential expression using a moderated *t*-statistic (Ritchie et al., 2015). Pathway analyses were done using gene set tests on the ranks of the *t*-values (Ritchie et al., 2015). Z value was calculated according to formula: $Z = (E - \bar{E})/SD$, where E is the quantile-normalized log2 signal intensity, $\bar{E}$ is the mean value of E, SD indicates the standard deviation across the samples.

4.2.8 Quantitative RT-PCR (qRT-PCR)

qRT-PCR was performed with the PerfeCTa SYBR Green FastMix (Quanta Biosciences) according to the manufacturer's instructions in the StepOnePlus™ Real-Time PCR System (Applied Biosystems) with the following temperature setting: initial denaturation for 20 seconds (s) at 95 ℃; 40 cycles of subsequent denaturation (3 s at 95 ℃) and elongation (30 s at 60 ℃); melting curve for 20 min. The secondary products and primer-dimers were excluded via melting curve and agarose gel electrophoresis. The specificity of amplification was verified by the presence of a single peak in the melting curve and also by sequencing (Microsynth SeqLab, Germany). *GAPDH* mRNA levels were evaluated in all cases as a reference, and other expression results were normalized to *GAPDH*.

Amplification efficiencies (E) of each primer pair were calculated using the following formula: E = 10(-1/slope), except for *MDA5, IFN-β, IFN-α, IL28A, U6*. The E of primers used in this study was within the range of 1.8-2.2 (Schmittgen and Livak, 2008) (Table 4.4).

Table 4.4 Amplification efficiencies (E) of each primer pair

Target genes	Efficiency (%)	slope	E
LncR 1	92.61	-3.513	1.847
LncR 2	100.5	-3.31	2.021
LncR 3	96.3	-3.414	1.929
LncR $3^{3'}$	99.81	-3.326	2.007
LncR 7-2	91.35	-3.548	1.818
LncR $7\text{-}2^{3'}$	109.5	-3.114	2.211
LncR 8	95.47	-3.435	1.911
LncR $8^{3'}$	109.4	-3.115	2.21
LncR 9	104.9	-3.209	2.116
LncR 10	98.96	-3.347	1.988
LncR $10^{3'}$	104.6	-3.217	2.108
GAPDH	95.71	-3.429	1.916
β-actin	95.49	-3.435	1.911
U99	92.25	-3.523	1.838
GPR55	97.6	-3.381	1.958
ITM2C	109.2	-3.12	2.205
CXCL10	102.1	-3.272	2.056
ISG15	98.85	-3.35	1.985
Mx1	95.27	-3.441	1.906
IFITM1	105.1	-3.205	2.12
GAS5	94.097	-3.472	1.880

To calculate the relative RNA levels in cytoplasmic/nuclear fractions, $2^{-\Delta Ct}$ was used, where Ct is the threshold cycle number, ΔCt = Ct of the gene in nucleus-Ct in cytoplasm. The expression fold change compared to control group was obtained using calculation: Fold change = $(E_{target})\text{^}\Delta Ct_{target}^{(control\text{-}sample)/}(E_{ref})\text{^}\Delta Ct_{ref}^{(control\text{-}sample)}$, where E_{target} and E_{ref} are the respective amplification efficiencies of target genes and reference gene *GAPDH*;

ΔCt = Ct of the control sample - Ct of the treatment sample. Fold change = $2^{\Delta Ct_{sample}^{(ref-target)}}/2^{\Delta Ct_{control}^{(ref-target)}}$, where ΔCt = Ct of the reference gene *GAPDH* - Ct of the target gene was also applied when E is not obtained (*MDA5, IFN-β, IFN-α, IL28A*). The relative expression level of lncRNAs after GmR knockdown was presented as $1000*2^{-\Delta Ct}$, ΔCt = Ct of the target gene - Ct of the reference gene *GAPDH*. The results of all biological replicates (minimum of three) and technical replicates (minimum of two) were used to derive the final data with standard error of the mean (SEM) graphed as error bars.

4.2.9 Protein Biochemical Techniques

4.2.9.1 Immunofluorescence

One day before transfection, coverslips were heated in pure Ethanol and covered for 30 min with 0.1 mg/mL Poly-L-Lysin (30000-70000). Two days after transfection of HCV full-length Jc1 genomes, cells were washed with PBS and fixed with 4% paraformaldehyde for 10 min. Cells were washed again 3 times (×) with ice cold PBS, permeabilized with cold acetone for 10 min at −20 °C and again washed. Then, cells were incubated with 1% BSA, 22.5 mg/mL glycine in PBST (1 × PBS, 0.5% Tween 20) (Glycin-PBST) for 10 min. For staining, cells were incubated with a 1:500 dilution of Anti-HCV NS3 antibody (8 G-2, Abcam) in 1% BSA for 1 h at room temperature. Cells were washed 3 ×with Glycin-PBST and then incubated with a 1:200 dilution of the secondary antibody (goat anti-mouse IgG1, Alexa Fluor® 488 conjugate) for 1 h at 37 ℃ in the dark. Cells were again washed 3 ×with Glycin-PBST, incubated with Fluoroshield Mounting Medium With DAPI (Abcam) for 5 min. Fluorescent images were obtained with a fluorescent microscope (Olympus).

4.2.9.2 Western blot

Cell pellets for western blots were lysed in 200 µL buffer. Following the pelleting of cell debris, 10 µL protein extracts were mixed with SDS loading buffer, denatured at 95 ℃ for 10 min, and subjected to 12% SDS-polyacrylamide gel electrophoresis.

	Stacking gel (5%)	Resolving gel (12%)
40% Bisacryamid (29:1)	375 µL	1800 µL
Tricine-Buffer	750 µL	2000 µL
Glycerol	-	650 µL
ddH_2O	1842 µL	1484 µL
APS	30 µL	60 µL
TEMED	3 µL	6 µL
Total	3 mL	6 mL

Next, proteins were transferred onto a PVDF membrane (Immobilon). PVDF membrane is first activated by immersing it in 100 % methanol for 1 min and placed in the blotting chamber along with the gel. The blotting chamber was assembled in the following order:

- 2 ×3 MM chromatography paper (Whatman paper)
- PVDF membrane
- Gel
- 2 ×3 MM chromatography paper (Whatman paper)

It is necessary to make sure that there are no bubbles between different layers of paper, membrane and gel. After assembly an electric current of 43 mA per membrane is applied for 1.5 hours. Membranes were blocked with 7.5% milk in PBS-T for 1 h and incubated with monoclonal antibodies against GAPDH diluted 1:15000 (clone GAPDH-71.1, Sigma-Aldrich), anti-HCV NS3 antibody 8G-2 (Abcam) diluted 1:500. After washing, membranes were incubated for another 1 h with a secondary goat-anti-mouse IgG HOR antibody conjugated with peroxidase diluted 1:40000 (Sigma-Aldrich). Western blots were developed with SuperSignal West Femto Chemiluminescent substrate (Pierce, Rockford, IL). The quantification of protein bands from western blotting films was performed by using Image J (NIH) (https://imagej.nih.gov/ij/index.html). The expression level was presented as IntDen ratio of each NS3 band relative to each GAPDH band.

4.2.10 RACE

3′RACE was performed using the conditions recommended by the 3′-Full RACE Core Set (TaKaRa, Japan) and RNA extracted from Huh-7.5 cells treated

with HCV and *miR-122* for 6 days. The outer PCR reaction mixture had a total volume of 50 μL and contained 5 μL of first-strand cDNA, 5 μL of 10×TrueStart Hot start Taq Reaction Buffer (ThermoFisher), 2 μL of 10 μM 3GSPouter, 2 μL of 10 μM AP, 0.4 μL of dNTP (25mM each), 5 μL of $MgCl_2$ (25 mM), 0.25 μL of TrueStart Hot start Taq DNA Polymerase (5 U/μL), and 30.35 μL of RNase-free water. PCR was conducted as follows: 95 ℃ for 2 min; 30 cycles of denaturation at 95 ℃ for 30 s, annealing at 50 ℃ for 30 s, extension at 72 ℃ for 1min 30 s, and a final extension at 72 ℃ for 10 min. The inner PCR reaction mixture contained 2 μL of outer PCR products, 5 μL of 10×TrueStart Hot start Taq Reaction Buffer, 2 μL of 10 μM 3GSPinner, 2 μL of 10 μM 3RACE-R, 0.4 μL of dNTP (25mM each), 5 μL of $MgCl_2$ (25 mM), 0.25 μL of TrueStart Hot start Taq DNA Polymerase (5 U/μL), and 33.35 μL of RNase-free water. The PCR procedure was the same as that described for the outer PCR, except to raise the annealing temperature (Tm) to 60 ℃.

Gene specific first strand cDNA for 5′ RACE was treated before PCR as described before (Cheng et al., 2011): First, apply RNaseH (NEB) to digest the RNA template in the cDNA solution following the protocol. Next, precipitate the cDNA by incubating with 100μL of RNase-free water and 500μL of 100% Ethanol for 30min at 40 ℃, then proceed with 70% Ethanol wash. Terminal deoxynucleotidyl-transferase (30U) (NEB) was used to add polyA tail to the 5′end of the purified cDNA at last. The PCR reaction mixture and procedure for the 5′ RACE were the same as that described above for the 3′ RACE. 5GSPouter and oligo dT(16)AP were used for the first round PCR. 5GSPinner and AP were used at the second round. Sequences of primers were listed in Table 4.3.

From preparative agarose gels the desired bands were cut out during UV light exposure, amplified products were resolved in agarose gels using the GeneJET Gel Extraction Kit, following the manufacturer's protocol, and insert into the vector from TA Cloning® Kit (Life Technologies), and transform into TOP10 cells. Sequencing was done at Microsynth SeqLab.

4.2.11 Protein-coding Potential

The features of lncRNA candidates, including the reference sequence, the length, Gene symbol and located chromosome of these lncRNAs were collected from NCBI (https://www.ncbi.nlm.nih.gov/) and are listed in Table 4.5. The

names used in this study were based on LNCipedia gene ID or HGNC Gene Symbol. The tissue specificity of lncRNA expression was evaluated according to RNA sequencing of total RNA from 20 human tissues with open access at https://www.ncbi.nlm.nih.gov/gene/. The data are normalized by RPKM (Reads Per Kilobase of transcript per Million mapped reads) (Figure 2.2 E).

Table 4.5 Characteristics of the lncRNA candidates

LncRNA	Ref.	Chr	Length(bp)	Gene symbol	Name
LncR 3	NR_033376.1	6	1753	lincRNA 222	LINC00222
LncR 7-2	NR_104615.1	5	3451	LOC100506688	*Lnc-SLC12A7-4:5*
LncR 8	NR_038238.1	2	1893	LOC151484	*Lnc-ITM2C-1*
LncR 10	NR_026974.1	8	3250	ZNF252P antisense RNA 1	*ZNF252P-AS1*

Ref.: NCBI Reference Sequence.

Coding potential of lncRNA candidates was evaluated by Open reading frame Finder (https://www.ncbi.nlm.nih.gov/orffinder/), and by searching the LNCipedia 5.2 (http://www.lncipedia.org) for the presence of our candidates in the Pride proteomics database and the Lee lists of novel coding RNAs or Bazzini lists of lncRNAs containing small open reading frames obtained in ribosome profiling experiments. The evaluation of our candidates by Phylogenetic Codon Substitution Frequencies (PhyloCSF) and the coding potential assessment tool (CPAT) were also included (Carnero et al., 2016; Volders et al., 2015). Results from LNCipedia are listed in Table 2.1.

4.2.12 Statistical Analysis

The graphs showed mean and standard error of mean (Mean ± SEM) of at least three independent experiments. SEM is represented by error bar. Comparisons between groups were performed using two-tailed Student's *t*-test by GraphPad. *p*-values lower than 0.05 were considered with statistical significance. * denotes $p \leq 0.05$, ** $p \leq 0.01$, *** $p \leq 0.001$, and **** $p \leq 0.0001$.

5. References

1. Ahmad, W., Ijaz, B., Hassan, S., 2012. Gene expression profiling of HCV genotype 3a initial liver fibrosis and cirrhosis patients using microarray. *Journal of translational medicine* 10.
2. Alazard-Dany, N., Denolly, S., Boson, B., Cosset, F.L., 2019. Overview of HCV Life Cycle with a Special Focus on Current and Possible Future Antiviral Targets. *Viruses* 11.
3. Appel, N., Schaller, T., Penin, F., Bartenschlager, R., 2006a. From structure to function: new insights into hepatitis C virus RNA replication. *The Journal of biological chemistry* 281, 9833-9836.
4. Appel, N., Schaller, T., Penin, F., Bartenschlager, R., 2006b. From structure to function: new insights into hepatitis C virus RNA replication. *J Biol Chem* 281, 9833-9836.
5. Arnaud, N., Dabo, S., Akazawa, D., Fukasawa, M., Shinkai-Ouchi, F., Hugon, J., Wakita, T., Meurs, E.F., 2011. Hepatitis C virus reveals a novel early control in acute immune response. *PLoS pathogens* 7, e1002289.
6. Ashfaq, U.A., Javed, T., Rehman, S., Nawaz, Z., Riazuddin, S., 2011. An overview of HCV molecular biology,replication and immune responses. *Virology journal* 8, 10.
7. Avidan U. Neumann, Nancy P. Lam, Harel Dahari, David R. Gretch, Thelma E. Wiley, Thomas J. Layden, Perelson, A.S., 1998. Hepatitis C Viral Dynamics *in Vivo* and the Antiviral Efficacy of Interferon-α Therapy. *Science* 282.
8. Barriocanal, M., Carnero, E., Segura, V., Fortes, P., 2014. Long Non-Coding RNA BST2/BISPR is Induced by IFN and Regulates the Expression of the Antiviral Factor Tetherin. *Frontiers in immunology* 5, 655.
9. Barriocanal, M., Fortes, P., 2017. Long Non-coding RNAs in Hepatitis C Virus-Infected Cells. *Frontiers in microbiology* 8, 1833.
10. Bartenschlager, R., Penin, F., Lohmann, V., Andre, P., 2011. Assembly of infectious hepatitis C virus particles. *Trends in microbiology* 19, 95-103.
11. Bayer, K., Banning, C., Bruss, V., Wiltzer-Bach, L., Schindler, M., 2016. Hepatitis C Virus Is Released via a Noncanonical Secretory Route. *Journal*

of virology 90, 10558-10573.

12. Berger, K.L., Cooper, J.D., Heaton, N.S., Yoon, R., Oakland, T.E., Jordan, T.X., Mateu, G., Grakoui, A., Randall, G., 2009. Roles for endocytic trafficking and phosphatidylinositol 4-kinase III alpha in hepatitis C virus replication. *Proceedings of the National Academy of Sciences of the United States of America* 106, 7577-7582.
13. Bevilacqua, V., Gioia, U., Di Carlo, V., Tortorelli, A.F., Colombo, T., Bozzoni, I., Laneve, P., Caffarelli, E., 2015. Identification of linc-NeD125, a novel long non coding RNA that hosts miR-125b-1 and negatively controls proliferation of human neuroblastoma cells. *RNA biology* 12, 1323-1337.
14. Blight, K.J., McKeating, J.A., Rice, C.M., 2002. Highly Permissive Cell Lines for Subgenomic and Genomic Hepatitis C Virus RNA Replication. *Journal of virology* 76, 13001-13014.
15. Boldanova, T., Suslov, A., Heim, M.H., Necsulea, A., 2017. Transcriptional response to hepatitis C virus infection and interferon-alpha treatment in the human liver. *EMBO molecular medicine* 9, 816-834.
16. Cao, H., Zhao, K., Yao, Y., Guo, J., Gao, X., Yang, Q., Guo, M., Zhu, W., Wang, Y., Wu, C., Chen, J., Zhou, Y., Hu, X., Lu, M., Chen, X., Pei, R., 2018. RNA binding protein 24 regulates the translation and replication of hepatitis C virus. *Protein & cell* 9, 930-944.
17. Cao, X., Ding, Q., Lu, J., Tao, W., Huang, B., Zhao, Y., Niu, J., Liu, Y.J., Zhong, J., 2015. MDA5 plays a critical role in interferon response during hepatitis C virus infection. *Journal of hepatology* 62, 771-778.
18. Carnero, E., Barriocanal, M., Prior, C., Pablo Unfried, J., Segura, V., Guruceaga, E., Enguita, M., Smerdou, C., Gastaminza, P., Fortes, P., 2016. Long noncoding RNA EGOT negatively affects the antiviral response and favors HCV replication. *EMBO reports* 17, 1013-1028.
19. Chan, J.H., Lim, S.H., Wong, W.F., 2006. Antisense oligonucleotides from design to therapeutic application. *Clinical and Experimental Pharmacology and Physiology* 33, 533-540.
20. Chang J., Nicolas E., Marks D., Sander C., Lerro A., Buendia M. A., Xu C., Mason W. S., Moloshok T., Bort R., Zaret K.S., M.., T.J., 2004. miR-122, a Mammalian Liver-Specific microRNA, is Processed from hcr mRNA and

MayDownregulate the High Affinity Cationic Amino Acid Transporter CAT-1. *RNA biology* 1, 106-113.

21. Chen, J.J., Hsueh, H.M., Delongchamp, R.R., Lin, C.J., Tsai, C.A., 2007. Reproducibility of microarray data: a further analysis of microarray quality control (MAQC) data. *BMC bioinformatics* 8, 412.
22. Cheng, H.L., Ji, N.J., Peng, Y.X., Shen, X., Wu, C.C., Xu, J.H., Dong, Z.G., 2011. Cloning and expression analysis of a full length cDNA encoding Glucokinase from PengZe CrucianCarp (*Carassius auratus* var. PengZe) (In Chinese). *Chinese Journal of Animal Nutrition* 23.
23. Chiurchiu, V., Lanuti, M., De Bardi, M., Battistini, L., Maccarrone, M., 2015. The differential characterization of GPR55 receptor in human peripheral blood reveals a distinctive expression in monocytes and NK cells and a proinflammatory role in these innate cells. *International immunology* 27, 153-160.
24. Choo, Q.-L., Kuo, G., Weiner, A.J., Overby, L.R., Bradley, D.W., Houghton, M., 1989. Isolation of a cDNA Clone Derived from a Blood-Borne Non-A, Non-B Viral Hepatitis Genome. *Science* 244, 359-362.
25. Domingues, P., Bamford, C.G., Boutell, C., McLauchlan, J., 2015. Inhibition of hepatitis C virus RNA replication by ISG15 does not require its conjugation to protein substrates by the HERC5 E3 ligase. *The Journal of general virology* 96, 3236-3242.
26. Dreux, M., Gastaminza, P., Wieland, S.F., Chisari, F.V., 2009. The autophagy machinery is required to initiate hepatitis C virus replication. *Proceedings of the National Academy of Sciences of the United States of America* 106, 14046-14051.
27. Dubuisson, J., Cosset, F.L., 2014. Virology and cell biology of the hepatitis C virus life cycle: an update. *Journal of hepatology* 61, S3-S13.
28. Durinck, K., Wallaert, A., Van de Walle, I., Van Loocke, W., Volders, P.J., Vanhauwaert, S., Geerdens, E., Benoit, Y., Van Roy, N., Poppe, B., Soulier, J., Cools, J., Mestdagh, P., Vandesompele, J., Rondou, P., Van Vlierberghe, P., Taghon, T., Speleman, F., 2014. The Notch driven long non-coding RNA repertoire in T-cell acute lymphoblastic leukemia. *Haematologica* 99, 1808-1816.
29. Dustin A. Cobb, Ok-Kyung Kim, Lucy Golden-Mason, Hugo R. Rosen,

Hahn, Y.S., 2018. Hepatocyte-Derived Exosomes Promote T Follicular Regulatory Cell Expansion During Hepatitis C Virus Infection. *Hepatology* 67.

30. Dustin, L.B., 2017. Innate and Adaptive Immune Responses in Chronic HCV Infection. Current drug targets 18, 826-843.
31. Dustin, L.B., Bartolini, B., Capobianchi, M.R., Pistello, M., 2016. Hepatitis C virus: life cycle in cells, infection and host response, and analysis of molecular markers influencing the outcome of infection and response to therapy. *Clinical microbiology and infection* 22, 826-832.
32. Fehr, C., Conrad, K.D., Niepmann, M., 2012. Differential stimulation of hepatitis C virus RNA translation by microRNA-122 in different cell cycle phases. *Cell cycle* 11, 277-285.
33. Feigelstock, D.A., Mihalik, K.B., Kaplan, G., M., F.S., 2010. Increased susceptibility of Huh7 cells to HCV replication does not require mutations in RIG-I. *Virology journal* 7.
34. Franciscus, A., 2016. An Overview of: Hepatitis C Transmission and Prevention. *Hepatitis C Support Project*.
35. Garcia-Alvarez, M., Berenguer, J., Jimenez-Sousa, M.A., Pineda-Tenor, D., Aldamiz-Echevarria, T., Tejerina, F., Diez, C., Vazquez-Moron, S., Resino, S., 2017. Mx1, OAS1 and OAS2 polymorphisms are associated with the severity of liver disease in HIV/HCV-coinfected patients: A cross-sectional study. *Scientific reports* 7, 41516.
36. Gentleman, R.C., Carey, V.J., Bates, D.M., Bolstad, B., Dettling, M., Dudoit, S., Ellis, B., Gautier, L., Ge, Y., Gentry, J., Hornik, K., Hothorn, T., Huber, W., Iacus, S., Irizarry, R., Leisch, F., Li, C., Maechler, M., Rossini, A.J., Sawitzki, G., Smith, C., Smyth, G., Tierney, L., Yang, J.Y., Zhang, J., 2004. Bioconductor: open software development for computational biology and bioinformatics. *Genome biology* 5, R80.
37. Gerresheim, G.K., Bathke, J., Michel, A.M., Andreev, D.E., Shalamova, L.A., Rossbach, O., Hu, P., Glebe, D., Fricke, M., Marz, M., Goesmann, A., Kiniry, S.J., Baranov, P.V., Shatsky, I.N., Niepmann, M., 2019. Cellular Gene Expression during Hepatitis C Virus Replication as Revealed by Ribosome Profiling. *International journal of molecular sciences* 20.
38. Ghada, F.H., Nancy, M.E.-A., 2009. Influence of HCV Infection on

Insulin-Like Growth Factor 1 and Proinflammatory Cytokines: Association with Risk for Growth Hormone Resistance Development. *The Egyptian Journal of Immunology* 16, 115-124.

39. Gokhale, N.S., Vazquez, C., Horner, S.M., 2014. Hepatitis C Virus. Strategies to Evade Antiviral Responses. *Future virology* 9, 1061-1075.
40. Heim, M.H., Thimme, R., 2014. Innate and adaptive immune responses in HCV infections. *Journal of hepatology* 61, S14-25.
41. Henke, J.I., Goergen, D., Zheng, J., Song, Y., Schuettler, C.G., Fehr, C., Juenemann, C., Niepmann, M., 2008. microRNA-122 stimulates translation of hepatitis C virus. *EMBO* 27, 3300-3310.
42. Hu, J., Gao, D.Z., 2012. Distinction immune genes of hepatitis-induced heptatocellular carcinoma. *Bioinformatics* 28, 3191-3194.
43. Huang, J., Li, Y., Lu, Z., Che, Y., Sun, S., Mao, S., Lei, Y., Zang, R., Li, N., Sun, N., He, J., 2018. Long non-coding RNA GAS5 is induced by interferons and plays an antitumor role in esophageal squamous cell carcinoma. *Cancer medicine* 7(7): 3157–3167.
44. Iwai, A., Takegami, T., Shiozaki, T., Miyazaki, T., 2011. Hepatitis C virus NS3 protein can activate the Notch-signaling pathway through binding to a transcription factor, SRCAP. *PloS one* 6, e20718.
45. Jackson, R.J., Hellen, C.U., Pestova, T.V., 2010. The mechanism of eukaryotic translation initiation and principles of its regulation. Nature reviews. *Molecular cell biology* 11, 113-127.
46. Jaksik, R., Iwanaszko, M., Rzeszowska-Wolny, J., Kimmel, M., 2015. Microarray experiments and factors which affect their reliability. *Biology direct* 10, 46.
47. Jirasko, V., Montserret, R., Lee, J.Y., Gouttenoire, J., Moradpour, D., Penin, F., Bartenschlager, R., 2010. Structural and functional studies of nonstructural protein 2 of the hepatitis C virus reveal its key role as organizer of virion assembly. *PLoS pathogens* 6, e1001233.
48. Jopling, C.L., Yi, M.K., Lancaster, A.M., Lemon, S.M., Sarnow, P., 2005. Modulation of Hepatitis C Virus RNA Abundance by a Liver-Specific MicroRNA. *Science* 309, 1577-1581.
49. Kambara, H., Niazi, F., Kostadinova, L., Moonka, D.K., Siegel, C.T., Post, A.B., Carnero, E., Barriocanal, M., Fortes, P., Anthony, D.D., Valadkhan, S.,

2014. Negative regulation of the interferon response by an interferon-induced long non-coding RNA. *Nucleic acids research* 42, 10668-10680.

50. Kasprzak, A., Adamek, A., 2012. The insulin-like growth factor (IGF) signaling axis and hepatitis C virus-associated carcinogenesis (review). *International journal of oncology* 41, 1919-1931.
51. Kim, M.J., Yoo, J.Y., 2010. Inhibition of hepatitis C virus replication by IFN-mediated ISGylation of HCV-NS5A. *Journal of immunology* 185, 4311-4318.
52. Klenerman, P., 2016. HCV vaccines—back to the future? *Annals of Blood* 2, 2-2.
53. Kohara, K.T., Iizuka, N., Kohara, M., Nomoto, A., 1992. Internal Ribosome Entry Site within Hepatitis C Virus RNA. *Journal of virology* 66, 1476-1483.
54. Kopp, F., Mendell, J.T., 2018. Functional Classification and Experimental Dissection of Long Noncoding RNAs. *Cell* 172, 393-407.
55. Kukla, M., Berdowska, A., Stygar, D., Gabriel, A., Mazur, W., Logiewa-Bazger, B., Sobala-Szczygiel, B., Buldak, R.J., Rokitka, M., Zajecki, W., Kepa, L., Sawczyn, T., Zwirska-Korczala, K., 2012. Serum FGF21 and RBP4 levels in patients with chronic hepatitis C. *Scandinavian journal of gastroenterology* 47, 1037-1047.
56. Lennox, K.A., Behlke, M.A., 2016. mini-review:current strategies to knockdown long non-coding RNAs. *J Rare Dis Res Treat* 1, 66-70.
57. Li, H. C., Lo, S. Y., 2015. Hepatitis C virus: Virology, diagnosis and treatment. *World journal of hepatology* 7, 1377-1389.
58. Li, K., Chen, Z., Kato, N., Gale, M., Jr., Lemon, S.M., 2005. Distinct poly(I-C) and virus-activated signaling pathways leading to interferon-beta production in hepatocytes. *The Journal of biological chemistry* 280, 16739-16747.
59. Lindenbach, B.D., Rice, C.M., 2005. Unravelling hepatitis C virus replication from genome to function. *Nature* 436, 933-938.
60. Lindenbach, B.D., Rice, C.M., 2013. The ins and outs of hepatitis C virus entry and assembly. Nature reviews. *Microbiology* 11, 688-700.
61. Liu, J., Wang, Z., Tang, J., Tang, R., Shan, X., Zhang, W., Chen, Q., Zhou,

F., Chen, K., Huang, A., Tang, N., 2011. Hepatitis C virus core protein activates Wnt/beta-catenin signaling through multiple regulation of upstream molecules in the SMMC-7721 cell line. *Archives of virology* 156, 1013-1023.

62. Liu, P., Feng, Y., Dong, D., Liu, X., Chen, Y., Wang, Y., Zhou, Y., 2016. Enhanced renoprotective effect of IGF-1 modified human umbilical cord-derived mesenchymal stem cells on gentamicin-induced acute kidney injury. *Scientific reports* 6, 20287.
63. Lohmann, V., 2013. Hepatitis C virus RNA replication. *Current topics in microbiology and immunology* 369, 167-198.
64. Masaki, T., Suzuki, R., Murakami, K., Aizaki, H., Ishii, K., Murayama, A., Date, T., Matsuura, Y., Miyamura, T., Wakita, T., Suzuki, T., 2008. Interaction of hepatitis C virus nonstructural protein 5A with core protein is critical for the production of infectious virus particles. *Journal of virology* 82, 7964-7976.
65. Messina, J.P., Humphreys, I., Flaxman, A., Brown, A., Cooke, G.S., Pybus, O.G., Barnes, E., 2015. Global Distribution and Prevalence of Hepatitis C Virus Genotypes. *Hepatology* 61, 77-87.
66. Morlando, M., Ballarino, M., Fatica, A., 2015. Long Non-Coding RNAs: New Players in Hematopoiesis and Leukemia. *Frontiers in medicine* 2, 23.
67. Morozov, V.A., Lagaye, S., 2018. Hepatitis C virus: Morphogenesis, infection and therapy. *World journal of hepatology* 10, 186-212.
68. Nam, D.K., Lee, S., Zhou, G., Cao, X., Wang, C., Clark, T., Chen, J., Rowley, J.D., Wang, S.M., 2002. Oligo(dT) primer generates a high frequency of truncated cDNAs through internal poly(A) priming during reverse transcription. *Proceedings of the National Academy of Sciences of the United States of America* 99, 6152-6156.
69. Narayana, S.K., Helbig, K.J., McCartney, E.M., Eyre, N.S., Bull, R.A., Eltahla, A., Lloyd, A.R., Beard, M.R., 2015. The Interferon-induced Transmembrane Proteins, IFITM1, IFITM2, and IFITM3 Inhibit Hepatitis C Virus Entry. *The Journal of biological chemistry* 290, 25946-25959.
70. Neumann-Haefelin, C., Thimme, R., 2013. Adaptive immune responses in hepatitis C virus infection. *Current topics in microbiology and immunology* 369, 243-262.

71. Niepmann, M., 2013. Hepatitis C virus RNA translation. *Current topics in microbiology and immunology* 369, 143-166.
72. Niepmann, M., Shalamova, L.A., Gerresheim, G.K., Rossbach, O., 2018. Signals Involved in Regulation of Hepatitis C Virus RNA Genome Translation and Replication. *Frontiers in microbiology* 9, 395.
73. Nishitsuji, H., Funami, K., Shimizu, Y., Ujino, S., Sugiyama, K., Seya, T., Takaku, H., Shimotohno, K., 2013. Hepatitis C virus infection induces inflammatory cytokines and chemokines mediated by the cross talk between hepatocytes and stellate cells. *Journal of virology* 87, 8169-8178.
74. Nishitsujia, H., Ujinoa, S., Yoshioa, S., Sugiyamaa, M., Mizokamia, M., Kantoa, T., Shimotohnoa, K., 2016. Long noncoding RNA #32 contributes to antiviral responses by controlling interferon-stimulated gene expression. *Proceedings of the National Academy of Sciences of the United States of America* 113, 10388–10393.
75. Nouroz, F., Shaheen, S., Mujtaba, G., Noreen, S., 2015. An overview on hepatitis C virus genotypes and its control. *Egyptian Journal of Medical Human Genetics* 16, 291-298.
76. Okabe, H., Delgado, E., Lee, J.M., Yang, J., Kinoshita, H., Hayashi, H., Tsung, A., Behari, J., Beppu, T., Baba, H., Monga, S.P., 2014. Role of leukocyte cell-derived chemotaxin 2 as a biomarker in hepatocellular carcinoma. *PloS one* 9, e98817.
77. Omura, H., Liu, F., Shimakami, T., Murai, K., Shirasaki, T., Kitabayashi, J., Funaki, M., Nishikawa, T., Nakai, R., Sumiyadorj, A., Hayashi, T., Yamashita, T., Honda, M., Kaneko, S., 2019. Establishment and Characterization of a New Cell Line Permissive for Hepatitis C Virus Infection. *Scientific reports* 9, 7943.
78. Ouyang, J., Zhu, X., Chen, Y., Wei, H., Chen, Q., Chi, X., Qi, B., Zhang, L., Zhao, Y., Gao, G.F., Wang, G., Chen, J.L., 2014. NRAV, a long noncoding RNA, modulates antiviral responses through suppression of interferon-stimulated gene transcription. *Cell host & microbe* 16, 616-626.
79. Ovejero, C., Cavard, C., Perianin, A., Hakvoort, T., Vermeulen, J., Godard, C., Fabre, M., Chafey, P., Suzuki, K., Romagnolo, B., Yamagoe, S., Perret, C., 2004. Identification of the leukocyte cell-derived chemotaxin 2 as a direct target gene of beta-catenin in the liver. *Hepatology* 40, 167-176.

80. Patsenker, E., Sachse, P., Chicca, A., Gachet, M.S., Schneider, V., Mattsson, J., Lanz, C., Worni, M., de Gottardi, A., Semmo, M., Hampe, J., Schafmayer, C., Brenneisen, R., Gertsch, J., Stickel, F., Semmo, N., 2015. Elevated levels of endocannabinoids in chronic hepatitis C may modulate cellular immune response and hepatic stellate cell activation. *International journal of molecular sciences* 16, 7057-7076.
81. Paul, D., Madan, V., Bartenschlager, R., 2014. Hepatitis C virus RNA replication and assembly: living on the fat of the land. *Cell host & microbe* 16, 569-579.
82. Pesce, M., D'Alessandro, A., Borrelli, O., Gigli, S., Seguella, L., Cuomo, R., Esposito, G., Sarnelli, G., 2018. Endocannabinoid-related compounds in gastrointestinal diseases. *Journal of cellular and molecular medicine* 22, 706-715.
83. Pessa, H.K., Will, C.L., Meng, X., Schneider, C., Watkins, N.J., Perala, N., Nymark, M., Turunen, J.J., Luhrmann, R., Frilander, M.J., 2008. Minor spliceosome components are predominantly localized in the nucleus. *Proceedings of the National Academy of Sciences of the United States of America* 105, 8655-8660.
84. Pezacki, J.P., Singaravelu, R., Lyn, R.K., 2010. Host-virus interactions during hepatitis C virus infection: a complex and dynamic molecular biosystem. *Molecular bioSystems* 6, 1131-1142.
85. Pietschmann, T., Kaul, A., Koutsoudakis, G., Shavinskaya, A., Kallis, S., Steinmann, E., Abid, K., Negro, F., Dreux, M., Cosset, F.L., Bartenschlager, R., 2006. Construction and characterization of infectious intragenotypic and intergenotypic hepatitis C virus chimeras. *Proceedings of the National Academy of Sciences of the United States of America* 103, 7408-7413.
86. Multiplex qPCR—how to get started. Available online: https://www.idtdna.com/pages/education/decoded/article/multiplex-qpcr-how-to-get-started (accessed on 4 January 2018).
87. Qian, X., Xu, C., Zhao, P., Qi, Z., 2016. Long non-coding RNA GAS5 inhibited hepatitis C virus replication by binding viral NS3 protein. *Virology* 492, 155-165.
88. Ramakrishnaiah, V., Thumann, C., Fofana, I., Habersetzer, F., Pan, Q., de Ruiter, P.E., Willemsen, R., Demmers, J.A., Stalin Raj, V., Jenster, G.,

Kwekkeboom, J., Tilanus, H.W., Haagmans, B.L., Baumert, T.F., van der Laan, L.J., 2013. Exosome-mediated transmission of hepatitis C virus between human hepatoma Huh7.5 cells. *Proceedings of the National Academy of Sciences of the United States of America* 110, 13109-13113.

89. Rios-Marco, P., Romero-Lopez, C., Berzal-Herranz, A., 2016. The *cis*-acting replication element of the Hepatitis C virus genome recruits host factors that influence viral replication and translation. *Scientific reports* 6, 25729.
90. Ritchie, M.E., Phipson, B., Wu, D., Hu, Y., Law, C.W., Shi, W., Smyth, G.K., 2015. limma powers differential expression analyses for RNA-sequencing and microarray studies. *Nucleic acids research* 43, e47.
91. Sarpel, D., Carter, D., Wasserman, I., Oxnard, M., T. Dieterich, D., 2017. An update on the management of chronic hepatitis B and C infection. *Clinical Pharmacist* 9 (8).
92. Schmittgen, T.D., Livak, K.J., 2008. Analyzing real-time PCR data by the comparative CT method. *Nature protocols* 3, 1101-1108.
93. Shen, J., Huang, C.K., Yu, H., Shen, B., Zhang, Y., Liang, Y., Li, Z., Feng, X., Zhao, J., Duan, L., Cai, X., 2017. The role of exosomes in hepatitis, liver cirrhosis and hepatocellular carcinoma. *Journal of cellular and molecular medicine* 21, 986-992.
94. Shimakami, T., Yamane, D., Jangra, R.K., Kempf, B.J., Spaniel, C., Barton, D.J., Lemon, S.M., 2012. Stabilization of hepatitis C virus RNA by an Ago2-miR-122 complex. *Proceedings of the National Academy of Sciences of the United States of America* 109, 941-946.
95. Silver, J.D., Ritchie, M.E., Smyth, G.K., 2009. Microarray background correction: maximum likelihood estimation for the normal-exponential convolution. *Biostatistics* 10, 352-363.
96. Stretch, C., Khan, S., Asgarian, N., Eisner, R., Vaisipour, S., Damaraju, S., Graham, K., Bathe, O.F., Steed, H., Greiner, R., Baracos, V.E., 2013. Effects of sample size on differential gene expression, rank order and prediction accuracy of a gene signature. *PloS one* 8, e65380.
97. Sumpter, R., Jr., Loo, Y.M., Foy, E., Li, K., Yoneyama, M., Fujita, T., Lemon, S.M., Gale, M., Jr., 2005. Regulating intracellular antiviral defense and permissiveness to hepatitis C virus RNA replication through a cellular

RNA helicase, RIG-I. *Journal of virology* 79, 2689-2699.

98. Sun, J., Rajsbaum, R., Yi, M., 2015. Immune and non-immune responses to hepatitis C virus infection. *World journal of gastroenterology* 21, 10739-10748.
99. Sung, P.S., Shin, E.C., Yoon, S.K., 2015. Interferon Response in Hepatitis C Virus (HCV) Infection: Lessons from Cell Culture Systems of HCV Infection. *International journal of molecular sciences* 16, 23683-23694.
100. Sur, S., Sasaki, R., Devhare, P., Steele, R., Ray, R., Ray, R.B., 2018. Association between microRNA-373 and long non-coding RNA NORAD in hepatitis C virus infected hepatocytes impairs Wee1 expression for growth promotion. *Journal of virology* 92(20).
101. Takacs, C.N., Andreo, U., Dao Thi, V.L., Wu, X., Gleason, C.E., Itano, M.S., Spitz-Becker, G.S., Belote, R.L., Hedin, B.R., Scull, M.A., Rice, C.M., Simon, S.M., 2017. Differential Regulation of Lipoprotein and Hepatitis C Virus Secretion by Rab1b. *Cell reports* 21, 431-441.
102. R Development Core Team. R: A language and environment for statistical computing. Available online: http://www.R-project.org (accessed on 1 March 2016).
103. Thimme, R., Binder, M., Bartenschlager, R., 2012. Failure of innate and adaptive immune responses in controlling hepatitis C virus infection. *FEMS microbiology reviews* 36, 663-683.
104. Tsukiyama-Kohara, K., Kohara, M., 2017. Hepatitis C Virus: Viral Quasispecies and Genotypes. *International journal of molecular sciences* 19.
105. Valadkhan, S., Fortes, P., 2018. Regulation of the Interferon Response by lncRNAs in HCV Infection. *Frontiers in microbiology* 9, 181.
106. Vieyres, G., Pietschmann, T., 2019. HCV Pit Stop at the Lipid Droplet: Refuel Lipids and Put on a Lipoprotein Coat before Exit. *Cells* 8 (3), 233.
107. Volders, P.J., Verheggen, K., Menschaert, G., Vandepoele, K., Martens, L., Vandesompele, J., Mestdagh, P., 2015. An update on LNCipedia: a database for annotated human lncRNA sequences. *Nucleic acids research* 43, 4363-4364.
108. Wang, N., Wang, Q., Shen, D., Sun, X., Cao, X., Wu, D., 2016. Downregulation of microRNA-122 promotes proliferation, migration, and

invasion of human hepatocellular carcinoma cells by activating epithelial-mesenchymal transition. *OncoTargets and therapy* 9, 2035-2047.

109. Wang, P., Xu, J.F., Wang, Y.J., Cao, X.T., 2017. An interferon-independent lncRNA promotes viral replication by modulating cellular metabolism. *Science* 358, 1051-1055.
110. White, J.M., Whittaker, G.R., 2016. Fusion of Enveloped Viruses in Endosomes. *Traffic* 17, 593-614.
111. Wienert, B., Shin, J., Zelin, E., Pestal, K., Corn, J.E., 2018. *In vitro*-transcribed guide RNAs trigger an innate immune response via the RIG-I pathway. *PLoS biology* 16, e2005840.
112. Wong, M.T., Chen, S.S., 2016. Emerging roles of interferon-stimulated genes in the innate immune response to hepatitis C virus infection. *Cellular & molecular immunology* 13, 11-35.
113. Xie, Q., Chen, S., Tian, R., Huang, X., Deng, R., Xue, B., Qin, Y., Xu, Y., Wang, J., Guo, M., Chen, J., Tang, S., Li, G., Zhu, H., 2018. Long Noncoding RNA ITPRIP-1 Positively Regulates the Innate Immune Response through Promotion of Oligomerization and Activation of MDA5. *Journal of virology* 92 (17): e00507-18.
114. Yang, H., Zhou, J., Lehmann, C., 2016. GPR55 - a putative "type 3" cannabinoid receptor in inflammation. *Journal of basic and clinical physiology and pharmacology* 27, 297-302.
115. Yang, Z., Lu, Y., Xu, Q., Tang, B., Park, C.K., Chen, X., 2015. HULC and H19 Played Different Roles in Overall and Disease-Free Survival from Hepatocellular Carcinoma after Curative Hepatectomy: A Preliminary Analysis from Gene Expression Omnibus. *Disease markers* 2015, 191029.
116. Yu, F., Zheng, J., Mao, Y., Dong, P., Lu, Z., Li, G., Guo, C., Liu, Z., Fan, X., 2015. Long Non-coding RNA Growth Arrest-specific Transcript 5 (GAS5) Inhibits Liver Fibrogenesis through a Mechanism of Competing Endogenous RNA. *The Journal of biological chemistry* 290, 28286-28298.
117. Zhang, J., Fan, D., Jian, Z., Chen, G.G., Lai, P.B., 2015. Cancer Specific Long Noncoding RNAs Show Differential Expression Patterns and Competing Endogenous RNA Potential in Hepatocellular Carcinoma. *PloS one* 10, e0141042.
118. Zhou, J., Burkovskiy, I., Yang, H., Sardinha, J., Lehmann, C., 2016. CB2

and GPR55 Receptors as Therapeutic Targets for Systemic Immune Dysregulation. *Frontiers in pharmacology* 7, 264.

6. Abbreviations

aa	Amino acids
Ago2	Argonaute 2
AP	Adaptor Primer
AP-1	Activator protein 1
Apo	Apolipoprotein
ATP	Adenosine triphosphate
BISPR	BST2 interferon stimulated positive regulator
bp	Base pair
BSA	Bovine serum albumin
BST2	Bone marrow stromal cell antigen 2
ceRNA	Competing endogenous RNA
CH25H	Cholesterol 25-hydroxylase
CREs	*Cis*-acting RNA elements
Ct	Threshold cycle
CTP	Cytosine triphosphate
DAA	Direct acting antivirals
DDX3X	DEAD box RNA helicase 3
DMEM	Dulbecco's Modified Eagle's Medium
DMSO	Dimethyl Sulfoxide
DNA	Deoxyribonucleic acid
DNase	Deoxyribonuclease
DTT	Dithiothreitol
E	Amplification efficiency
EC	Endogenous cannabinoid
EDTA	Ethyendiamintetraacetic acid
EGOT	Eosinophil granule ontogeny transcript
eIFs	Eukaryotic initiation factors
eIF2a	Eukaryotic translation initiation factor 2A
ER	Endoplasmic reticulum
eRNA	Enhancer RNA
EWSR1	Ewing sarcoma breakpoint region 1
FBS	Fetal Bovine Serum

FFU	Focus-forming units
GAPDH	Glyceraldehyde 3-phosphate dehydrogenase
GAS	Gamma-activated sequences
GAS5	Growth arrest-specific 5
GBP1	Interferon induced guanylate-binding protein 1
GmR	GapmeR
GPR55	G protein-coupled receptor 55
GSP	Gene specific primer
GSH	Glutathione
GTP	Guanosine triphosphate
h	hour
HCC	Hepatocellular carcinoma
HCV	Hepatitis C virus
HMGB1	High mobility group box 1
HMW	High molecular weight
HOTAIR	HOX transcript antisense RNA
HSP90	Heat shock protein 90
hnRNPA1	Heterogeneous nuclear ribonucleoprotein A1
IFIT	Interferon induced protein with tetratricopeptide repeats
IFITM1	Interferon induced transmembrane protein 1
IFN	Interferon
IL-6	Interleukin-6
IL28A	Interleukin-28 isoform A
IRES	Internal ribosome entry site
IRF3	IFN regulatory factor 3
IRF9	IFN regulatory factor 9
ISG	Interferon stimulated genes
ISG15	Interferon stimulated gene 15
ISGF3	Interferon stimulated gene factor 3
ISGylation	ISG15 conjugation
ISRE	Interferon stimulated response elements
JAK-STAT	Janus kinase/signal transducers and activators of transcription
Jc1	Plasmid pFK-JFH1-J6 C-846_dg
LDL	Low density lipoproteins

LGP2	Laboratory of genetics and physiology 2
LNA	Locked nucleic acid
LncRNAs/lncRs	Long non-coding RNAs
LncRNA#32/LUARIS	LncRNA upregulator of antiviral response interferon signaling
LPS	Lipopolysaccharides
MDA5	Melanoma differentiation factor 5
min	minute
MIP1	Macrophage inflammatory protein 1
MiR-122	MicroRNA-122
mRNA	Messenger RNA
Mx1	MX dynamin like GTPase 1
NCBI	National Center for Biotechnology Information
Neg. ctr. GmR	Negative control GapmeR
NF-κB	Nuclear factor kappa-light-chain-enhancer of activated B cells
NGS	Next generation sequencing
NIH	National Institutes of Health
NK	Natural killer
NLR	NOD-like receptor
NRC	No reverse transcription control
NRIR	Negative regulator of interferon response
NRAV	Negative regulator of antiviral response lncRNA
NTC	No template control
NTRs	Nontranslated regions
OAS	2'-5'-oligoadenylate synthetase
ORF	Open reading frame
PAMPs	Pathogen-associated molecular patterns
PBS	Phosphate buffered saline
PCBP2	Poly(rC)-binding protein 2
pDCs	Plasmacytoid dendritic cells
Pen/Strep	Penicillin-streptomycin solution
PKR	Protein kinase R
Poly(I:C)	Polyinosinic-polycytidylic acid
PRRs	Pattern recognition receptors
PVDF	Polyvinylidenfluoride

qRT-PCR	Quantitative real-time polymerase chain reaction
RIG-I	Retinoic acid-inducible gene I
RIN	RNA Integrity Number
RLH	RIG-I–like helicase
RNA	Ribonucleic acid
RNase L	Ribonuclease L
RPKM	Reads per kilobase of transcript per million mapped reads
RSAD	Radical S-adenosyl methionine domain containing 2
RT	Reverse transcription
s	second
SD	Standard deviation
SDS	Sodium dodecyl dulfate
SEM	Standard error of the mean
SFV	Semliki forest virus
SIRT1	Sirtuin family member 1
SLC12A7	Solute carrier family 12 member 7
Tfr	T follicular regulatory cell
Tfh	T follicular helper cell
TGF-β	Transforming growth factor beta
TLR	Toll-like receptor
Tm	Annealing temperature
TRIF	TIR-domain-containing adapter-inducing interferon-β
TRIM	The tripartite motif family
UCA1	Urothelial cancer associated 1
USP18	Ubiquitin specific peptidase 18
U99	Small nucleolar RNA U99, H/ACA box 57, snoRNA U99
µg	Microgram
µL	Microliter
µM	Micromolar
UTP	Uridine triphosphate
UTR	Untranslated region
VLDL	Very low-density lipoproteins
ZNF252P-AS1	ZNF252P Antisense RNA 1

7. Appendix

7.1 Test for Possible Cross Reactions between GmRs

(https://www.ebi.ac.uk/Tools/services/web_clustalo/toolform.ebi)

```
lncR_7-GmR_2        ----ATAAGTGTCTAGTTAG---------          16
lncR_3-GmR_2        -----GACGATAAGAGGTAAC--------          16
lncR_8-GmR_1        --------GTTACCAGTGAAGCGG-----          16
Random_GmR_         ----AACAC-----GTCTATACGC-----          15
lncR_3-GmR_1        ----------GCGTGATTAAATGGAT---          16
lncR_7-GmR_1        -------------TGATTAACAGAACGGA          16
lncR_8-GmR_2        -------TCGGATTGGTCACATG------          16
lncR_10-GmR_1       GTTAATCTGATCTTGC-------------          16
lncR_10-GmR_2       -----TCTGAGCTTGATCACT--------          16
```

Conclusion:

All used GapmeRs do not show any cross reactions among each other.

GapmeR specificities

GapmeR sequences were matched against Human genomic plus transcript (Human G-T) sequences using NBLAST (https://blast.ncbi.nlm.nih.gov/Blast.cgi?PROGRAM=blastn&PAGE_TYPE=BlastSearch&LINK_LOC=blasthome) using default parameters but without any filtering of repeat sequences. For each GapmeR, the best 5 matches to human transcripts (except the genuine target) are shown.

Conclusions (for details please see below):

The Randomized control GapmeR does not bind specifically to any target in the human transcriptome. Virtually all GapmeRs specific for lncRNAs used in this study are very specific for their genuine targets. Only lncR 10-GmR 1 can bind to only one other target RNA with a temperature difference of only at least 1 °C (value calculated for DNA), to the next target with at least 5 °C difference.

Random_GmR; Query: AACACGTCTATACGC (15 nts)

5 best matches (binding to RNA splice variants removed from output):

Homo sapiens zinc finger CCHC-type containing 23 (ZCCHC23), mRNA, Sequence ID: NM_001039778.2

```
Query  1    AACACGTCTATAC  13
           |||||||||||||
Sbjct  973  AACACGTCTATAC  961
```

PREDICTED: Homo sapiens uncharacterized LOC107984587 (LOC107984587), ncRNA

Sequence ID: XR_001749928.1

```
Query  1    AACACGTCTATAC  13
           |||||||||||||
Sbjct  578  AACACGTCTATAC  590
```

Homo sapiens long intergenic non-protein coding RNA 645 (LINC00645), long non-coding RNA

Sequence ID: NR_039992.2

```
Query  1     AACACGTCTATAC  13
            |||||||||||||
Sbjct  1476  AACACGTCTATAC  1464
```

PREDICTED: Homo sapiens DNA polymerase eta (POLH), transcript variant X2, mRNA

Sequence ID: XM_024446466.1

```
Query  1     AACACGTCTATA  12
            ||||||||||||
Sbjct  3057  AACACGTCTATA  3046
```

Homo sapiens chromosome 2, GRCh38.p12 Primary Assembly

Sequence ID: NC_000002.12

```
Query  1          AACACGTCTATACG  14
                 ||||||||||||||
Sbjct  112349170  AACACGTCTATACG  112349183
```

Conclusion: Random_GmR (15 nts) has at least 2 mismatches to any human transcript. For standard DNA oligonucleotides this would correspond to a drop in T_M by 11 °C compared to full hybridization.

lncR 3-GmR 1; Query: GCGTGATTAAATGGAT (16 nts)

5 best matches (except genuine target, binding to RNA splice variants removed from output):

PREDICTED: Homo sapiens EYA transcriptional coactivator and phosphatase 4 (EYA4), transcript variant X1, mRNA, Sequence ID: XM_017010368.2

```
Query  3   GTGATTAAATGGAT  16
           ||||||||||||||
Sbjct  60  GTGATTAAATGGAT  7
```

PREDICTED: Homo sapiens macrophage scavenger receptor 1 (MSR1), transcript variant X1, mRNA, Sequence ID: XM_024447160.1

```
Query  4     TGATTAAATGGAT  16
             |||||||||||||
Sbjct  1554  TGATTAAATGGAT  1542
```

PREDICTED: Homo sapiens transmembrane protein 181 (TMEM181), transcript variant X5, mRNA, Sequence ID: XM_005267074.4

```
Query  4     TGATTAAATGGAT  16
             |||||||||||||
Sbjct  2295  TGATTAAATGGAT  2307
```

PREDICTED: Homo sapiens zinc finger FYVE-type containing 16 (ZFYVE16), transcript variant X18, mRNA, Sequence ID: XM_024446273.1

```
Query  4     TGATTAAATGGAT  16
             |||||||||||||
Sbjct  8457  TGATTAAATGGAT  8469
```

PREDICTED: Homo sapiens SMAD family member 5 (SMAD5), transcript variant X3, mRNA, Sequence ID: XM_024446047.1

```
Query  4     TGATTAAATGGAT  16
             |||||||||||||
Sbjct  4433  TGATTAAATGGAT  4421
```

Conclusion: lncR 3-GmR 1 (16 nts) has at least 2 mismatches to any other human transcript. For standard DNA oligonucleotides this would correspond to a drop in T_M by 10 °C compared to full hybridization.

lncR 3-GmR 2; Query: GACGATAAGAGGTAAC (16 nts)

5 best matches (except genuine target, binding to RNA splice variants removed from output):

PREDICTED: Homo sapiens PRELI domain containing 2 (PRELID2), transcript variant X2, mRNA, Sequence ID: XM_017009127.1

```
Query  4    GATAAGAGGTAAC  16
            |||||||||||||
Sbjct  982  GATAAGAGGTAAC  994
```

PREDICTED: Homo sapiens chromosome 8 open reading frame 34 (C8orf34), transcript variant X3, misc_RNA, Sequence ID: XR_928756.3

```
Query  4     GATAAGAGGTAA  15
             ||||||||||||
Sbjct  6998  GATAAGAGGTAA  7009
```

PREDICTED: Homo sapiens inner mitochondrial membrane peptidase subunit 2 (IMMP2L), transcript variant X13, mRNA, Sequence ID: XM_024446959.1

```
Query  5     ATAAGAGGTAAC  16
             ||||||||||||
Sbjct  2239  ATAAGAGGTAAC  2250
```

PREDICTED: Homo sapiens Cbl proto-oncogene like 1 (CBLL1), transcript variant X7, mRNA, Sequence ID: XM_011516580.3

```
Query  3     CGATAAGAGGTA  14
             ||||||||||||
Sbjct  1974  CGATAAGAGGTA  1963
```

PREDICTED: Homo sapiens parkin coregulated (PACRG), transcript variant X6, mRNA, Sequence ID: XM_011535461.3

```
Query  5     ATAAGAGGTAAC  16
             ||||||||||||
Sbjct  2089  ATAAGAGGTAAC  2100
```

Conclusion: lncR 3-GmR 2 (16 nts) has at least 3 mismatches to any other human transcript. For standard DNA oligonucleotides this would correspond to a drop in T_M by 11 °C compared to full hybridization.

lncR 7-GmR 1; Query: TGATTAACAGAACGGA (16 nts)

5 best matches (except genuine target, binding to RNA splice variants removed from output):

PREDICTED: Homo sapiens MCF.2 cell line derived transforming sequence (MCF2), transcript variant X6, mRNA, Sequence ID: XM_017029532.2

```
Query  3     ATTAACAGAACGG  15
             |||||||||||||
Sbjct  2871  ATTAACAGAACGG  2883
```

PREDICTED: Homo sapiens proline rich 26 (PRR26), transcript variant X4, mRNA, Sequence ID: XM_024448024.1

```
Query  1    TGATTAACAGAAC  13
            |||||||||||||
Sbjct  854  TGATTAACAGAAC  866
```

PREDICTED: Homo sapiens uncharacterized LOC285500 (LOC285500), transcript variant X3, mRNA, Sequence ID: XM_011532460.2

```
Query  1     TGATTAACAGAAC  13
             |||||||||||||
Sbjct  1435  TGATTAACAGAAC  1423
```

PREDICTED: Homo sapiens UTP18, small subunit processome component (UTP18), transcript variant X2, mRNA, Sequence ID: XM_011524870.2

```
Query  4     TTAACAGAACGGA  16
             |||||||||||||
Sbjct  1542  TTAACAGAACGGA  1554
```

PREDICTED: Homo sapiens mal, T cell differentiation protein like (MALL), transcript variant X1, mRNA, Sequence ID: XM_011511809.1

```
Query  2    GATTAACAGAACG  14
            |||||||||||||
Sbjct  602  GATTAACAGAACG  614
```

Conclusion: lncR 7-GmR 1 (16 nts) has at least 3 mismatches to any other human transcript. For standard DNA oligonucleotides this would correspond to a drop in T_M by 9 °C compared to full hybridization.

lncR 7-GmR 2; Query: ATAAGTGTCTAGTTAG (16 nts)

5 best matches (except genuine target, binding to RNA splice variants removed from output):

PREDICTED: Homo sapiens myotubularin related protein 10 (MTMR10), transcript variant X4, mRNA, Sequence ID: XM_005254508.3

```
Query  3     AAGTGTCTAGTTAG  16
             ||||||||||||||
Sbjct  3699  AAGTGTCTAGTTAG  3712
```

Homo sapiens PCNA clamp associated factor (PCLAF), transcript variant 3, non-coding RNA, Sequence ID: NR_109934.1

```
Query  2    TAAGTGTCTAGTT  14
            |||||||||||||
Sbjct  768  TAAGTGTCTAGTT  780
```

Homo sapiens proline rich 9 (PRR9), mRNA, Sequence ID: NM_001195571.1

```
Query  1    ATAAGTGTCTAGT  13
            |||||||||||||
Sbjct  184  ATAAGTGTCTAGT  196
```

PREDICTED: Homo sapiens chromosome X open reading frame 38 (CXorf38), transcript variant X5, mRNA, Sequence ID: XM_006724527.4

```
Query  5     GTGTCTAGTTAG  16
             ||||||||||||
Sbjct  3143  GTGTCTAGTTAG  3154
```

PREDICTED: Homo sapiens branched chain keto acid dehydrogenase E1 subunit beta (BCKDHB), transcript variant X6, mRNA, Sequence ID: XM_011536023.3

```
Query  3     AAGTGTCTAGTT  14
             ||||||||||||
Sbjct  1536  AAGTGTCTAGTT  1525
```

Conclusion: lncR 7-GmR 2 (16 nts) has at least 2 mismatches to any other human transcript. For standard DNA oligonucleotides this would correspond to a drop in T_M by 1 °C compared to full hybridization.

lncR 8-GmR 1; Query: GTTACCAGTGAAGCGG (16 nts)

5 best matches (except genuine target, binding to RNA splice variants removed from output):

PREDICTED: Homo sapiens schlafen family member 12 (SLFN12), transcript variant X6, mRNA, Sequence ID: XM_017024811.2

```
Query  1    GTTACCAGTGAAG  13
            |||||||||||||
Sbjct  452  GTTACCAGTGAAG  440
```

PREDICTED: Homo sapiens citrate lyase beta like (CLYBL), transcript variant X10, mRNA, Sequence ID: XM_024449330.1

```
Query  2     TTACCAGTGAAGC  14
             |||||||||||||
Sbjct  1682  TTACCAGTGAAGC  1670
```

PREDICTED: Homo sapiens COP1, E3 ubiquitin ligase (COP1), transcript variant X25, mRNA, Sequence ID: XM_017002080.2

```
Query  1     GTTACCAGTGAAG  13
             |||||||||||||
Sbjct  5564  GTTACCAGTGAAG  5576
```

PREDICTED: Homo sapiens uncharacterized LOC105375318 (LOC105375318), transcript variant X1, ncRNA, Sequence ID: XR_001745236.1

```
Query  2    TTACCAGTGAAGC  14
            |||||||||||||
Sbjct  572  TTACCAGTGAAGC  584
```

PREDICTED: Homo sapiens uncharacterized LOC105375101 (LOC105375101), ncRNA
Sequence ID: XR_001744179.1

```
Query  2    TTACCAGTGAAGC  14
            |||||||||||||
Sbjct  866  TTACCAGTGAAGC  878
```

Conclusion: lncR 8-GmR 1 (16 nts) has at least 3 mismatches to any other human transcript. For standard DNA oligonucleotides this would correspond to a drop in T_M by 12 °C compared to full hybridization.

lncR 8-GmR 2; Query: TCGGATTGGTCACATG (16 nts)

5 best matches (except genuine target, binding to RNA splice variants removed from output):

PREDICTED: Homo sapiens LIF receptor alpha (LIFR), transcript variant X4, mRNA, Sequence ID: XM_011514042.3

```
Query  4     GATTGGTCACATG  16
             |||||||||||||
Sbjct  6201  GATTGGTCACATG  6213
```

PREDICTED: Homo sapiens regulator of G protein signaling 9 (RGS9), transcript variant X1, mRNA, Sequence ID: XM_011525426.3

```
Query  1     TCGGATTGGTCAC  13
             |||||||||||||
Sbjct  1080  TCGGATTGGTCAC  1068
```

Homo sapiens long intergenic non-protein coding RNA 1550 (LINC01550), transcript variant 2, long non-coding RNA, Sequence ID: NR_152746.1

```
Query  3     GGATTGGTCACAT  15
             |||||||||||||
Sbjct  1862  GGATTGGTCACAT  1850
```

Homo sapiens dispatched RND transporter family member 1 (DISP1), transcript variant 2, mRNA, Sequence ID: NM_001350630.1

```
Query  4    GATTGGTCACATG  16
            |||||||||||||
Sbjct  891  GATTGGTCACATG  903
```

Homo sapiens glutathione peroxidase 3 (GPX3), transcript variant 1, mRNA
Sequence ID: NM_002084.4

```
Query  2    CGGATTGGTCACA  14
            |||||||||||||
Sbjct  127  CGGATTGGTCACA  139
```

Conclusion: lncR 8-GmR 2 (16 nts) has at least 3 mismatches to any other human transcript. For standard DNA oligonucleotides this would correspond to a drop in T_M by 5 °C compared to full hybridization.

lncR 10-GmR 1; Query: GTTAATCTGATCTTGC (16 nts)

5 best matches (except genuine target, binding to RNA splice variants removed from output):

PREDICTED: Homo sapiens solute carrier family 4 member 4 (SLC4A4), transcript variant X6, mRNA, Sequence ID: XM_024454272.1

```
Query  2     TTAATCTGATCTTGC  16
             ||||||||||||||||
Sbjct  4333  TTAATCTGATCTTGC  4319
```

PREDICTED: Homo sapiens tRNA-yW synthesizing protein 5 (TYW5), transcript variant X2, misc_RNA, Sequence ID: XR_001738610.2

```
Query  2     TTAATCTGATCTTG  15
             ||||||||||||||
Sbjct  1979  TTAATCTGATCTTG  1992
```

PREDICTED: Homo sapiens embigin (EMB), transcript variant X1, mRNA, Sequence ID: XM_011543146.2

```
Query  2     TTAATCTGATCTTG  15
             ||||||||||||||
Sbjct  3760  TTAATCTGATCTTG  3773
```

PREDICTED: Homo sapiens roundabout guidance receptor 2 (ROBO2), transcript variant X26, mRNA, Sequence ID: XM_017007006.1

```
Query  3     TAATCTGATCTTGC  16
             ||||||||||||||
Sbjct  7680  TAATCTGATCTTGC  7693
```

PREDICTED: Homo sapiens ATPase family, AAA domain containing 2 (ATAD2), transcript variant X4, misc_RNA, Sequence ID: XR_928326.3

```
Query  4     AATCTGATCTTGC  16
             |||||||||||||
Sbjct  1731  AATCTGATCTTGC  1719
```

Conclusion: lncR 10-GmR 1 (16 nts) has at least 1 mismatch to any other human transcript. For standard DNA oligonucleotides this would correspond to a drop in T_M by 3 °C compared to full hybridization. Hybridization to the next target (2 mismatches) would correspond to a drop in T_M by 9 °C.

lncR 10-GmR 2; Query: TCTGAGCTTGATCACT (16 nts)

5 best matches (except genuine target, binding to RNA splice variants removed from output):

PREDICTED: Homo sapiens solute carrier family 35 member B4 (SLC35B4), transcript variant X2, misc_RNA, Sequence ID: XR_001744887.2

```
Query  3     TGAGCTTGATCACT  16
             ||||||||||||||
Sbjct  1725  TGAGCTTGATCACT  1738
```

PREDICTED: Homo sapiens ring finger protein 14 (RNF14), transcript variant X6, mRNA, Sequence ID: XM_005268541.4

```
Query  2    CTGAGCTTGATCA  14
            |||||||||||||
Sbjct  619  CTGAGCTTGATCA  607
```

PREDICTED: Homo sapiens uncharacterized LOC107986317 (LOC107986317), ncRNA, Sequence ID: XR_002959804.1

```
Query  4     GAGCTTGATCACT  16
             |||||||||||||
Sbjct  1859  GAGCTTGATCACT  1847
```

PREDICTED: Homo sapiens OPA1, mitochondrial dynamin like GTPase (OPA1), transcript variant X2, misc_RNA, Sequence ID: XR_001740159.2

```
Query  2     CTGAGCTTGATCA  14
             |||||||||||||
Sbjct  6007  CTGAGCTTGATCA  6019
```

PREDICTED: Homo sapiens neuron navigator 3 (NAV3), transcript variant X14, mRNA, Sequence ID: XM_017020173.2

```
Query  1     TCTGAGCTTGATC  13
             |||||||||||||
Sbjct  1388  TCTGAGCTTGATC  1376
```

Conclusion: lncR 10-GmR 2 (16 nts) has at least 2 mismatches to any other human transcript. For standard DNA oligonucleotides this would correspond to a drop in T_M by 5 °C compared to full hybridization.

7.2 Potential full length sequence of lncR 8

RACE experiments extended sequences of both 3′ and 5′ end of lncR 8 in addition to sequence obtained from the RefSeq database (NR_038238.1) (label in red). Sequence of qRT-PCR primers and GapmeRs were also indicated.

7.3 Negative Control β-actin

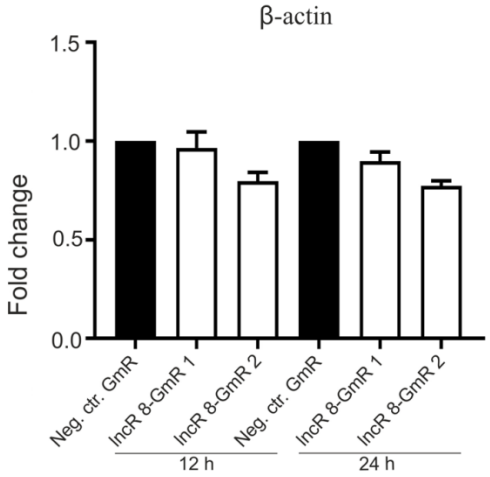

Since *GAPDH* was used for data normalization, an additional house-keeping gene (β-actin) was used as a negative control target. One day prior to HCV treatment, GmRs targeting lncR 8 and Neg. ctr. GmR were transfected in Huh-7.5 cells. Cells were collected at 12 h and 24 h post HCV transfection. qRT-PCR data of targeted genes was normalized to *GAPDH*. The data are shown as the mean ± SEM of at least three independent experiments.

7.4 Plasmid Map of pFK-JFH1-J6 C-846_dg (Jc1)_12961

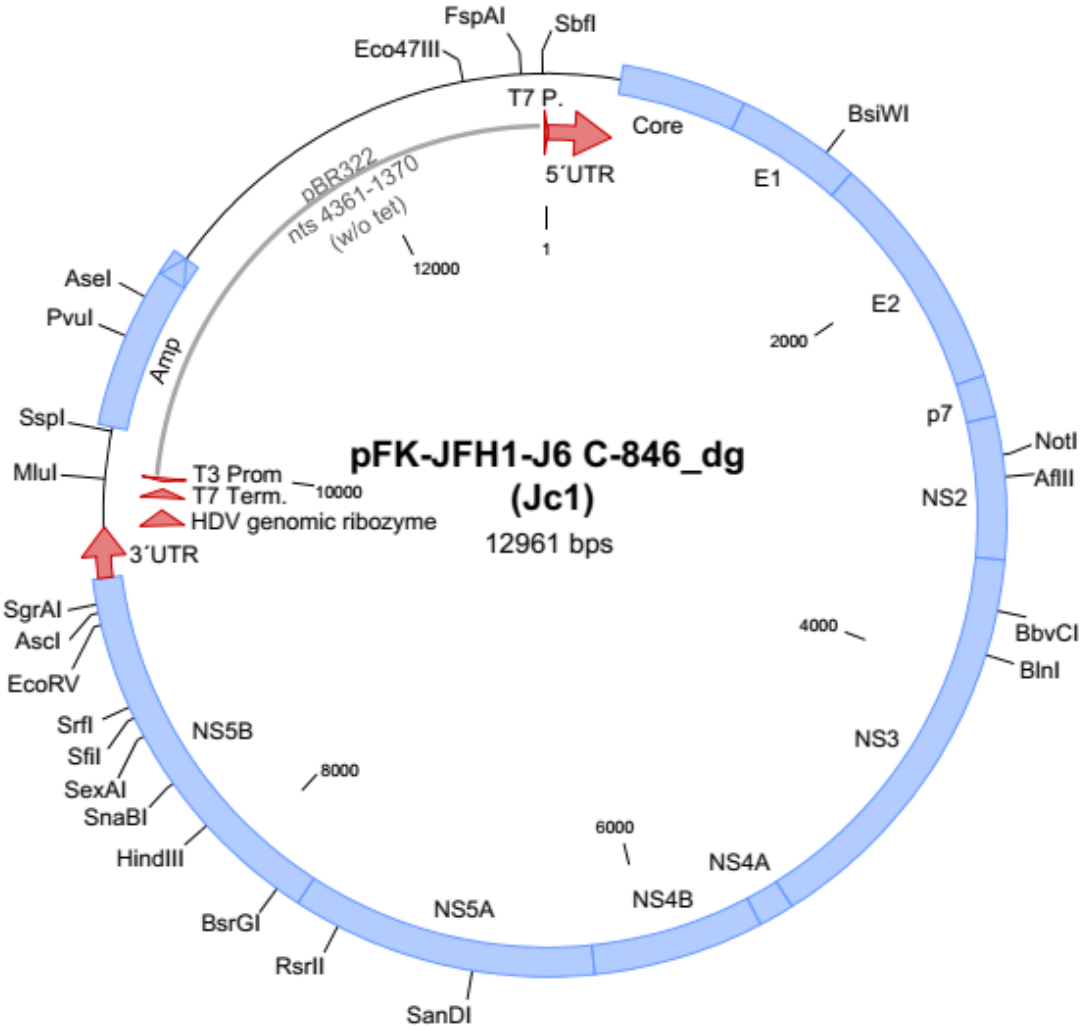

Feature	Description	Start – Stop (nt)
T7	T7 RNA Polymerase promoter	1-18
5′UTR	HCV 5′ untranslated region	18-357
Core	HCV Core-coding sequence	358-930
E1	HCV E1 glycoprotein coding sequence	931-1506
E2	HCV E2 glycoprotein coding sequence	1507-2607
p7	HCV p7 polypeptide coding sequence	2608-2796
NS2	HCV NS2 protein coding sequence	2797-3447
NS3	HCV NS3 protein coding sequence	3448-5340
NS4A	HCV NS4A protein coding sequence	5341-5502
NS4B	HCV NS4B protein coding sequence	5503-6285
NS5A	HCV NS5A protein coding sequence	6286-7683
NS5B	HCV NS5B protein coding sequence	7684-9459
3′UTR	HCV 3′ untranslated region	9460-9695
HDV	Hepatitis D Virus genomic ribozyme	9696-9779
T7T	T7 RNA Polymerase terminator	9845-9891

T3	T3 RNA Polymerase promoter	9931-9950
pBR322 ori	pBR322 origin of replication	9954-12945
Amp R	Ampicillin resistance gene	10162-11019

8. Publications

8.1 Peer-reviewed Journal

Pan Hu*, Jochen Wilhelm, Gesche K. Gerresheim, Lyudmila A. Shalamova and Michael Niepmann*. *Lnc-ITM2C-1* and *GPR55* Are Proviral Host Factors for Hepatitis C Virus. *Viruses*. 2019, 11, (6) (***Corresponding author**)
This paper was chosen by the Editors as the title cover story of this journal issue.

Gesche K. Gerresheim, Jochen Bathke, Audrey M. Michel, Dmitri E. Andreev, Lyudmila A. Shalamova, Oliver Rossbach, **Pan Hu**, Dieter Glebe, Markus Fricke, Manja Marz, Alexander Goesmann, Stephen J. Kiniry, Pavel V. Baranov, Ivan N. Shatsky and Michael Niepmann. Cellular Gene Expression during Hepatitis C Virus Replication as Revealed by Ribosome Profiling. *International Journal of Molecular Sciences*. 2019, 15; 20 (6).

8.2 Contributions to Congresses

Oct. 8-11 2018, chosen for “poster walk” on 25th International symposium on Hepatitis C Virus and Related Viruses, Dublin, Irland.

Oct. 5-8 2019, 26th International symposium on Hepatitis C Virus and Related Viruses, Seoul, South Korea, Poster.

9. Acknowledgements

First of all, I would like to thank Prof. Michael Niepmann for providing the research topic, funding and laboratory space for conducting this work. Big thanks for his understanding and support during the whole process, especially for his encouragement in times of hardship.

Special thanks go to Prof. Albrecht Bindereif for being my first supervisor in the faculty of biology at Justus Liebig University Giessen.

I also want to thank the Land Hessen LOEWE grant (Medical RNomics) for providing the funding for travels and symposiums allowing me to improve presenting skills and scientific thinking.

I express my great thanks also to my colleagues Gesche K. Gerresheim, Lyudmila Shalamova, Anika Nieder-Röhrmann, Nadia Dünnes for sharing their experimental experiences with me. I thank Dimitar Nachev, Selena A. Guggenberger, Dennis Metzger, Stefanie M. Herbel, and Lisa Loew as well for all the good times we spent together inside and outside the lab.

Additionally, I want to thank Jochen Wilhelm for his support on bioinformatical analysis. Big thanks to Prof. Dieter Glebe for allowing me to perform experiments in the S3** lab in BFS. My sincere thanks also go to members of the research groups at the Institute of Biochemistry, Prof. Lienhard Schmitz and Prof. Ritva Tikkanen. I also want to thank members of Prof. Albrecht Bindereif's group for initial discussions about the project and helps with the experiments.

Also, I want to thank my Chinese friends Kai Ni and Lu Liu for their kindness and valuable help. And special thanks to Xiaohan Wang for accompanying me through difficult times, for "he is truly his brother's keeper and the finder of lost children".

I am forever and ever indebted to my parents for their understanding and support. Special thanks to Siqi Li for being a conscientious husband and a faithful partner, his unconditional love makes me brave.